# NON-CANONICAL ROLES FOR RAG1 IN LYMPHOCYTE DEVELOPMENT

Julie E. Horowitz

A DISSERTATION

in

Immunology

Presented to the Faculties of the University of Pennsylvania

in

Partial Fulfillment of the Requirements for the

Degree of Doctor of Philosophy

2015

Supervisor of Dissertation

_____

Craig H. Bassing, Ph.D.

Associate Professor, Pathology and Laboratory Medicine

Graduate Group Chairperson

_____

David M. Allman, Ph.D., Associate Professor, Pathology and Laboratory Medicine

Dissertation Committee

Rahul M. Kohli, M.D., Ph.D., Assistant Professor, Medicine (Chair)

Marisa Bartolomei, Ph.D., Professor, Cell and Developmental Biology

Michael P. Cancro, Ph.D., Professor, Pathology and Laboratory Medicine

Michael M. May, Ph.D., Associate Professor, Animal Biology

NON-CANONICAL ROLES FOR RAG1 IN LYMPHOCYTE DEVELOPMENT

## DEDICATION

To my parents, Susan and Peter, who have taken the road less traveled by—from the South Bronx and West Philly to Riyadh and everywhere in between—and that has made all the difference.

**ACKNOWLEDGEMENT**

I owe a debt of thanks for the time I have spent at Penn, especially:

To Craig Bassing, thank you for your patience, guidance, and support as a mentor. You taught me to think critically and to fight for my science, pushed me to succeed all the times I was afraid, and gave me a steady five-year supply of animal crackers, without which none of the experiments described in this thesis would've been analyzed;

To the women of the Bassing Lab, Katherine, Amy, Meg, Sarah, Brenna, and Natalie, thank you for making the lab a place where I could work hard and laugh harder. You are phenomenal scientists and even better friends;

To my thesis committee, thank you for listening to hours of V(D)J recombination and for pushing me to think carefully about my science and my future;

To David G. Schatz for finding RAG1, for being a supporter and advocate of my work, and for setting a stellar example of how to be a good scientist;

To my extraordinarily good-looking, brilliant, funny, talented siblings, Nicky, Eric, Andy, and Matt, for being my reality check;

To my good friends, Jaclyn Gidel, Martin Naradikian, and Ellen de Obaldia for showing me that life should be filled with joy and that happiness comes from being true to yourself;

And to *all* the mice, for giving me a place to hide out and think and for keeping me organized.

# ABSTRACT


NON-CANONICAL ROLES FOR RAG1 IN LYMPHOCYTE DEVELOPMENT

Julie E. Horowitz

Craig H. Bassing, Ph.D.

The RAG1/RAG2 (RAG) endonuclease recombines accessible antigen receptor (AgR) genes through DNA double strand break (DSB) intermediates to generate a diverse AgR repertoire. RAG-mediated DSBs signal changes in expression of genes encoding proteins involved in cellular survival, lymphocyte differentiation, and AgR selection. RAG proteins are each comprised of “core” endonuclease domains and dispensable “non-core” regions. Humans with mutations in non-core RAG1 regions exhibit fatal primary immunodeficiencies, and mice expressing truncated core, but not full-length, Rag1 protein ($Rag1^{C/C}$ mice) exhibit impaired early lymphocyte development associated with reduced levels of AgR gene rearrangements. In addition to serving with RAG2 as the V(D)J endonuclease, the RAG1 protein has been proposed to utilize non-core regions to regulate V(D)J recombination by enhancing AgR locus accessibility, promoting efficient RAG endonuclease activity, and/or generating RAG DSB-induced survival and differentiation signals. The experiments described in this thesis use a variety of mouse genetic models to investigate how mutations in RAG1 protein that preserve RAG endonuclease activity impair V(D)J recombination efficiency and lymphocyte development. First, these studies have identified roles for non-core Rag1 regions in regulating normal $\alpha\beta$ T cell development and TCR$\beta$ recombination by promoting V$\beta$ rearrangements and diverse usage of V$\beta$ gene segments in both primary and secondary V$\beta$D$\beta$J$\beta$ rearrangements. Second, these studies show that non-core Rag1 regulates normal B cell development by inducing transcriptional activation of the pro-survival kinase Pim2 in response to RAG cleavage and by promoting the survival of

developing Igκ$^+$ and Igλ$^+$ B cells. These studies have also identified roles for Rag1 in enhancing Igκ and Igλ locus accessibility in pre-B cells prior to RAG cleavage. Collectively, the data presented in this thesis demonstrate that RAG1 has critical functions outside of V(D)J recombination that enhance AgR gene segment accessibility, promote V(D)J recombination at multiple AgR loci, and transduce pro-survival signals during AgR recombination to establish a broad AgR repertoire and thereby foster normal lymphocyte development.

## TABLE OF CONTENTS

## LIST OF FIGURES

# CHAPTER 1

## Antigen Receptor Assembly and the RAG Recombinase

### Antigen Receptor Assembly

In response to infection, antigen-activated lymphocytes clear antigen from the host and protect against future stimulation with the same antigen. Thus, antigen-specific lymphocyte activation is the cornerstone of effective adaptive immunity. Antigen recognition is mediated by antigen receptors (AgRs) expressed on the surface of mature B and T lymphocytes. The B cell receptor (BCR) is comprised of immunoglobulin heavy (IgH) and immunoglobulin light (IgL) protein chains (encoded by *IgH* loci and either *Igκ* or *Igλ* loci, respectively), while the T cell receptor (TCR) is comprised of either TCRβ and TCRα protein chains (encoded by *TCRβ* and *TCRα* loci, respectively) or, in a subset of cells, TCRδ and TCRγ protein chains (encoded by *TCRδ* and *TCRγ* loci, respectively). AgRs are composed of variable regions that mediate antigen recognition as well as constant regions that mediate effector function in response to antigen stimulation. Most lymphocytes express a single AgR of unique specificity, yielding a population of lymphocyte AgRs with ~$10^8$ different antigenic specificities (Janeway, 2005).

The lymphocyte-specific RAG1/RAG2 (RAG) endonuclease complex generates AgR gene diversity by catalyzing the assembly of Ig and TCR genes from germline variable (V), diversity (D), and joining (J) gene segments and downstream constant (C) gene segments (Fugmann et al., 2000) (Figure 1.1). The RAG1 protein binds DNA and exhibits DNA endonuclease activity in the presence of RAG2 protein, a co-factor essential for RAG cleavage but with no inherent DNA cleavage activity of its own (Schatz and Swanson, 2011). The RAG protein complex, which forms a Y-shaped

hetero-tetrameric complex (Kim et al., 2015; Yin et al., 2009), generates DNA double-strand breaks (DSBs) between individual variable (V), diversity (D), and joining (J) gene segments and adjacent recombination signal sequences (RSSs). RSSs are composed of conserved heptamer and nonamer sequences separated by either 12 or 23 base pair spacer sequences, which are less conserved (Fugmann et al., 2000; Schatz and Swanson, 2011). The RAG proteins independently localize at a single RSS and then capture a second RSS, forming a pre-break synaptic complex. RAG synaptic complexes form between one 12-RSS and one 23-RSS, thus restricting potential V(D)J rearrangements by the 12/23 rule (Schatz and Ji, 2011). This 12/23 restriction is strongly enforced at the IgH locus, where $V_H$ and $J_H$ gene segments have 23-RSSs and $D_H$ segments are flanked by 12-RSSs, ensuring that $D_H$ segments are included in *IgH* gene assembly and that direct $V_H$-$J_H$ recombination does not occur (Schatz and Ji, 2011; Schatz and Swanson, 2011). Additional mechanisms enforce 12/23 restriction at the TCRβ locus, where *Vβ* and *Jβ* segments are 12/23-compatible (Bassing et al., 2000), to ensure *Dβ* segments are included in *TCRβ* gene assembly. During synapsis, the RAG protein complex first induces a single-strand DNA nick, which then attacks the second strand to generate a DNA DSB at each RSS. The resultant hairpin-sealed coding ends and blunt signal ends remain held together in a post-cleavage complex. RAG DSBs activate the DNA-dependent protein kinase catalytic subunit, which together with the Artemis nuclease, forms an endonuclease that processes RAG coding ends for non-homologous end-joining (Helmink and Sleckman, 2012; Lieber, 2010). RAG DSBs also activate the ataxia telangiectasia mutated (ATM) kinase, which coordinates the cellular DSB response. ATM substrates stabilize, process, and repair DNA ends, creating V(D)J coding joins and signal joins (Alt et al., 2013; Boboila et al., 2012; Helmink and Sleckman, 2012; Lieber, 2010), and RAG DSBs signal in part though ATM to activate a

genetic program encompassing cell survival and lymphocyte differentiation genes (Bednarski and Sleckman, 2012; Bredemeyer et al., 2008; Helmink and Sleckman, 2012). RAG coding ends undergo non-templated nucleotide addition by the terminal deoxynucleotidyl transferase before joining, while RAG signal ends are simply end-ligated (Helmink and Sleckman, 2012). The number of possible RAG-mediated V(D)J joining events coupled with the imprecise manner in which coding ends are processed together combine to generate AgR diversity.

**Antigen Receptor Assembly is Developmentally Regulated**

AgRs are assembled in the bone marrow or thymus through a series of ordered, cell-type and developmental-stage specific V(D)J recombination events (Clark et al., 2014; Rothenberg, 2014). BCR assembly initiates at the *IgH* locus, which spans 3 Mb and is comprised of several regions: the distal 5' end, consisting of 150 $V_H$ gene segments, a 2 kb region consisting of ~10 $V_D$ and 4 $J_H$ gene segments, and the 3' region, consisting of 8 $C_H$ genes (Perlot and Alt, 2008) (Figure 1.1). In pre-pro B cells, RAG accumulates over transcriptionally active D and J gene segments marked by high levels of tri-methylated histone H3 at lysine 4 (H3K4Me3), acetylated histone H3 at lysine 9 (H3K9Ac), and RNA polymerase II (RNAPII) binding to initiate $D_H$-*to*-$J_H$ rearrangements on both *IgH* alleles (Jung et al., 2006; Schatz and Ji, 2011). These localized "recombination centers" are proposed to facilitate subsequent $V_H$-*to*-$DJ_H$ recombination events via large-scale looping of the IgH locus that bring distal $V_H$ gene segments in proximity to $DJ_H$ rearrangements (Chaumeil and Skok, 2012; Degner-Leisso and Feeney, 2010; Schatz and Ji, 2011) and form independently of RAG (Majumder et al., 2015). Productive, in-frame $V_HDJ_H$ gene rearrangements together with downstream $C_H$ genes are expressed as IgH proteins that pair with surrogate light chain complexes comprised of λ5 and VpreB to form pre-BCRs (Clark et al., 2014). Signaling from the

pre-BCR leads to cessation of RAG expression and induction of Cyclin D3 protein, which drives pro-to-pre-B cell differentiation concomitant but independent of proliferation expansion (Clark et al., 2014; Sicinska et al., 2003). At this time, developmental stage-specific changes in $V_H$ chromatin and $V_H/DJ_H$ looping likely cooperate to silence transcription and recombination of $V_H$ segments in pre-B cells (Chaumeil and Skok, 2012). The subsequent developmental transition from the large to small Pre-B cell stage is associated with attenuation of interleukin-7 (IL-7) cytokine signals, cell cycle exit, re-induction of RAG proteins, transcriptional activation of germline *Igκ* loci, and consequent *Vκ-Jκ* recombination (Clark et al., 2014; Schlissel, 2007). The *Igκ* locus spans ~3.5 Mb and is comprised of two regions: the 5' end, consisting of 140 *Vκ* gene segments, and the 3' end, consisting of 4 functional *Jκ* gene segments and a single *Cκ* exon (Schatz and Ji, 2011) (Figure 1.1). Successful, in-frame *Vκ-Jκ* rearrangements are expressed as proteins for pairing with IgH proteins, and the resultant BCRs are tested for auto-reactivity. Cells that successfully undergo productive *Igκ* rearrangements and pass self-tolerance checkpoints exit the bone marrow to complete maturation in the spleen. However, recognition of self-proteins results in down-regulation of the BCR, re-induction of RAG transcripts, and secondary *Vκ-Jκ* rearrangements. Pre-B cells with receptors that fail to yield productive, non-autoreactive *Vκ-Jκ* rearrangements exhaust/inactivate the Igκ locus via RS element deletion and initiate *Vλ-Jλ1* rearrangements at *Igλ* loci (Clark et al., 2014; Schlissel, 2007). The Igλ locus is ~240 kb and is comprised of two *V-J* domains, each containing one or two *Vλ* gene segments that rearrange to *Jλs* across total distances of 30-80 kb (Sanchez et al., 1991; Schlissel, 2007) (Figure 1.1). These late-stage *Igλ* rearrangements depend on developmentally regulated *Igλ* locus accessibility (Beck et al., 2009) as well as NF-κB-induced Pim2 signals to provide pro-survival signals in pre-B cells attempting productive rearrangements (Beck et al., 2009;

Bednarski et al., 2012; Derudder et al., 2009; Schlissel, 2007). Cells that successfully undergo IgL rearrangements (*Igκ or Igλ*) and pass tolerance checkpoints exit the bone marrow to complete maturation in the spleen (Luning Prak et al., 2011).

The assembly of αβ T cell receptor genes is similarly coordinated with programmed differentiation in the thymus (Rothenberg, 2014). The *TCRβ* locus is ~700 kb and is comprised of two regions: the 5' end, consisting of 30 *Vβ* gene segments, and the 3' end, consisting of two *DβJβ* clusters and an additional V*β14* gene segment at the extreme 3' end of the locus (Schatz and Ji, 2011) (Figure 1.1). RAG initiates V(D)J recombination in CD4/CD8 double negative (DN) thymocytes by generating *Dβ-to-Jβ* recombination events on both *TCRβ* alleles. The DN stage is subdivided into four developmental stages based on cell surface expression of c-Kit and CD25. *Dβ-to-Jβ* recombination is initiated in DN1 (c-Kit$^+$, CD25$^-$) and DN2 (c-Kit$^+$, CD25$^+$) cells. *Dβ-to-Jβ* rearrangements on both alleles are completed by the DN3 (c-Kit$^-$, CD25$^+$) stage, where *Vβ-to-DβJβ* recombination occurs, one allele at a time (Krangel, 2009). Here, tissue-specific cis-elements in the *TCRβ* locus promote large-scale looping that brings distal *Vβ* gene segments in proximity to *DJβ* clusters, facilitating *Vβ-to-DJβ* rearrangements in DN cells (Chaumeil and Skok, 2012; Majumder et al., 2015; Shih and Krangel, 2013). In-frame *VβDβJβ* joins are expressed as proteins that pair with pre-Tα to form the pre-TCR signaling complex. Developmental state-specific changes in *Vβ* chromatin and *Vβ/DJβ* looping likely cooperate to silence transcription and recombination of *Vβ* segments in pre-T cells. Signals downstream of the pre-TCR inhibit further *Vβ* rearrangements on either allele, drive Cyclin D3-mediated proliferation, and promote differentiation through the DN4 (c-Kit$^-$, CD25$^-$) to the CD4/CD8 double-positive (DP) stage, wherein *Vα-to-Jα* recombination at the *TCRα* locus is initiated (Krangel, 2009; Sicinska et al., 2003; von

Boehmer and Melchers, 2010). The *TCR*$\alpha$ locus spans ~2 Mb and is comprised of two regions: the 5' end, consisting of 100 interspersed *V*$\alpha/\delta$ gene segments, and the 3' end, consisting a *D*$\delta$/*J*$\delta$ array upstream of ~60 *J*$\alpha$ gene segments (Figure 1.1). *TCR*$\alpha$ genes assemble through *V*$\alpha$*-to-J*$\alpha$ rearrangements on both alleles (Chen et al., 2001; Krangel, 2009). Functional *TCR*$\alpha$ *gene* rearrangements lead to expression of *TCR*$\alpha$ chains that can pair with *TCR*$\beta$ chains. Cell surface-expressed $\alpha\beta$ TCRs in CD4/CD8 DP cells are then selected based on interactions with self-peptide:MHC complexes, which drive differentiation into either CD4 or CD8 single positive (SP) thymocytes or allow for additional *V*$\alpha$*-to-J*$\alpha$ rearrangements to potentially rescue self-peptide responsive cells from negative selection (Krangel, 2009). Positively selected SP cells then exit the thymus to enter the naïve peripheral T cell pool (von Boehmer and Melchers, 2010).

**Regulation of V(D)J Recombination by RAG Expression, RAG Binding, AgR Locus Accessibility**

RAG DSBs are essential for AgR assembly yet pose risks to developing lymphocytes in the form of genomic instability and apoptosis (Helmink and Sleckman, 2012). Accordingly, V(D)J is regulated by several cell-type and stage-specific mechanisms that both maximize AgR diversity and minimize immune deficiency and oncogenic lesions in the host. First, V(D)J recombination is restricted to G1-phase of the cell cycle. The RAG1 protein is expressed throughout the cell cycle. However, phosphorylation of RAG2 by CyclinA/Ckd2 at threonine 490, results in proteosomal degradation of RAG2 at the G1/S transition by the Skp2-SCF ubiquitin ligase complex (Li et al., 1996; Lin and Desiderio, 1993; Lin and Desiderio, 1994). Loss of this regulation promotes aberrant recombination and results in chromosomal translocations involving AgR genes (Zhang et al., 2011). Thus, the cell cycle-restriction of RAG expression limits

V(D)J recombination, likely preventing cells with unrepaired RAG DSBs from propagating through the cell cycle.

Second, RAG expression is restricted to two discrete phases of lymphocyte development. Initial Rag expression in pre-pro B cells and DN2 thymocytes results in *IgH/TCR*$\beta$ gene assembly, respectively (Kuo and Schlissel, 2009). Signaling downstream of the pre-BCR/TCR results in transcriptional down-regulation of *RAG* in pro B/T cells (Amin and Schlissel, 2008; Kuo and Schlissel, 2009) coincident with a period of cellular proliferation and differentiation. Subsequent RAG re-expression in pre-B/T cells is permanently silenced in mature, self-tolerant cells by tonic PI3K/Akt signaling downstream of a functional BCR and by Akt, LAT, and SLP-76 signaling downstream of a functional TCR. The absence of this regulation, as in constitutive expression of RAG throughout development, causes severe B cell and T cell lymphopenia, immune deficiency, and potential increases in genomic stress due to accumulated unrepaired RAG DSBs (Wayne et al., 1994). Thus, developmental-stage restriction of RAG expression is critical.

The modulation of RAG expression throughout lymphocyte development is regulated by a network of transcription factors, enhancers, and other cis-regulatory elements within the *RAG* locus that function in a cell-type specific manner (Amin and Schlissel, 2008; Hsu et al., 2003). The *RAG* locus contains both *RAG1* and *RAG2* genes, which are separated by 8 kb and lie in reverse transcriptional orientation. Cell stage-appropriate expression of *RAG* is driven by the *Rag1* promoter, which is active in both lymphoid and non-lymphoid cell types, and the lymphocyte-specific *Rag2* promoter (Lauring and Schlissel, 1999). While both promoters share common transcription factor binding elements, the variable expression of these factors (Bain et al., 1994; Degner et al., 2009; Kuo and Schlissel, 2009; Reynaud et al., 2008; Verkoczy et al., 2005; Zhang et al., 2006a) result in cell-type specific RAG regulation. *RAG* expression is further

regulated in cis by the *Erag* enhancer, which lies ~20 kb upstream of the *Rag2* promoter and blocks early B but not T cell development (Hsu et al., 2003), as well as a silencer element found between the *Rag1* and *Rag2* genes that antagonizes an anti-silencer element ~70 Kb upstream of the *Rag2* gene. Deletion of the anti-silencer causes decreased *RAG* expression in DP T cells but not B cells (Yannoutsos et al., 2004). Thus cis-regulatory elements within in the RAG locus contribute the regulation of V(DJ) recombination via RAG expression.

Finally, the long-standing V(D)J accessibility model links V(D)J recombination to an open chromatin environment that is both permissive to RAG binding and subsequent cleavage (Yancopoulos and Alt, 1985). Active AgR loci exhibit increased germline transcripts, RNAPII binding, histone H3K4me3 and H3K9Ac (Schatz and Ji, 2011), and DNA hypomethylation (Jung et al., 2006; Krangel, 2007). Recombining AgR loci also exhibit shifts in nucleosome density and positioning that promote dissociation of RSSs from chromatin (Cobb et al., 2006; Oltz and Osipovich, 2007; Osipovich et al., 2007; Schatz and Ji, 2011) and activation of locus-specific cis-elements that enable RAG binding at *D/J* gene segments and render *D/J* RSSs accessible for RAG cleavage (Ji et al., 2010a; Kondilis-Mangum et al., 2011; Oltz and Osipovich, 2007). Additional transcription factors like c-Fos and Runx1 in T cells (Cieslak et al., 2014; Wang et al., 2008) promote RAG binding at *Dβ* and *Dδ* gene segments, respectively (Cieslak et al., 2014; Wang et al., 2008; Zhang et al., 2006b). Recombination is also driven by large-scale contractions at AgR loci that facilitate recombination of distal AgR gene segments, mediate ordered recombination, and promote diverse AgR gene usage (Chaumeil and Skok, 2012; Ebert et al., 2011; Guo et al., 2011; Jhunjhunwala et al., 2009; Shih and Krangel, 2013; Xiang et al., 2013). Collectively, these observations support a model in which RAG recruitment over transcriptionally active D and J gene segments initiate *D-to-J* rearrangements and promote looping of distal *V* gene segments for *V-to-DJ*

recombination within a focal recombination center (Schatz and Ji, 2011). Thus, the regulation of V(D)J recombination is intimately linked with RAG accessibility to AgR genes.

**Structure and Biochemical Activities of the RAG Proteins**

Until recently, studies investigating the role of the RAG endonuclease complex used truncated “core” RAG enzymes due to insolubility of the full-length recombinant proteins (Sadofsky, 2004; Sadofsky et al., 1993). The RAG1 core protein, which lacks 40% of full-length RAG1, is the minimal portion capable of catalyzing V(D)J recombination with the RAG2 core protein, which lacks 25% of full-length RAG2, in vitro (Sadofsky, 2004) (Figure 1.2). The carboxy-terminal non-core RAG2 region contains a PHD domain that binds tri-methylated histone H3 proteins along transcribing genes to increase V(D)J recombination (Liu et al., 2007; Matthews et al., 2007) and a motif that restricts RAG2 expression and therefore RAG cleavage to G1 phase cells (Li et al., 1996) (Figure 1.2). The amino-terminal non-core regions of RAG1 include a Really Interesting New Gene (RING) domain with E3 ubiquitin ligase activity and sequences that interact with the VprBP kinase, the Roc1/Cul4A/DDB1 ubiquitin ligase complex, histones H3 and variant H3.3, the MDC1 and Ku70/Ku80 DNA damage response proteins, and the Gmeb1 transcription factor (Coster et al., 2012; Grazini et al., 2010; Jones et al., 2011; Kassmeier et al., 2012; Kim et al., 2013; Maitra and Sadofsky, 2009; Raval et al., 2008) (Figure 1.2). The discoveries of these biochemical activities have led to hypotheses linking the non-core regions of RAG1 to the modulation of antigen receptor gene assembly through ubiquitylating proteins to promote Ig/TCR locus accessibility and through transducing signals following RAG DNA breaks (Dudley et al., 2003; Grazini et al., 2010; Horowitz and Bassing, 2014; Jones et al., 2011; Sadofsky, 2004; Simkus et al., 2007). Yet, specific evidence for roles of non-core RAG1 regions in

regulating these or other aspects of antigen receptor gene assembly within the context of developing lymphocytes *in vivo* remain poorly understood.

**Roles for Non-Core RAG1 Regions *In Vivo***

Although dispensable for V(D)J recombination, non-core RAG regions are essential for normal lymphocyte development. Human *RAG* mutations that completely block V(D)J recombination cause B cell$^{-}$, T cell$^{-}$, Natural Killer (NK) cell$^{+}$ severe combined immunodeficiency (SCID) associated with a complete lack of circulating B or T cells (Lee et al., 2014). Hypomorphic RAG mutations that disrupt the biochemical activities of non-core RAG1 regions but preserve recombination activity cause a variety of atypical SCID-like conditions, including combined immunodeficiency (CID) with granuloma and/or autoimmunity, late-onset SCID, and Omenn Syndrome (OS), an immune deficiency associated with lack of circulating B cells, oligoclonal TCR repertoire, autoimmunity, T cell infiltration of the skin and gut, high serum IgE levels, and erythroderma (Aleman et al., 2001; Santagata et al., 2000; Wong and Roth, 2007). However, how mutations in non-core RAG regions that preserve V(D)J recombination activity but cause autoimmunity and altered AgR repertoire remain poorly understood. Untreated OS is typically fatal (Aleman et al., 2001), and current therapies are limited to hematopoietic stem cell transplantation from healthy donors (Caglayan Sozmen et al., 2015). Further, the late onset and immune and autoimmune phenotypes observed in these atypical-SCID and OS patients may complicate treatment (Jspeert et al., 2014). Thus, defining how RAG mutations that preserve recombination activity but compromise lymphocyte development may generate novel and/or targeted therapeutics for SCID and OS patients.

While dispensable *in vitro*, the non-core regions of Rag1 promote efficient V(D)J recombination *in vivo.* Mice expressing “core” but not full-length Rag1 (Rag1$^{C/C}$ mice)

exhibit a partial block in early lymphocyte development and reduced numbers of mature B and T lymphocytes that are associated with reduced *D-J* and *V-to-DJ* at $Ig_H$ and *TCRβ* loci (Dudley et al., 2003). Specifically, Rag1$^{C/C}$ mice exhibit reduced Dβ-Jβ and Vβ-DβJβ recombination in non-selected DN3 thymocytes, a partial block at the DN-to-DP transition, and a 50% reduction in mature splenic T cell numbers as well as reduced $D_H$-$J_H$ and $V_H$-$D_HJ_H$ recombination in pre-B cells, a partial block at the pro-B-to-pre-B cell transition, and a 50% reduction in mature splenic B cell numbers (Dudley et al., 2003). These phenotypes implicate non-core Rag1 regions in promoting efficient V(D)J recombination. Yet, the specific roles of non-core Rag1 domains in the context of V(D)J recombination or lymphocyte differentiation *in vivo* are unknown. For instance, because *D-to-J* recombination is required for *V-to-DJ* recombination to occur, and as RAG binding over *D* and *J* segments is proposed to promote *V-to-DJ* recombination, Rag1$^{C/C}$ mouse phenotypes may be due to defects in *D-to-J*, *V-to-DJ*, or both steps. Data shown in Chapter 2 of this thesis shows that expression of a pre-assembled endogenous *VβDβJβ* allele, but not a *DβJβ* allele, rescues αβ T cell development in Rag1$^{C/C}$ mice, indicating non-core Rag1 regions primarily function during V(D)J recombination to promote *Vβ-to-DJβ* recombination. Data in Chapter 2 also demonstrates that Rag1$^{C/C}$ αβ T cells express a *Vβ* repertoire that is skewed during both primary and secondary *Vβ-to-DβJβ* recombination and that Rag1$^{C/C}$ thymocytes undergo altered αβ TCR selection, implicating non-core Rag1 regions in promoting a diverse *TCRβ* repertoire. Further experiments in Chapter 2 demonstrate that replacement of a single non-consensus *Vβ* RSS for an efficient with a consensus RSS nearly rescues αβ T cell development in Rag1$^{C/C}$ mice, implicating non-core Rag1 in establishing *Vβ* diversity through overcoming inherent *Vβ* RSS inefficiencies. Together, the data presented in Chapter 2 demonstrate

novel roles for non-core Rag1 regions in primary V(D)J rearrangements and αβ TCR selection to promote the generation of a diverse naïve αβ TCR repertoire *in vivo.*

In addition to promoting V(D)J recombination, the non-core regions of RAG1 have been proposed to be important for AgR gene segment accessibility, V(D)J efficiency, RAG DSB repair, and/or signaling following RAG DSBs. Yet, the specific roles of these domains in the context of V(D)J recombination or lymphocyte differentiation *in vivo* are unknown. Data presented in Chapter 3 of this thesis shows that $Rag1^{C/C}$ mice have decreased accessibility of *Jλ1* gene segments and that the Rag1 protein promotes accessibility of both *Jκ* and *Jλ* gene segments, implicating Rag1 in promoting AgR locus accessibility independent of Rag cleavage activity. Further, RAG DSBs in pre-B cells induce hundreds of transcriptional changes in genes encoding proteins associated with cell survival, lymphocyte differentiation, and AgR selection. These include the NF-κB-dependent pro-survival factor *Pim2*, which promotes $Igλ^+$ B cell development. Data shown in Chapter 4 of this thesis shows that $Rag1^{C/C}$ mice exhibit impaired late B cell development with profound defects in $Igλ^+$ B cell development that is associated with reduced *Vλ-to-Jλ* recombination. Additional experiments show that $Rag1^{C/C}$ pre-B cells do not upregulate *Pim2* during RAG DSBs and that expression of pro-survival BCL2 protein rescues $Igλ^+$ cell development in $Rag1^{C/C}$ mice, indicating that non-core Rag1 regions promote survival signals in response to RAG DSBs in pre-B cells that promote the development of $Igλ^+$ cells. Collectively, the data presented in this thesis demonstrates novel, non-cleavage functions for the RAG endonuclease in establishing a normal immune repertoire and also implicates RAG1 as a chromatin-modifying factor that promotes accessibility of AgR genes prior to recombination and as a signal transduction molecule that promotes the survival and differentiation of developing lymphocytes.

**Figure 1.1**

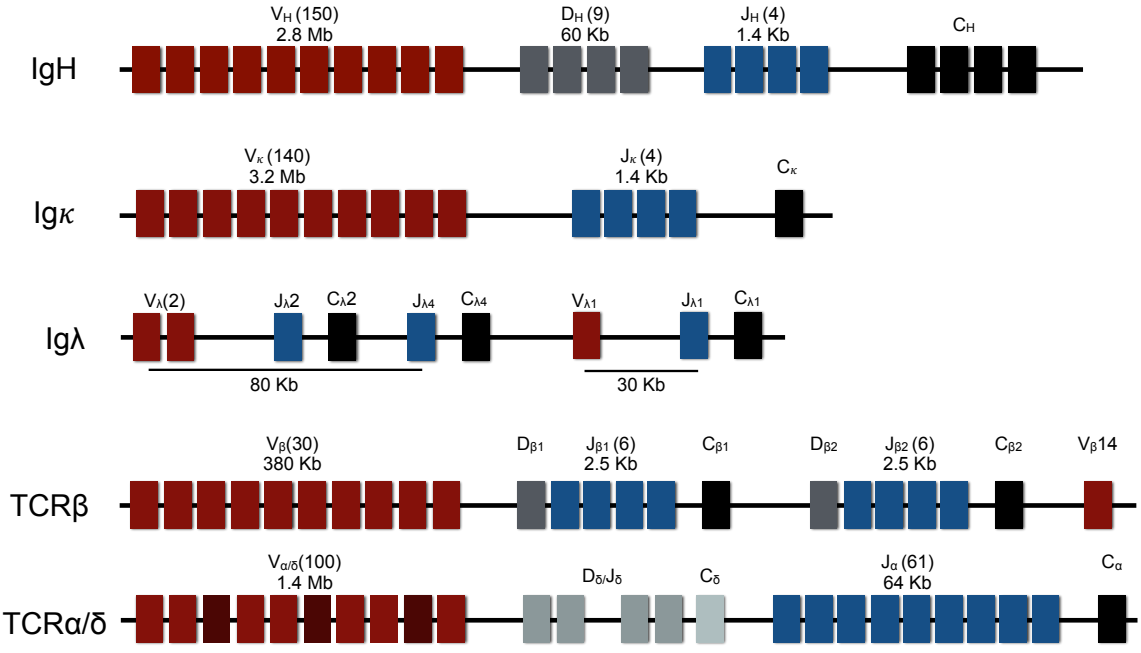


**Figure 1.1 The structure of AgR receptor loci**. Schematics indicating mouse AgR receptor loci, with variable (V) gene segments shown in red, diversity (D) gene segments are shown in grey, joining (J) gene segments are shown in blue, with constant (C) genes shown in black. Approximate locus sizes are indicated and numbers of gene segments per locus are indicated in parentheses, where relevant.

**Figure 1.2**

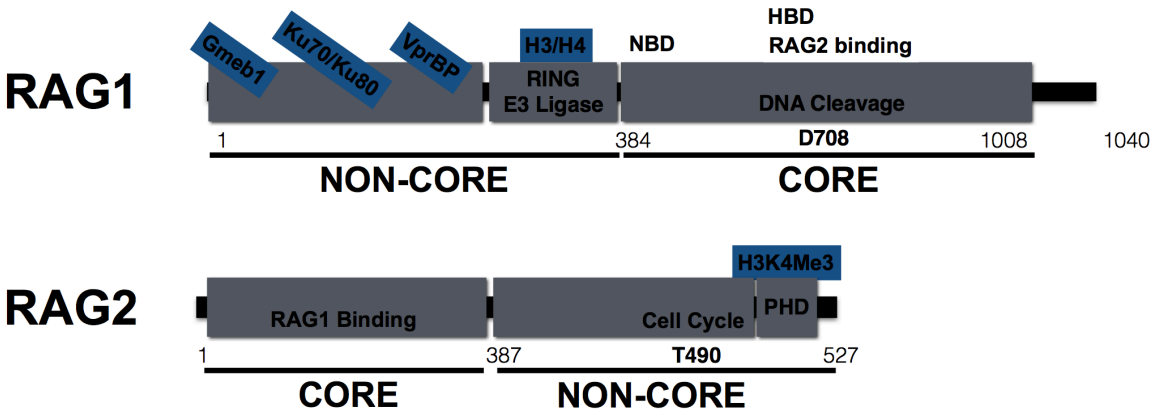


**Figure 1.2 The RAG proteins.** Schematics of RAG1 and RAG2 protein domains. Indicated "core" regions are critical for V(D)J recombination, while "non-core" regions are dispensable for this reaction *in vitro*. The core-RAG1 domain possesses DNA cleavage activity, catalyzed at the indicated D708A residue, a RSS nonamer-binding domain (NBD), a RSS heptamer-binding domain (HBD), and sequences that bind the V(D)J co-factor RAG2. The non-core regions of RAG1 include a RING domain with E3 ligase activity that can ubiquitylate histones H3 and H4 as well as sequences that bind the VprBP component of the VprBP/Roc1/Cul4/DDB E3 ligase complex, DNA damage response proteins Ku70/Ku80, and the transcription factor Gmeb1. The core RAG2 protein interacts with RAG1, and the non-core regions of RAG2 include a PHD domain, which binds H3K4me3, and the indicated T490 residue, which regulates cell-cycle dependent degradation of RAG2.

## CHAPTER 2

## Noncore RAG1 Regions Promote Vβ Rearrangements and αβ T Cell Development by Overcoming Inherent Inefficiency of Vβ Recombination Signal Sequences[1]


### Abstract

The RAG proteins are comprised of core endonuclease domains and non-core regions that modulate endonuclease activity. Mutation or deletion of non-core RAG regions in humans causes immunodeficiency and altered TCR repertoire, and mice expressing core but not full-length Rag1 (Rag1$^{C/C}$) or Rag2 (Rag2$^{C/C}$) exhibit lymphopenia, reflecting impaired V(D)J recombination and lymphocyte development. Rag1$^{C/C}$ mice display reduced *D-to-J* and *V-to-DJ* rearrangements of *TCRβ* and *IgH loci*, while Rag2 $^{C/C}$ mice show decreased *V-to-DJ* rearrangements and altered *Vβ/V$_H$* repertoire. Since *Vβs/V$_H$s* only recombine to *DJ* complexes, the Rag1$^{C/C}$ phenotype could reflect roles for non-core RAG1 regions in promoting recombination during only the *D-to-J* step or during both steps. Here, we demonstrate that a pre-assembled *TCRβ* gene, but not a pre-assembled *DβJβ* complex or the pro-survival BCL2 protein, completely rescues *αβ* T cell development in Rag1$^{C/C}$ mice. We find that Rag1$^{C/C}$ mice exhibit altered *Vβ* utilization in *Vβ-to-DJβ* rearrangements, increased usage of 3'*Jα* gene segments in *Vα-to-Jα* rearrangements, and abnormal changes in Vβ repertoire during αβ TCR selection. Inefficient *Vβ/V$_H$* recombination signal sequences (RSSs) have been hypothesized to cause impaired *V-to-DJ* recombination on the background of a defective recombinase as in core-Rag mice. We show that replacement of the *Vβ14* RSS with a


[1] Originally published in *The Journal of Immunology*. Horowitz, J.E., and Bassing, C.H. 2014. Noncore RAG1 regions promote Vβ rearrangements and αβ T cell development by overcoming inherent inefficiency of Vβ recombination signal sequences. *J. Immunol*. Vol: 192, 4, pp1609-1619. 

more efficient RSS increases *Vβ14* recombination and rescues αβ T cell development in Rag1$^{c/c}$ mice. Our data indicate that non-core RAG1 regions establish a diverse TCR repertoire by overcoming *Vβ* RSS inefficiency to promote *Vβ* recombination and αβ T cell development, and by modulating TCRβ and TCRα gene segment utilization.

## Introduction

The lymphocyte-specific RAG1/RAG2 (Fugmann et al., 2000) endonuclease generates Ag receptor diversity by recombining germline variable (V), diversity (D), and joining (J) gene segments of T cell receptor (TCR) and immunoglobulin (Ig) loci. RAG cleavage between two participating gene segments and their adjacent RSSs yields DNA double strand breaks (DSBs) comprised of hairpin-sealed coding ends and blunt signal ends (Fugmann et al., 2000; Schatz and Ji, 2011). RAG proteins along with DNA damage response/repair proteins hold these DNA ends in a stable post-cleavage complex and facilitate their repair by non-homologous end-joining (NHEJ) factors (Helmink and Sleckman; Lieber). The combination of possible V(D)J joining events and the imprecise manner by which coding ends are processed cooperate to generate Ag receptor diversity.

The RAG1 and RAG2 proteins are each comprised of core endonuclease domains, defined as the minimal sequences required for DNA cleavage *in vitro*, and non-core regions that modulate this activity (Sadofsky, 2004; Schatz and Swanson, 2011). *RAG1* or *RAG2* mutations that alter or delete non-core RAG1 or RAG2 region amino acids and reduce overall V(D)J recombinase activity cause Omenn Syndrome (OS) or other fatal severe combined immunodeficiencies associated with oligoclonal TCR repertoire and increased T cell mediated autoimmunity (Notarangelo, 2010; Villa et al., 2008; Villa et al., 2001; Wong and Roth, 2007). However, the contribution of diminished recombinase activity to aberrant TCR repertoire and autoreactive T cells in OS patients remains undetermined (Wong and Roth, 2007). $Rag1^{C/C}$ and $Rag2^{C/C}$ mice each display reduced numbers of mature T and B cells, reflecting impaired lymphocyte development beyond the progenitor stages associated with reduced *TCR*$\beta$ and *IgH* recombination (Akamatsu et al., 2003; Dudley et al., 2003; Liang et al., 2002). While $Rag1^{C/C}$ mice

display reduced levels of both *D-to-J* and *V-to-DJ* recombination of *TCRβ* and *IgH* loci (Dudley et al., 2003), Rag2$^{C/C}$ mice show predominantly decreased *V-to-DJ* rearrangements associated with altered *Vβ/V$_H$* usage (Akamatsu et al., 2003; Liang et al., 2002). Although no reductions in the levels of *V-to-J* recombination of *Igκ* or *TCRα* loci were discovered in either Rag1$^{C/C}$ or Rag2$^{C/C}$ mice, potential changes in the utilization of individual *Igκ* or *TCRα* gene segments have not been assayed (Akamatsu et al., 2003; Liang et al., 2002). Considering that *Vβs* and *V$_H$s* only recombine to *DJ* complexes, the Rag1$^{C/C}$ phenotype could reflect roles for non-core RAG1 regions in promoting recombination during only the *D-to-J* step or during both the *D-to-J* and *V-to-DJ* steps (Dudley et al., 2003). Since *Vβ* and *V$_H$* rearrangements are selectively impaired in Rag2$^{C/C}$ mice, it has been hypothesized that the Rag2$^{C/C}$ mouse phenotype is due to the interaction of a defective recombinase with unique features of *Vβ/V$_H$* RSSs (Liang et al., 2002). In support of this notion, *Vβ/V$_H$* RSSs that more closely resemble those of *Dβ* and *Vλ/Vα/Vγ/Vδ* segments are more efficiently cleaved by core-RAG proteins *in vitro* and their associated *Vβ/V$_H$* segments are recombined and expressed at higher frequencies in Rag2$^{C/C}$ mice relative to normal mice (Liang et al., 2002). Yet, neither this decade-old model nor its prediction that Rag1$^{C/C}$ mice also would exhibit altered *Vβ* and *V$_H$* utilization has been tested.

In humans and mice, αβ T cells develop in the thymus through a differentiation program that involves the ordered assembly, expression, and selection of TCR genes. TCRβ genes assemble through *Dβ-to-J*β and then *Vβ-to-DβJβ* rearrangements in CD4$^-$ CD8$^-$ "double-negative" (DN) thymocytes (Krangel, 2009). The *Dβ-to-Jβ* recombination step initiates in c-Kit$^+$CD25$^-$ DN1 cells and continues in c-Kit$^+$CD25$^+$ DN2 cells, while *Vβ-to-DβJβ* recombination occurs in c-Kit$^-$CD25$^+$ DN3 cells (Krangel, 2009). Since *TCRβ* loci

contain 31 *Vβ* segments (*Trbv1* through *Trbv31*) and two Dβ-Jβ-Cβ clusters (*Trbd1-Trbj1-Trbc1* and *Trbd2-Trbj2-Trbc2*) each with one *Dβ* and six functional *Jβ* segments, secondary *Vβ* rearrangements can occur to *Dβ2Jβ2* (*Trbd2Trbj2*) complexes on alleles with primary *Vβ* rearrangements to assembled *Dβ1Jβ1 (Trbd1Trbj1*) complexes (Brady et al., 2010). Utilization of individual *Vβ* segments in primary *Vβ-to-Dβ1Jβ1* rearrangements is biased independent of *Vβ* position (Wilson et al., 2001). However, *Vβ* position relative to a pre-assembled *VβDβJβ1Cβ1* gene can influence the usage of *Vβ* segments in secondary *Vβ-to-Dβ2Jβ2* rearrangements (Brady et al., 2010; Steinel et al., 2010). Assembly and expression of a functional *TCRβ* gene generates *TCRβ* chains that pair with pre-Tα proteins to form pre-TCRs, which promote survival and differentiation, down-regulate RAG expression, and induce expression of the Cyclin D3 (Ccnd3) protein (Sicinska et al., 2003; von Boehmer and Melchers, 2010). Ccnd3 drives proliferation as DN3 cells down-regulate RAG expression and differentiate into c-Kit$^-$CD25$^-$ DN4 and then CD4$^+$CD8$^+$ "double-positive" (DP) thymocytes. *TCRα* genes assemble through *Vα-to-Jα* rearrangements on both alleles in DP cells, where *Vβ-to-DβJβ* recombination is silenced (Sicinska et al., 2003; von Boehmer and Melchers, 2010). The assembly and expression of a functional *VαJαCα* gene generates TCRα chains that can pair with TCRβ chains to generate ab TCRs, which are selected based on interactions with thymic epithelial cells (Chen et al., 2001; Krangel, 2009). Positive selection increases expression of αβ TCRs and promotes differentiation of DP thymocytes into CD4$^+$CD8$^-$ or CD4$^-$CD8$^+$ "single-positive" thymocytes that emigrate from the thymus as mature naive *αβ* T cells (von Boehmer and Melchers, 2010). Since *TCRα* loci contain ~100 *Vα* and ~50 *Jα* segments, successive *Vα-to-Jα* rearrangements can occur until positive selection or until all Vα or Jα segments have been utilized (von Boehmer and Melchers,

2010). Although pre-TCR selection and thymocyte expansion does not significantly change *Vβ* repertoire during DN-to-DP thymocyte differentiation (Krangel, 2009), positive selection can substantially alter Vβ representation in *ab* TCRs during DP-to-SP thymocyte development (Wilson et al., 2001).

The mouse *αβ* T cell differentiation program provides a useful experimental model to elucidate roles for non-core RAG1 regions in promoting V(D)J recombination and controlling *TCR* gene repertoire. Rag1$^{C/C}$ mice exhibit reduced *Dβ-Jβ* and *Vβ-DβJβ* recombination in DN3 thymocytes and impaired DN3-to-DP thymocyte development from accumulation of cells at the DN3 stage (Blackman et al., 1989; Carpenter et al., 2009; Kappler et al., 1987; Kappler et al., 1988; MacDonald et al., 1988; Wade et al., 1988; Wu et al., 2003). These phenotypes may arise from impaired *Dβ-to-Jβ* and/or *Vβ-to-DβJβ* recombination in the absence of non-core RAG1 regions. Yet, considering that RAG DSBs induce changes in the expression of proteins involved in cellular survival, lymphocyte differentiation, and Ag gene receptor selection (Dudley et al., 2003), these phenotypes also may arise from impaired signaling in response to RAG DSBs induced in Rag1$^{C/C}$ DN3 thymocytes. To determine how non-core RAG1 regions promote *TCRβ* gene assembly and αβ T cell development, we have created and analyzed Rag1$^{C/C}$ mice containing a pre-assembled DβJβ complex or pre-assembled functional *TCRβ* gene, expressing the pro-survival EμBCL2 transgene, or with the 3'*Dβ*1 RSS in place of the *Vβ14* RSS. We demonstrate that this *TCRβ* gene, but not the *DβJβ* complex or BCL2, completely rescues DN3-to-DP thymocyte development in Rag1$^{C/C}$ mice, indicating that the predominant function of non-core RAG1 regions in differentiating αβ T cells is to promote Vβ recombination. We show that Rag1$^{C/C}$ mice exhibit altered *Vβ* utilization in *Vβ-to-DJβ* rearrangements and that neither apoptosis of

cells attempting *Vβ* recombination nor *TCRβ*-dependent expansion of DN3 thymocytes contributes to this abnormal *Vβ* repertoire. We detect increased usage of 3'*Jα* segments in *Vα-to-Jα* rearrangements and abnormal selection of the *Vβ* repertoire in Rag1$^{C/C}$ mice, revealing that non-core RAG1 regions also function during *TCRα* recombination in DP thymocytes. Finally, we show that the 3'*Dβ1* RSS increases Vβ14 recombination and partially rescues αβ T cell development in Rag1$^{C/C}$ mice. Collectively, our data indicate that non-core RAG1 regions establish a diverse αβ TCR repertoire by overcoming *Vβ* RSS inefficiency to promote *Vβ* recombination and αβ T cell development and by modulating *TCRβ* and *TCRα* gene segment utilization.

## Materials and Methods

### Mice

Rag1$^{C/C}$ (Bredemeyer et al., 2008), EμBCL2 (Dudley et al., 2003), Jβ1$^{DJ/DJ}$ (Strasser et al., 1991), Vβ1$^{NT/NT}$ (Carpenter et al., 2009), and Ccnd3$^{-/-}$ (Brady et al.) mice were obtained and utilized to generate the mice described in this study. The germline Vβ14$^{3'Db1RSS}$ mice were generated by Cre-loxP-mediated gene-targeting using W4 mouse embryonic stem cells and the construct previously employed to make chimeric Vβ14$^{3'Db1RSS}$ mice (Sicinska et al., 2003). All experimental mice were on a mixed 129SvEv and C57BL/6 background and were littermate or age-matched mice between 4-6 weeks of age. All experiments were conducted in accordance with national guidelines and approved by the Institutional Animal Care and Use Committee of the Children's Hospital of Philadelphia.

### Flow Cytometry

Single cell suspensions were stained with antibodies in PBS containing 2% BSA. All antibodies were purchased from BD Pharmingen. CD4 and CD8 analysis was performed using anti-CD4 (553653), anti-CD8 (553031), and anti-TCRβ (553174) antibodies. DN stage analysis was performed on lineage-negative cells stained with a mixture of PE-conjugated anti-CD4 (553653), anti-CD8α (553033), anti-TCRβ (553172), anti-TCRγ (553178), anti-B220 (553090), anti-CD19 (553786), anti-CD11b (553311), anti-CD11c (557401), anti-NK1.1 (553165), and anti-Ter119 (553673) antibodies in addition to anti-CD25 (552880) and anti-CD117 (553356) antibodies. Vβ analysis was performed using antibodies against TCRβ (553174) as well as Vβ5 (553189), Vβ6 (553192), Vβ8 (553861), Vβ10 (553285), Vβ14 (553258), and Streptavidin-FITC (554060). Data was

acquired on a FACSCalibur (BD Biosciences, San Jose, CA) using CellQuest software (BD Biosciences) and analyzed using FlowJo software (Tree Star).

**PCR**

Genomic DNA from sorted DP thymocytes (on 100 ng and 1:5 serial dilutions) was subjected to long-range PCR with the use of primers and PCR conditions as described (Wu et al., 2003)

## Results

### Transgenic BCL2 expression partially rescues early αβ T cell development in Rag1$^{C/C}$ mice.

To determine whether impaired cellular survival in response to RAG DSBs causes impaired DN3-to-DP thymocyte development in Rag1$^{C/C}$ mice, we created and analyzed Rag1$^{C/C}$ mice containing the EμBCL2 transgene (EμBCL2:Rag1$^{C/C}$ mice) since expression of the anti-apoptotic BCL2 protein increases survival of DN3 cells attempting TCRβ rearrangements (Guo et al., 2002; Riegert and Gilfillan, 1999). Consistent with the pro-survival effect of BCL2, we detected ~3-fold increases in the numbers DN and DP thymocytes in EμBCL2:Rag1$^{C/C}$ mice compared to Rag1$^{C/C}$ mice, although the difference in DN thymocyte numbers did not reach statistical significance (Figure 2.1 *A and B*). Similarly, we found equivalent numbers of DN3 and DN4 thymocytes in EμBCL2:Rag1$^{C/C}$ and Rag1$^{C/C}$ mice (Figure 2.1 *C* and *D*). We also detected ~4.5-fold decreased numbers of total and DP thymocytes in EμBCL2:Rag1$^{C/C}$ mice relative to EμBCL2 mice (Figure 2.1 *A and B*), indicating that BCL2 expression does not completely rescue impaired DN-to-DP thymocyte development in Rag1$^{C/C}$ mice. These observations indicate that BCL2 expression does not substantially enhance the survival of Rag1$^{C/C}$ DN3 thymocytes, yet has a more pronounced effect on promoting survival of DP thymocytes or cells during DN-to-DP thymocyte expansion and differentiation in Rag1$^{C/C}$ mice. Therefore, we conclude that reduced survival of DN3 thymocytes in response to RAG DSBs is not a major cause of impaired TCRβ gene assembly and DN-to-DP thymocyte development in Rag1$^{C/C}$ mice.

**A pre-assembled TCRβ gene completely rescues early αβ T cell development in Rag1$^{C/C}$ mice.**

To determine potential functions of non-core Rag1 regions in promoting Dβ-to-Jβ recombination and Vβ-to-DJβ recombination, we generated and analyzed Rag1$^{C/C}$ mice that contain a pre-assembled DβJβ complex (Jβ1$^{DJ}$) or pre-assembled functional TCRβ gene (Vβ1$^{NT}$) on both TCRβ alleles. The Jβ1$^{DJ}$ allele contains a pre-assembled Dβ1Jβ1.1 (*Trbd1Trbj1.1)* complex, lacks Dβ2 (*Trbd2*) and Jβ2 (*Trbj2*) segments, and must recombine one of 35 Vβ segments to the Dβ1Jβ1.1 complex to promote αβ T lymphocyte development (Brady et al., 2013) The Vβ1$^{NT}$ allele contains a pre-assembled functional endogenous Vβ1Dβ1Jβ1.4Cβ1 (*Trbv5Trbd1Trbj1.4Trbc1*) gene that promotes αβ T cell development independent of TCRβ recombination We detected ~2-fold more DP thymocytes in Rag1$^{C/C}$Jβ1$^{DJ/DJ}$ mice relative to Rag1$^{C/C}$ mice (Figure 2.2 *A* and *B*). However, the DP cell numbers in Rag1$^{C/C}$Jβ1$^{DJ/DJ}$ mice and Rag1$^{C/C}$ mice were 2-fold or more lower as compared to EμBCL2 and WT mice, respectively (Figure 2.2 *B* versus *Figure 2.*1 *B*). We also detected ~8-fold more DN4 cells in Rag1$^{C/C}$Jβ1$^{DJ/DJ}$ mice relative to Rag1$^{C/C}$ mice (Figure 2.2 *C* and *D*), with DN4 thymocyte numbers in Rag1$^{C/C}$Jβ1$^{DJ/DJ}$ mice and Rag1$^{C/C}$ mice significantly lower than in EμBCL2 and WT mice, respectively (*Figure 2.2 D* versus *Figure 2.1 E*). These data demonstrate that a pre-assembled DβJβ1 complex on both TCRβ alleles partially rescues DN3-to-DN4 and DN-to-DP thymocyte development in Rag1$^{C/C}$ mice. In Rag1$^{C/C}$Vβ1$^{NT/NT}$ mice relative to Rag1$^{C/C}$ mice, we observed greater numbers of DP (4-fold more) and DN4 (11-fold more) thymocytes (Figure 2.2 *E* - *H*). Notably, the numbers of DP and DN4 thymocytes in Rag1$^{C/C}$Vβ1$^{NT/NT}$ mice were similar to those in Vβ1$^{NT/NT}$ and WT mice (Figure 2.2 *E* - *H*), showing that a pre-assembled functional TCRβ gene completely rescues both DN3-to-

DN4 and DN-to-DP thymocyte development in Rag1$^{C/C}$ mice. Therefore, our data indicates that non-core RAG1 regions promote both Dβ-to-Jβ and Vβ-to-DJβ rearrangements and that reduced Vβ-to-DJβ recombination is the major cause of accumulation of cells at the DN3 stage and impaired DN-to-DP thymocyte development in Rag1$^{C/C}$ mice.

**Rag1$^{C/C}$ mice exhibit altered Vβ utilization in primary and secondary Vβ rearrangements.**

The TCRβ locus architecture permits primary Vβ rearrangements to Dβ1Jβ1 complexes and then secondary Vβ rearrangements to Dβ2Jβ2 complexes, which occur on the Vβ1$^{NT}$ allele (Carpenter et al., 2009). Our current analysis of thymocyte development in Rag1$^{C/C}$Jβ1$^{DJ/DJ}$ and Rag1$^{C/C}$Vβ1$^{NT/NT}$ mice and our previous analysis of Vβ8 (*Trbv13.1, Trbv13.2,* and *Trbv13.3*) and Vβ10 (*Trbv4*) rearrangements in DN3 cells of Rag1$^{C/C}$ mice (Brady et al., 2010) demonstrate that primary Vβ-to-DJβ rearrangements are impaired in the absence of non-core Rag1 regions. However, these analyses cannot address potential function of non-core Rag1 regions in secondary Vβ rearrangements nor quantify relative usage of individual Vβ segments in Vβ-to-DβJβ rearrangements. Since DN-to-DP thymocyte differentiation does not significantly alter Vβ repertoire (Dudley et al., 2003), the use of flow cytometry to monitor Vβ expression on TCRβ$^{intermediate}$ DP thymocytes provides a more sensitive means than PCR to quantify relative Vβ usage in Vβ rearrangements (Wilson et al., 2001). Thus, to determine the contributions of non-core Rag1 regions in Vβ utilization during primary Vβ-to-DβJβ rearrangements, we assayed Vβ5 (*Trbv12.1* and *Trbv12.2*), Vβ6 (*Trbv19*), Vβ8, Vb10, and Vβ14 (*Trbv31*) expression on DP thymocytes of Rag1$^{C/C}$Jβ1$^{DJ/DJ}$ and Jβ1$^{DJ/DJ}$ mice,

as only primary Vβ rearrangements occur on the Jb1$^{DJ}$ allele (Brady and Bassing, 2011; Brady et al., 2010; Wilson et al., 2001; Wu et al., 2003). We observed lower percentages of Vβ5$^{+}$ (5-fold less) and Vβ10$^{+}$ (~3-fold less) DP thymocytes in Rag1$^{C/C}$Jβ1$^{DJ/DJ}$ mice as compared to Jβ1$^{DJ/DJ}$ mice (Figure *A* and *B*). We detected increases in the percentages of Vβ8$^{+}$ (2-fold more) and Vβ14$^{+}$ (3-fold more) DP thymocytes, but no difference in the percentages of Vβ6$^{+}$ DP cells, in Rag1$^{C/C}$Jβ1$^{DJ/DJ}$ mice relative to Jβ1$^{DJ/DJ}$ mice (Figure 2.3 *A* and *B*). Since only secondary Vβ-to-DβJβ rearrangements involving Vβ10 occur on the Vβ1$^{NT}$ allele (Carpenter et al., 2009), we next quantified Vβ10 expression on DP thymocytes of Rag1$^{C/C}$Vβ1$^{NT/NT}$ and Vβ1$^{NT/NT}$ mice to evaluate whether non-core Rag1 regions promote such secondary Vβ rearrangements. We found a 7-fold lower percentage of Vβ10$^{+}$ DP thymocytes in Rag1$^{C/C}$Vβ1$^{NT/NT}$ mice as compared to Vβ1$^{NT/NT}$ mice (Figure 2.3 *C* and *D*). Collectively, these data indicate that non-core Rag1 regions affect Vβ utilization in primary and secondary Vβ rearrangements, at least on Jβ1$^{DJ}$ and Vβ1$^{NT}$ alleles.

To evaluate whether non-core Rag1 regions affect Vβ utilization in total Vβ rearrangements on normal TCRβ alleles, we quantified expression of Vβ5, Vβ6, Vβ8, Vβ10, and Vβ14 on DP thymocytes of Rag1$^{C/C}$ and WT mice. We detected lower percentages of Vβ5$^{+}$ (~6-fold less) and Vβ10$^{+}$ (~2-fold less) DP cells in *Rag1$^{C/C}$* mice relative to WT mice (Figure 2.3 *E* and *F*). We also detected ~2-fold increased percentage of Vβ8$^{+}$ and ~3-fold increased percentage of Vβ14$^{+}$ DP thymocytes, but no difference in the percentage of Vβ6$^{+}$ DP cells, in Rag1$^{C/C}$ mice as compared to WT mice (Figure 2.3 *E* and *F*). These data demonstrate that non-core Rag1 regions influence Vβ utilization in total Vβ rearrangements on normal TCRβ alleles.

While we did not observe a major role for impaired survival of Rag1$^{C/C}$ thymocytes in response to RAG DSBs during TCRβ recombination, altered survival of DN3 thymocytes during rearrangements of particular Vβ segments could influence Vβ repertoire in Rag1$^{C/C}$ mice. To investigate this possibility, we quantified the expression of Vβ5, Vβ6, Vβ8, Vβ10, and Vβ14 on DP thymocytes of EμBCL2:Rag1$^{C/C}$ and Rag1$^{C/C}$ mice. We detected no significant differences in the frequencies of Vβ6$^{+}$, Vβ5$^{+}$, Vβ10$^{+}$ or Vβ14$^{+}$ DP thymocytes between EμBCL2:Rag1$^{C/C}$ and Rag1$^{C/C}$ mice (Figure 2.3 *E* and *F*), however we did observe a slightly higher frequency of Vβ8$^{+}$ DP cells in EμBCL2:Rag1$^{C/C}$ mice as compared to Rag1$^{C/C}$ mice (Figure 2.3 *E* and *F*). These data suggest that impaired survival of DN3 cells in response to RAG DSBs does not cause the altered relative representation of Vβ5, Vβ6, Vβ8, Vβ10, and Vβ14 on DP thymocytes of Rag1$^{C/C}$ mice.

While Vβ representation is not significantly altered during DN-to-DP thymocyte differentiation in mice with normal levels of Vβ rearrangements (Brady et al., 2010), altered expansion of DN cells expressing particular Vβ segments could contribute to the altered Vb repertoire in DP thymocytes of Rag1$^{C/C}$ mice which have reduced numbers of thymocytes caused by impaired Vβ-to-DβJβ recombination. To assess this possibility, we generated and analyzed Rag1$^{C/C}$Ccnd3$^{-/-}$ mice since expression of TCRβ chains drive DN-to-DP thymocyte expansion through Ccnd3, and Ccnd3$^{-/-}$ mice exhibit normal Vb repertoire in DP thymocytes (Wilson et al., 2001). We found equivalent numbers of DN thymocytes, but ~10-fold lower numbers of DP cells, in Rag1$^{C/C}$Ccnd3$^{-/-}$ mice as compared to Ccnd3$^{-/-}$ mice (Figure 2.4 *A* and *B*), indicating that TCRβ-mediated DN-to-DP thymocyte development is profoundly impaired in Rag1$^{C/C}$Ccnd3$^{-/-}$ mice relative to Ccnd3$^{-/-}$ mice. Notably, the numbers of DP cells in Rag1$^{C/C}$Ccnd3$^{-/-}$ mice were reduced

~40-fold as compared to Rag1$^{C/C}$ mice versus ~17 fold for Ccnd3$^{-/-}$ mice relative to WT mice (Compare Figure 2.4 *B* and Figure 2.1 *B*). We also found a ~5-fold lower frequency of V$\beta$10$^{+}$ DP cells but a ~2-fold increase frequency of V$\beta$14$^{+}$ DP thymocytes in Rag1$^{C/C}$Ccnd3$^{-/-}$ mice as compared to Ccnd3$^{-/-}$ mice (Figure 2.4 *C* and *D*). Considering that we observed similar increased and deceased frequencies of V$\beta$10$^{+}$ and V$\beta$14$^{+}$ DP thymocytes, respectively, in Rag1$^{C/C}$ mice relative to WT mice (Figure 2.3 *E* and *F*), our data indicate that the altered representation of V$\beta$10 and V$\beta$14 on DP thymocytes of Rag1$^{C/C}$ mice is not caused by differences in TCR$\beta$-mediated proliferation of DN cells expressing particular V$\beta$ segments. Therefore, based on our quantification of V$\beta$ expression on DP thymocytes of mice expressing wild-type or core-Rag1 proteins in combination with other genetic modifications, we conclude that Rag1 non-core regions control V$\beta$ repertoire at the level of relative V$\beta$ usage in primary and secondary V$\beta$-to-D$\beta$J$\beta$ rearrangements.

**Rag1$^{C/C}$ mice exhibit altered J$\alpha$ utilization in V$\alpha$-to-J$\alpha$ rearrangements and abnormal changes in V$\beta$ repertoire during ab TCR selection.**

In DP thymocytes of wild-type mice, TCR$\alpha$ recombination occurs on both alleles and normally involves successive rounds of V$\alpha$-to-J$\alpha$ rearrangements on each allele (Brady and Bassing, 2011; Sicinska et al., 2003). Although both TCR$\alpha$ alleles are recombined in mature $\alpha\beta$ T cells of Rag1$^{C/C}$ mice (Krangel, 2009), whether the absence of non-core Rag1 regions results in a modest reduction in V$\alpha$-to-J$\alpha$ rearrangements in DP thymocytes is not known. Since reduced V(D)J recombinase activity in DP cells leads to increased representation of 5'J$\alpha$s and decreased representation of 3'J$\alpha$s in V$\alpha$-to-J$\alpha$ rearrangements (Dudley et al., 2003), we investigated whether V$\alpha$ rearrangements

in DP cells of Rag1$^{C/C}$ mice are similarly biased. For this purpose, we used PCR primers that hybridize to the Vα3 (*Trav9-4*) family of gene segments or to Jα61 (*Traj61*), Jα42 (*Traj42*), Jα17 (*Traj17*), or Jα4 (*Traj4*) to amplify Vα3-to-Jα rearrangements involving these 5' (Jα61, Jα42) or 3' (Jα17, Jα4) Jα gene segments from sort-purified DP cells of WT or Rag1$^{C/C}$ mice. The levels of PCR products representing Vα3 rearrangements to Jα61 and Jα42 were reduced in DP thymocytes from Rag1$^{C/C}$ mice relative to WT mice (Figure 2.5 *A*). In contrast, the levels of PCR products representing Vα3 rearrangements to Jα17 and Jα4 were elevated in DP thymocytes from Rag1$^{C/C}$ mice as compared to WT mice (Figure 2.5 *A*). These data reveal that loss of non-core Rag1 regions results in decreased usage of 5'Jαs and increased usage of 3'Jαs in Vα-to-Jα rearrangements. Although this biased targeting of Vα3 rearrangements toward 3'Jα gene segments is not consistent with diminished recombinase activity at the TCRα locus, our results demonstrate that non-core Rag1 regions control formation of the TCRα gene repertoire during Vα-to-Jα recombination in DP thymocytes.

Since positive selection of αβ TCRs expressed on DP thymocytes shapes TCRβ repertoire (Yannoutsos et al., 2004) and Jα repertoire is altered in DP thymocytes of Rag1$^{C/C}$ mice (Figure 2.5 A), we investigated the impact of non-core Rag1 regions on Vβ repertoire during DP-to-SP thymocyte development. We detected ~4-fold lower frequencies of Vβ5$^{+}$ TCRβ$^{high}$ SP thymocytes and higher frequencies of Vβ6$^{+}$ (~2-fold more) Vβ8$^{+}$ (~2-fold more), and Vβ14$^{+}$ (~5-fold more) TCRβ$^{high}$ SP cells in Rag1$^{C/C}$ mice relative to WT mice (Figure 2.5 *B* and *C*). Considering that we observed ~2-fold lower frequencies of Vβ10$^{+}$ DP thymocytes and equivalent frequencies of Vβ6$^{+}$ DP cells in Rag1$^{C/C}$ mice relative to WT mice (Figure 2.3 *E* and *F)*, these data indicate that positive selection of DP thymocytes alters Vβ repertoire differently in αβ TCRs of Rag1$^{C/C}$ and

WT mice. To confirm this notion, we calculated the ratios of the frequencies of cells expressing Vβ5, Vβ6, Vβ8, or Vβ14 on TCRβ$^{high}$ versus TCRβ$^{intermediate}$ thymocytes in Rag1$^{C/C}$ and WT mice (Figure 2.5 *D*). This analysis indicated enhanced selection for Vβ6$^{+}$, Vβ8$^{+}$, Vβ10$^{+}$, and Vβ14$^{+}$ cells and increased selection against Vβ5$^{+}$ cells during positive selection of DP thymocytes in Rag1$^{C/C}$ mice as compared to WT mice (Figure 2.5 *D*). Collectively, these data show that loss of non-core Rag1 regions leads to abnormal changes in Vβ repertoire during αβ TCR selection.

**Replacement of the Vβ14 RSS with the more efficient 3'Dβ1 RSS increases Vβ14 recombination frequency and rescues αβ T cell development in Rag1$^{C/C}$ mice.**

We have shown that Rag1$^{C/C}$ mice exhibit impaired DN3-to-DP thymocyte development caused by reduced levels of Vβ-to-DJβ rearrangements, and that this impaired Vβ recombination is associated with altered recombination frequencies of individual Vβ segments. A similar phenotype in Rag2$^{C/C}$ mice lead to the hypothesis that conserved sequence features of Vβ/V$_H$ RSSs that make them inefficient relative to 3'Dβ and Vκ/Vλ/Vδ/Vα RSSs contributes to impaired V-to-DJ recombination on the background of a diminished recombinase (Blackman et al., 1989; Carpenter et al., 2009; Kappler et al., 1987; Kappler et al., 1988; MacDonald et al., 1988; Speiser et al., 1989; Wade et al., 1988). In support of this model, the Vβ8 RSS more closely resembles the consensus Vκ/Vλ/Vδ/Vα RSS than canonical Vβ RSSs, and Vβ8 exhibits a 1.8-fold higher rearrangement and expression in Rag1$^{C/C}$ and Rag2$^{C/C}$ mice compared to WT mice (Liang et al., 2002); Figure 2.3 *E* and *F*). In addition, the Vβ5 and Vβ10 RSSs more closely resemble the consensus Vβ/V$_H$ RSS than canonical Vβ RSSs, and Vβ5 and Vβ10 exhibit ~2-fold lower rearrangement and expression in Rag1$^{C/C}$ mice relative to WT

mice (Figure 2.3 *E* and *F*). However, the Vβ14 RSS more closely resembles the Vβ/$V_H$ RSS consensus than other Vβ RSSs, yet Vβ14 exhibits 2-fold higher recombination and expression in Rag1$^{C/C}$ mice relative to WT mice (Figure 2.3 *E* and *F*). This latter finding suggests that factors in addition to Vβ RSS inefficiency may contribute the altered relative frequency of Vβ segments in Rag1$^{C/C}$ mice.

To directly test the prediction that Vβ RSS inefficiency causes impaired Vβ rearrangement in Rag1$^{C/C}$ mice, we sought to determine whether replacement of a Vβ RSS with a 3'Dβ or Vκ/Vλ/Vδ/Vα RSS increases recombination and expression of this Vβ to the same extent in Rag1$^{C/C}$ and WT mice. For this purpose, we established mice with gene-targeted replacement of the Vβ14 RSS with the 3'Dβ1 RSS on an otherwise normal TCRβ allele (Vβ14$^{3'D_\beta 1RSS/+}$ mice) since we previously showed in chimeric mice that this RSS replacement increases the frequencies of Vβ14 rearrangement and expression on a wild-type RAG background (Liang et al., 2002). We then made and analyzed in parallel Vb14$^{3'D_\beta 1RSS/+}$ and Rag1$^{C/C}$Vβ14$^{3'D_\beta 1RSS/+}$ mice, as well as control Rag1$^{C/C}$ and WT mice. Consistent with our previous findings (Wu et al., 2003), we detected a ~20-fold increase in the frequency of Vβ14$^+$ TCRβ$^{intermediate}$ DP thymocytes in Vβ14$^{3'Db1RSS/+}$ mice relative to WT mice (Figure 2.6 *A* and *B*). We observed a similar ~20-fold increase in the frequency of Vβ14$^+$ TCRβ$^{intermediate}$ DP thymocytes in Rag1$^{C/C}$Vβ14$^{3'D_\beta 1RSS/+}$ mice relative to Rag1$^{C/C}$ mice (Fig. 6 *A* and *B*), revealing that sequence of the RSS attached to Vβ14 is a major determinant of the frequency of Vβ14 rearrangement and expression in both WT and Rag1$^{C/C}$ mice. Therefore, our data provide direct support for the decade-old model that sequence features of Vβ/$V_H$ RSSs that renders them less efficient than 3'Dβ and Vκ/Vλ/Vδ/Vα RSSs contributes to impaired V rearrangements on the background of a defective recombinase as in Rag2$^{C/C}$

and Rag1$^{C/C}$ mice. Yet, we still detected ~2-fold greater frequencies of Vβ14 rearrangements and expression in Rag1$^{C/C}$Vβ14$^{3'D_\beta 1RSS/+}$ mice as compared to Vβ14$^{3'D_\beta 1RSS/+}$ mice (Fig. 6 *A* and *B*) as we observed between Rag1$^{C/C}$ and WT mice (Figure 2.3 *E* and *F*), highlighting that non-core Rag1 regions may modulate Vβ usage in Vβ rearrangements through mechanisms in addition to their function with inefficient Vβ RSSs.

Since the 3'Dβ1 RSS replacement drives increased Vβ14 rearrangement in Rag1$^{C/C}$ DN3 cells, we next investigated the effect of this single RSS replacement on the impaired DN3-to-DP thymocyte development of Rag1$^{\mathbf{C/C}}$ mice. We found ~5-fold greater numbers of total and DP thymocytes in Rag1$^{\mathbf{C/C}}$Vβ14$^{3'D_\beta 1RSS/+}$ mice as compared to Rag1$^{\mathbf{C/C}}$ mice (Figure 2.6 *C* and *D*), with no significant differences in total and DP cell numbers or the percentages of thymocytes at the DP stage among Rag1$^{\mathbf{C/C}}$Vb14$^{3'D_\beta 1RSS/+}$, Vb14$^{3'D_\beta 1RSS/+}$, and WT mice (Figure 2.6 *D* and *E*). While DN cell numbers were similar among all four genotypes (Figure 2.6 *D*), the percentages of thymocytes at the DN stage were lower in Rag1$^{\mathbf{C/C}}$Vb14$^{3'D_\beta 1RSS/+}$ mice compared to Rag1$^{\mathbf{C/C}}$ mice (Figure 2.6 *C*), yet higher in Rag1$^{\mathbf{C/C}}$Vb14$^{3'D_\beta 1RSS/+}$ mice relative to Vb14$^{3'D_\beta 1RSS/+}$ and WT mice (Figure 2.6 *C*). Consistent with these observations, we detected increased numbers of DN4 cells and an increased percentage of DN thymocytes at the DN4 stage in Rag1$^{\mathbf{C/C}}$Vβ14$^{3'D_\beta 1RSS/+}$ mice as compared to Rag1$^{\mathbf{C/C}}$ mice (Figure 2.6 *E*), but lower values for these two parameters in Rag1$^{\mathbf{C/C}}$Vβ14$^{3'D_\beta 1RSS/+}$ mice relative to Vβ14$^{3'D_\beta 1RSS/+}$ and WT mice (Figure 2.6 *E*). These data indicate that replacement of the RSS of only one of the 20 functional Vβ segments with the more efficient 3'Dβ1 RSS partially rescues DN3-to-DN4 thymocyte development and completely rescues DN-to-DP thymocyte development in Rag1$^{\mathbf{C/C}}$ mice. Therefore,

we conclude that non-core Rag1 regions drive αβ T cell development by overcoming inherent inefficiencies of Vβ RSSs to promote Vβ rearrangements.

**Discussion**

We have taken a genetic approach with Rag1$^{C/C}$ mice to determine how non-core RAG1 regions promote TCRβ gene assembly and αβ T cell development. The reduced levels of Dβ-Jβ and Vβ-DβJβ recombination in DN3 thymocytes and impaired DN-to-DP thymocyte development from accumulation of cells at the DN3 stage of Rag1$^{C/C}$ mice could arise from decreased efficiency of TCRβ recombination and/or survival of DN3 thymocytes in response to RAG DSBs. Our observation that expression of the anti-apoptotic BCL2 protein does not substantially enhance the survival of Rag1$^{C/C}$ DN3 cells and only minimally rescues thymocyte development in Rag1$^{C/C}$ mice indicates that preventing death of DN3 cells in response to RAG DSBs is not the major means through which non-core RAG1 regions promote TCRβ recombination and αβ T cell development. Our finding that a pre-assembled DβJβ complex partially rescues thymocyte development in Rag1$^{C/C}$ mice confirms the hypothesis that non-core RAG1 regions promote αβ T cell development in part by stimulating Dβ-to-Jβ recombination (Wu et al., 2003), and also provides unequivocal evidence that non-core RAG1 regions drive Vβ-to-DJβ recombination. Combined with these data, our observation that a pre-assembled TCRβ gene completely rescues thymocyte development in Rag1$^{C/C}$ mice proves that non-core RAG1 regions promote TCRβ gene assembly and αβ T cell development by stimulating Vβ recombination. However, because Dβ-to-Jβ recombination precedes Vβ-to-DβJβ recombination, our data cannot differentiate the relative contribution of non-core RAG1 regions in each of these steps of TCRβ gene assembly in driving αβ T cell development.

In contrast to Rag1$^{C/C}$ mice, which we have shown exhibit substantial defects in both Dβ-to-Jβ and Vβ–to-DJβ recombination and altered Vβ repertoire, Rag2$^{C/C}$ mice

have a major impairment in only Vβ-to-DJβ recombination that is associated with altered Vβ usage (Dudley et al., 2003). Since Rag2$^{C/C}$ mice also have a reduction in overall recombinase activity in thymocytes but no apparent defect in TCRα recombination, it was proposed that the interaction of a diminished recombinase with RSS sequences unique to Vβs may cause the Vβ-to-DJβ recombination defect, rather than loss of specific properties of the non-core RAG2 region in stimulating Vβ rearrangements (Liang et al., 2002). Our findings that a pre-assembled DβJβ complex or functional TCRβ gene each rescues αβ T cell development to some extent cannot distinguish between impaired TCRβ gene assembly caused by diminished recombinase activity versus by the loss of specific functions of Rag1 non-core regions that stimulate Dβ-to-Jβ and/or Vβ-to-DJβ recombination. However, our demonstration that replacement of the Vβ14 RSS with the more efficient 3'Dβ1 RSS dramatically increases the frequency of Vβ14 rearrangement in Rag1$^{C/C}$ thymocytes and partially rescues thymocyte development proves that sequence features of the Vβ14 RSS that distinguishes it from the 3'Dβ1 RSS contributes to impaired Vβ-to-DJβ recombination in Rag1$^{C/C}$ mice. Notably, in the presence or absence of this Vβ14 RSS replacement, we have shown that loss of non-core Rag1 regions results in increased Vβ14 rearrangements, indicating that the interaction of a defective recombinase with inefficient Vβ RSSs is not the sole cause of impaired Vβ recombination in Rag1$^{C/C}$ mice. Furthermore, our discovery that Vα3 rearrangements are biased toward 3'Jα segments in DP thymocytes of Rag1$^{C/C}$ mice is opposite the prior observation of increased usage of 5'Jαs in mice with diminished recombinase activity in DP thymocytes (Liang et al., 2002). Therefore, we conclude that specific activities of non-core RAG1 regions modulate Vβ and Jα gene segment utilization during V(D)J recombination.

How might non-core RAG1 regions modulate Vβ and Jα usage? Both Vβ-to-DJβ and Vα-to-Jα recombination are driven by TCR enhancers and promoters that enable RAG2 binding to histone H3 proteins tri-methylated on lysine 4 located over D/J segments and also render D/J RSSs nucleosome-free and accessible for RAG cleavage (Yannoutsos et al., 2004). The RAG1/RAG2 proteins in D/J recombination centers capture accessible V RSSs to mediate V-to-(D)J rearrangements (Ji et al., 2010a; Kondilis-Mangum et al., 2011; Osipovich et al., 2007). Changes in locus topology that place V segments near D/J segments are likely critical for the formation of synaptic complexes between V and D/J RSSs (Ji et al., 2010b), which may dissociate more often than they are cleaved by RAG to assemble V(D)J joins (Jhunjhunwala et al., 2009; Schatz and Ji, 2011). The relative usage of individual Vβ and Jα gene segments in rearrangements should be determined by accessibility of their RSSs, frequencies at which they enter synaptic complexes, efficiencies of their flanking RSSs, and physical forces that destabilize pre-cleavage synaptic complexes (Schatz and Ji, 2011; Wu et al., 2003). Since differences in TCRα locus conformation have been observed between DP cells that lack Rag1 protein or express a cleavage-defective mutant Rag1 protein (Bassing et al., 2008; Schatz and Ji, 2011; Wu et al., 2003),non-core RAG1 regions may promote or preserve changes in TCRβ and TCRα locus topology that, respectively, help assemble or stabilize synaptic complexes for some Vb and Ja segments over others. The non-core RAG1 regions contain a Really Interesting New Gene domain with E3 ubiquitin ligase activity (Chaumeil et al., 2013) and other sequences that bind the RING E3 ubiquitin ligase complex VprBP/DDB1/Cul4A/Roc1 (Jones and Gellert, 2003; Yurchenko et al., 2003) The RAG1 RING domain catalyzes histone H3 mono-ubiquitylation, which reduces core histone binding and promotes transcription of genes (Kassmeier et al., 2012) and *RAG1* mutations that reduce this E3 ubiquitin ligase activity

impair V(D)J recombination (Grazini et al., 2010; Jones et al., 2011; Zentner and Henikoff, 2013). While targets of VprBP/DDB1/Cul4A/Roc1 in the context of V(D)J recombination are not known, deletion of VprBP initiating in pro-B cells causes a block in B cell development at this stage that correlates with greater impairment of $V_H$-to-$D_HJ_H$ recombination than $D_H$-to-$J_H$ recombination (Grazini et al., 2010; Jones et al., 2011; Simkus et al., 2007). Differences in accessibility and transcription among germline Vβ and Jα gene segments are observed in DN and DP thymocytes, respectively (Kassmeier et al., 2012), while changes in TCRα locus topology control Jα usage in Vα-to-Jα rearrangements (Abarrategui and Krangel, 2009; Chen et al., 2001; Krangel, 2009). Thus, non-core RAG1 regions could modulate Vβ and Jα usage by ubiquitylating H3 histones or other proteins to remove nucleosomes from some Vβ and Jα RSSs more than others and/or similarly function to modify proteins that organize TCRβ and TCRα locus topology. The increased utilization of 3'Jα segments in $Rag1^{C/C}$ mice suggests that non-core RAG1 regions might inhibit successive Vα-to-Jα rearrangements. Although transcription from Vα promoters stimulates such rearrangements to shape TCRα repertoire (Seitan et al., 2011) mechanisms that suppress Vα-to-Jα recombination and provide DP thymocytes time to express and select TCRα genes are not known. Considering that the RAG1 RING domain promotes RAG1 poly-ubiquitylation (Abarrategui and Krangel, 2009), and ubiquitylation targets proteins for proteasomal degradation and changes in cellular localization, our data is consistent with a regulatory role of the RAG1 non-core region in constraining RAG1 protein expression to ensure time for assembled TCRα genes to be expressed and selected before initiation of further Vα-to-Jα recombination. Another possibility is that RAG1-mediated ubiquitylation of histones cooperates with ATM-dependent histone H2A ubiquitlyation (Jones and Gellert,

2003) to transiently inhibit accessibility and transcription of germline Vα gene segments in response to RAG DSBs induced during Vα-to-Jα rearrangements.

Generation, selection, and expression of a broad αβ TCR and IgH/IgL repertoires are critical for effective adaptive immunity. *RAG1* or *RAG2* mutations that diminish RAG endonuclease activity cause inefficient TCR gene assembly, reduced numbers of αβ T cells beyond the progenitor stage, restricted TCRβ and TCRα repertoires, and immunodeficiency (Shanbhag et al., 2010), revealing that efficient V(D)J recombination is critical for generation of αβ TCR diversity. TCRβ-mediated, Ccnd3-dependent thymocyte expansion contributes to αβ TCR diversity by allowing multiple chances for each unique TCRβ gene assembled in DN thymocyte to be selected with a different TCRα chain in DP cells (Notarangelo, 2010; Villa et al., 2008; Villa et al., 2001; Wong and Roth, 2007). Our demonstration that impaired TCRβ recombination is the predominant cause of reduced DP thymocyte numbers in $Rag1^{C/C}$ mice and that DP cell numbers are lower in $Rag1^{C/C}Ccnd3^{-/-}$ mice than in $Rag1^{C/C}$ and $Ccnd3^{-/-}$ mice indicates that TCRβ recombination efficiency and TCRβ-mediated thymocyte expansion cooperate to generate ab TCR diversity. A polymorphism in the human VκA2 RSS impairs VκA2 recombination efficiency, reduces VκA2 representation in the Vκ repertoire, and confers susceptibility to *Haemophilus Influenzae* (Sicinska et al., 2003), revealing that alterations to the mechanisms that control utilization of individual V gene segments can have deleterious consequences. Our study indicates that, similar to loss of the non-core Rag2 region (Nadel et al., 1998), absence of non-core RAG1 regions decreases Vβ-to-Jβ recombination and alters the primary Vβ repertoire generated during Vβ-to-DJβ recombination. Our study also reveals that the loss of non-core RAG1 regions leads to abnormal changes in Vβ repertoire during TCR selection, which could arise from altered

Jα usage in TCRα rearrangements and/or impaired signaling of gene expression changes in response to RAG DSBs in DP thymocytes. Regardless, our findings suggest that non-core regions of RAG1 may have co-evolved with the non-core RAG2 domain and Vβ RSS sequences to protect host organisms from pathogens by promoting sufficient TCRβ gene diversity and advantageous representation of individual Vβ segments in the naive αβ TCR repertoire.

## Figures

## Figure 2.1

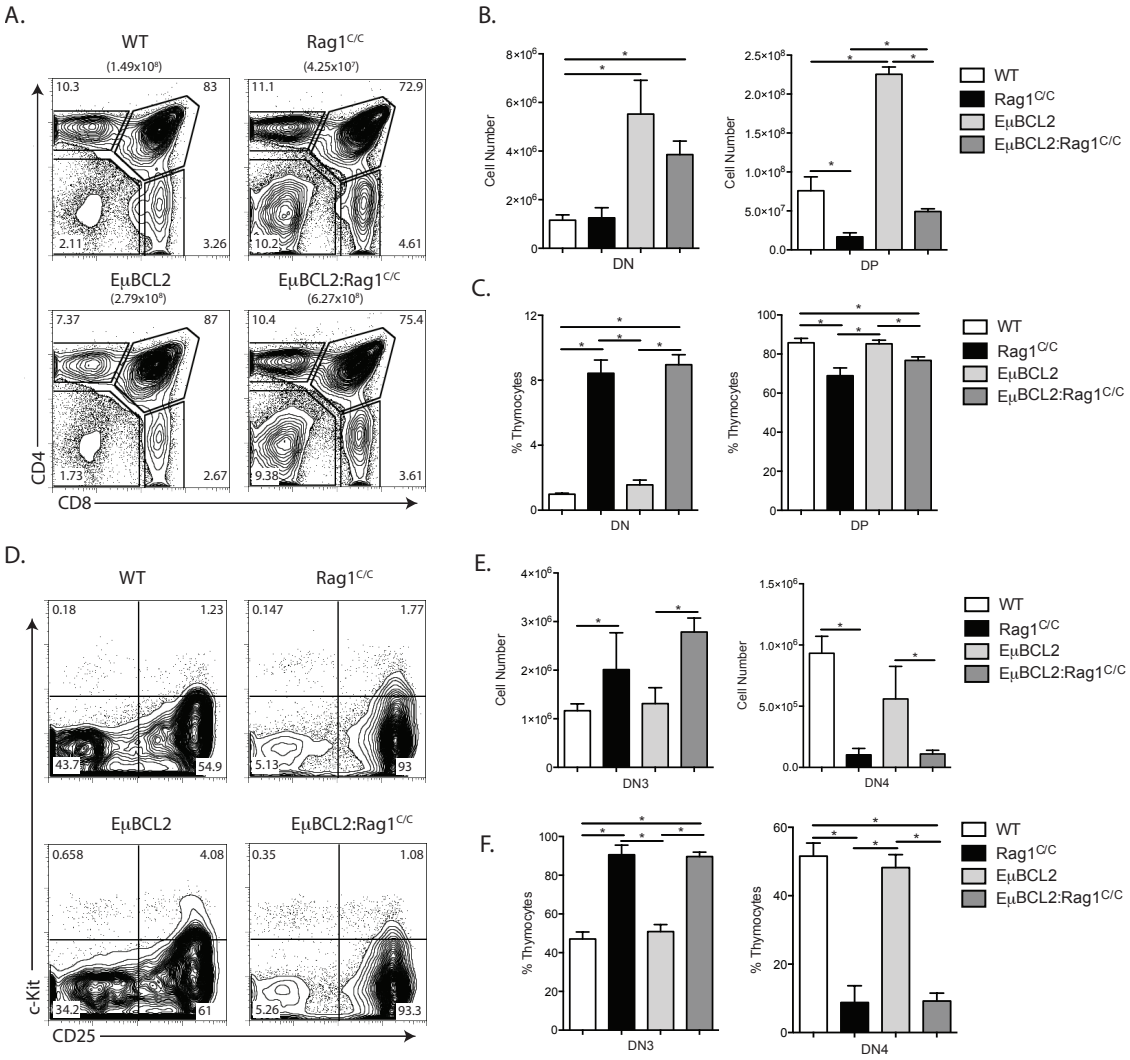

**Figure 2.1. Transgenic BCL2 expression partially rescues αβ T cell development in Rag1$^{C/C}$ mice.** *A.* Representative flow cytometry analysis of CD4 and CD8 expression on total thymocytes isolated from littermate or age-matched WT (n=3), Rag1$^{C/C}$ (n=3), EμBCL2 (n=3), or EμBCL2:Rag1$^{C/C}$ (n=3) mice. The average number of total thymocytes for mice of each genotype is indicated in parentheses, and the frequencies of cells in the DN, DP, CD4$^{+}$ SP, and CD8$^{+}$ SP quadrants are indicated on the plots. *B*. Graphs showing the average numbers of DN and DP thymocytes from mice of the indicated genotypes. Error bars are standard error of the mean. Lines with asterisks above indicate significant differences ($p \leq 0.05$). *A and B*. This experiment was independently performed three times, each time on one mouse of each genotype. *C.* Representative flow cytometry analysis of c-Kit and CD25 expression on DN thymocytes isolated from littermate or age-matched WT (n=3), Rag1$^{C/C}$ (n=3), EμBCL2 (n=3), or EμBCL2:Rag1$^{C/C}$ (n=3) mice. The frequencies of DN cells in the DN1, DN2, DN3, and DN4 quadrants are indicated on the plots. *D.* Graphs showing the average numbers of DN3 and DN4 thymocytes from mice of the indicated genotypes. Error bars are standard error of the mean. Lines with asterisks above indicate significant differences ($p \leq 0.05$). *C and D*. This experiment was independently performed three times, each time on one mouse of each genotype.

**Figure 2.2**

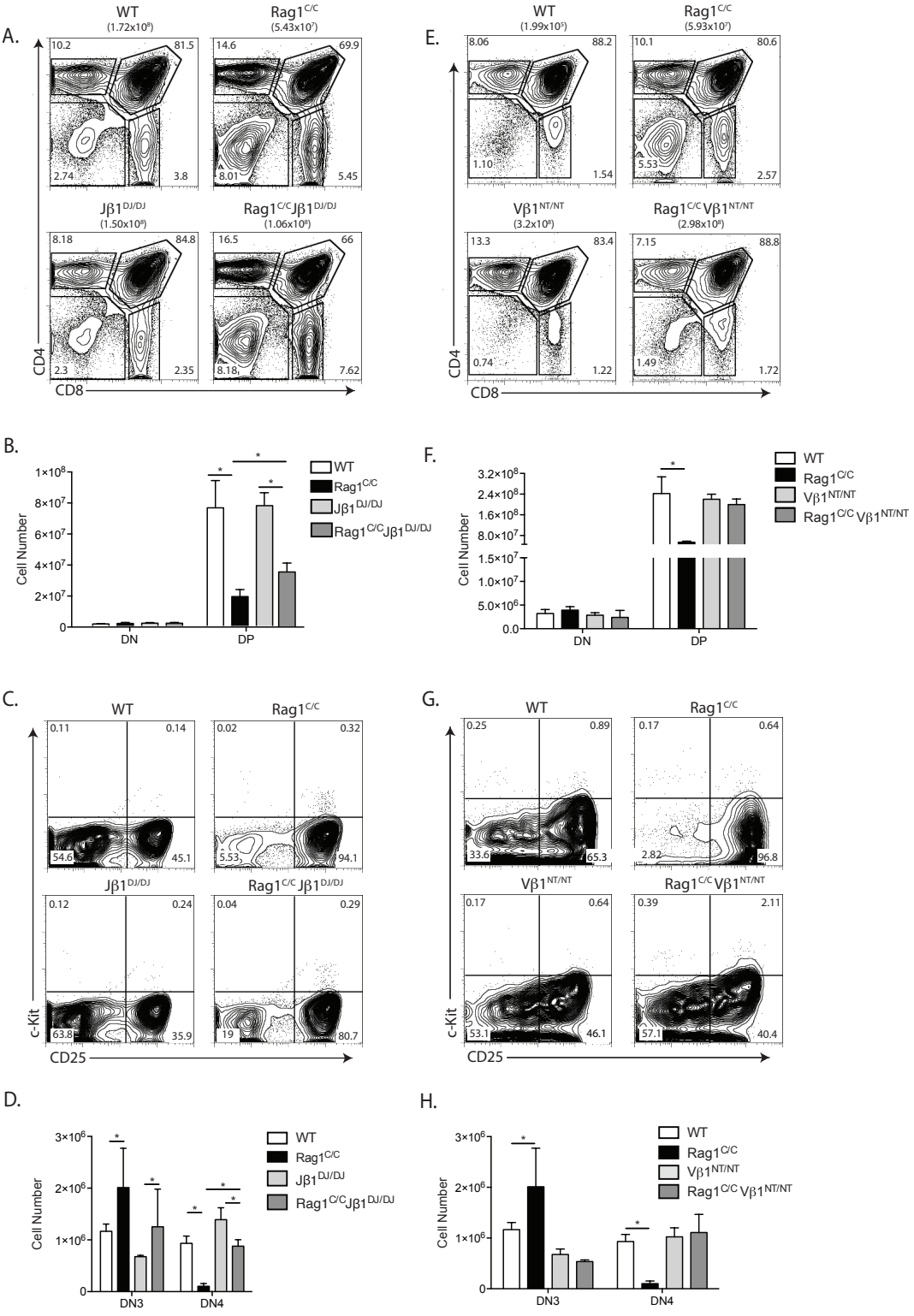
A.
WT
(1.72x10^8)
Rag1^C/C
(5.43x10^7)
Jβ1^DJ/DJ
(1.50x10^8)
Rag1^C/C Jβ1^DJ/DJ
(1.06x10^8)
CD4
CD8
E.
WT
(1.99x10^5)
Rag1^C/C
(5.93x10^7)
Vβ1^NT/NT
(3.2x10^8)
Rag1^C/C Vβ1^NT/NT
(2.98x10^8)
B.
Cell Number
DN
DP
WT
Rag1^C/C
Jβ1^DJ/DJ
Rag1^C/C Jβ1^DJ/DJ
F.
Vβ1^NT/NT
Rag1^C/C Vβ1^NT/NT
C.
c-Kit
CD25
G.
H.
DN3
DN4

**Figure 2.2. A pre-assembled TCRβ gene completely rescues early αβ T cell development in Rag1$^{C/C}$ mice.** *A.* Representative flow cytometry analysis of CD4 and CD8 expression on total thymocytes isolated from littermate or age-matched WT (n=3), Rag1$^{C/C}$ (n=3), Jβ1$^{DJ/DJ}$ (n=3), and Rag1$^{C/C}$Jβ1$^{DJ/DJ}$ mice (n=3). The average number of total thymocytes for each genotype is indicated in parentheses, and the frequencies of cells in the DN, DP, CD4$^+$ SP, and CD8$^+$ SP quadrants are indicated on the plots. *B*. Graphs showing the average numbers of DN and DP thymocytes from mice of the indicated genotypes. Error bars are standard error of the mean. Lines with asterisks above indicate significant differences ($p \leq 0.05$). *A and B*. This experiment was independently performed three times, each time on one mouse of each genotype. *C.* Representative flow cytometry analysis of c-Kit and CD25 expression on DN thymocytes isolated from littermate or age-matched WT (n=3), Rag1$^{C/C}$ (n=3), Jβ1$^{DJ/DJ}$ (n=3), and Rag1$^{C/C}$Jβ1$^{DJ/DJ}$ (n=3) mice. The frequencies of DN cells in the DN1, DN2, DN3, and DN4 quadrants are indicated. *D.* Graphs showing the average numbers of DN3 and DN4 thymocytes from mice of the indicated genotypes. Error bars are standard error of the mean. Lines with asterisks above indicate significant differences ($p \leq 0.05$). *C and D*. This experiment was independently performed three times, each time on one mouse of each genotype. *E.* Representative flow cytometry analysis of CD4 and CD8 expression on total thymocytes isolated from littermate or age-matched WT (n=3), Rag1$^{C/C}$ (n=3), Vβ1$^{NT/NT}$ (n=6), and Vβ1$^{NT/NT}$Rag1$^{C/C}$ (n=6) mice. The average number of total thymocytes for each genotype is indicated in parentheses, and the frequencies of cells in the DN, DP, CD4$^+$ SP, and CD8$^+$ SP quadrants are indicated on the plots. *F*. Graphs showing the average numbers of DN and DP thymocytes from mice of the indicated genotypes. Error bars are standard error of the mean. The line with an asterisk above indicates a significant difference ($p \leq 0.05$). *E and F*. This experiment was independently

performed three times, each time on at least mouse of each genotype. *G.* Representative flow cytometry analysis of c-Kit and CD25 expression on DN thymocytes isolated from littermate or age-matched WT (n=3), $Rag1^{C/C}$ (n=3), $V\beta1^{NT/NT}$ (n=3), and $V\beta1^{NT/NT}Rag1^{C/C}$ (n=3) mice. The frequencies of DN cells in the DN1, DN2, DN3, and DN4 quadrants are indicated. *H.* Graphs showing the average numbers of DN3 and DN4 thymocytes from mice of the indicated genotypes. Error bars are standard error of the mean. Lines with asterisks above indicate significant differences ($p \leq 0.05$). *G and H*. This experiment was independently performed three times, each time on one mouse of each genotype.

## Figure 2.3

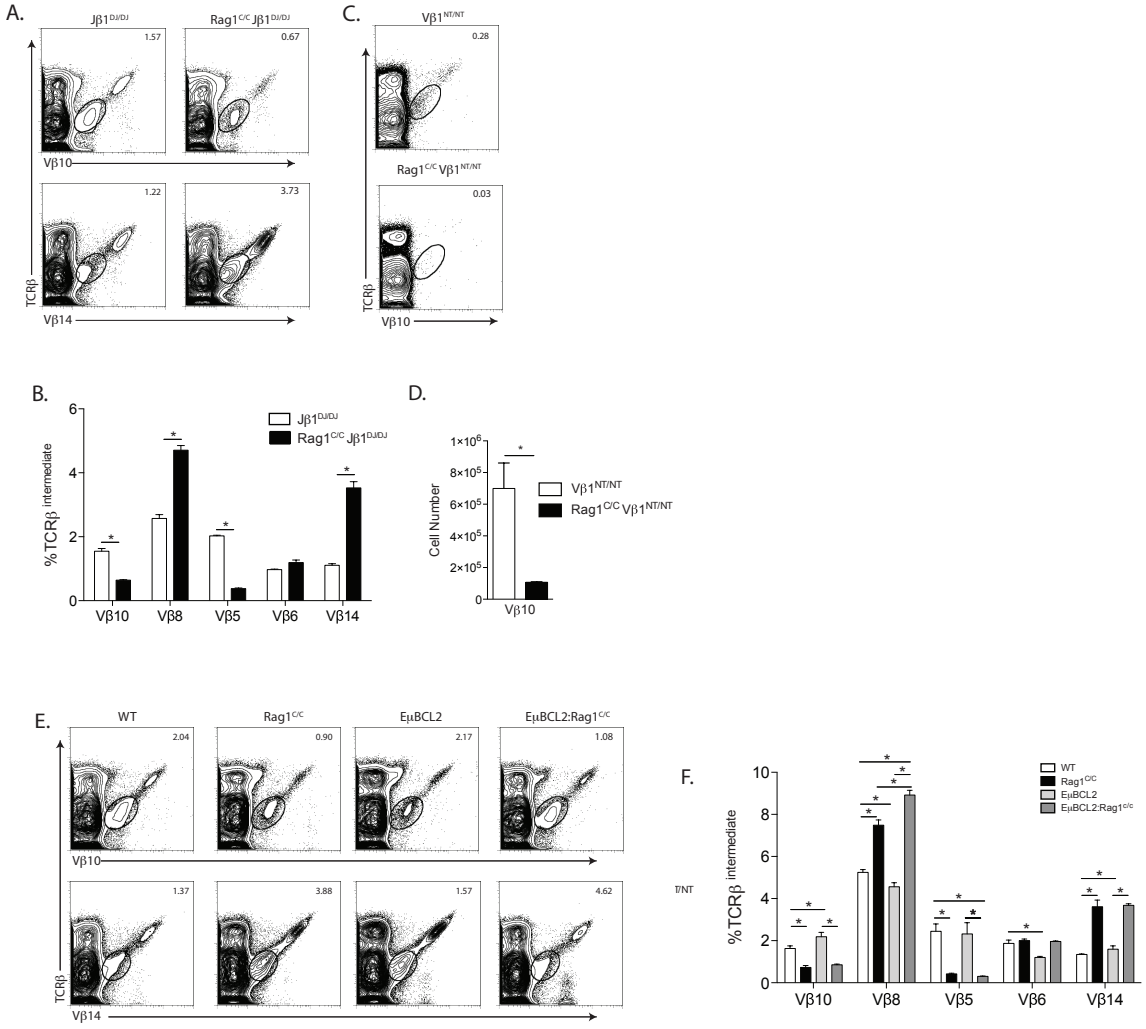
A.
Jβ1 DJ/DJ
Rag1 C/C Jβ1 DJ/DJ
1.57
0.67
Vβ10
1.22
3.73
TCRβ
Vβ14
C.
Vβ1 NT/NT
0.28
Rag1 C/C Vβ1 NT/NT
0.03
TCRβ
Vβ10
B.
Jβ1 DJ/DJ
Rag1 C/C Jβ1 DJ/DJ
% TCRβ intermediate
Vβ10
Vβ8
Vβ5
Vβ6
Vβ14
D.
Vβ1 NT/NT
Rag1 C/C Vβ1 NT/NT
Cell Number
Vβ10
E.
WT
Rag1 C/C
EμBCL2
EμBCL2:Rag1 C/C
2.04
0.90
2.17
1.08
Vβ10
1.37
3.88
1.57
4.62
TCRβ
Vβ14
F.
WT
Rag1 C/C
EμBCL2
EμBCL2:Rag1 C/C
% TCRβ intermediate
T/NT
Vβ10
Vβ8
Vβ5
Vβ6
Vβ14

**Figure 2.3.** Rag1$^{C/C}$ mice exhibit altered Vβ utilization in primary and secondary Vβ rearrangements. *A.* Representative flow cytometry analysis of TCRβ and Vβ expression shown for Vβ10 or Vβ14 on total thymocytes isolated from littermate or age-matched Jβ1$^{DJ/DJ}$ (n=3) and Rag1$^{C/C}$Jβ1$^{DJ/DJ}$ (n=3) mice. The frequencies of cells in the depicted TCRβ$^{intermediate}$ gate are indicated. *B.* Graph showing the average frequencies of TCRβ$^{intermediate}$ cells expressing Vβ10, Vβ8, Vβ5, Vβ6, or Vβ14 in thymocytes from Jβ1$^{DJ/DJ}$ and Rag1$^{C/C}$Jβ1$^{DJ/DJ}$ mice. Error bars are standard error of the mean. Lines with asterisks above indicate significant differences ($p \leq 0.05$). *A and B*. This experiment was independently performed three times, each time on one mouse of each genotype. *C.* Representative flow cytometry analysis of TCRβ and Vβ10 expression on total thymocytes isolated from littermate or age-matched Vβ1$^{NT/NT}$ (n=6) and Vβ1$^{NT/NT}$Rag1$^{C/C}$ (n=6) mice. The frequencies of cells in the depicted TCRβ$^{intermediate}$ gate are indicated. *D.* Graph showing the average number of TCRβ$^{intermediate}$ cells expressing Vβ10 in cells from Vβ1$^{NT/NT}$ and Vβ1$^{NT/NT}$Rag1$^{C/C}$ mice. Error bars are standard error of the mean. The line with an asterisk above indicates a significant difference ($p \leq 0.05$). *C and D*. This experiment was independently performed three times, each time on at least one mouse of each genotype. *E.* Representative flow cytometry analysis of TCRβ and Vβ10 or Vβ14 expression on total thymocytes isolated from littermate or age-matched WT (n=3), Rag1$^{C/C}$ (n=3), EμBCL2 (n=3), or EμBCL2:Rag1$^{C/C}$ (n=3) mice. The frequencies of cells in the depicted TCRβ$^{intermediate}$ gate are indicated. *F.* Graph showing the average frequencies of TCRβ$^{intermediate}$ cells expressing Vβ10, Vβ8, Vβ5, Vβ6, or Vβ14 in cells from mice of the indicated genotypes. Error bars are standard error of the mean. Lines with asterisks above indicate significant differences ($p \leq 0.05$). *E and F*. This experiment was independently performed three times, each time on one mouse of each genotype.

## Figure 2.4

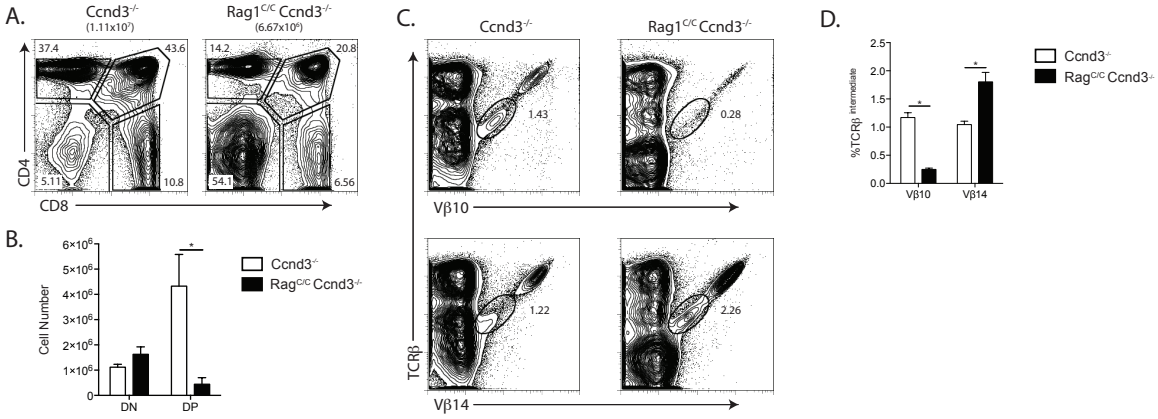
A.
Ccnd3-/-
(1.11x10^7)
Rag1C/C Ccnd3-/-
(6.67x10^6)
37.4
43.6
5.11
10.8
14.2
20.8
54.1
6.56
CD4
CD8
B.
Cell Number
6×10^6
5×10^6
4×10^6
3×10^6
2×10^6
1×10^6
0
DN
DP
*
Ccnd3-/-
RagC/C Ccnd3-/-
C.
Ccnd3-/-
Rag1C/C Ccnd3-/-
1.43
0.28
1.22
2.26
Vβ10
TCRβ
Vβ14
D.
%TCRβ+ intermediate
2.5
2.0
1.5
1.0
0.5
0.0
Vβ10
Vβ14
*
*
Ccnd3-/-
RagC/C Ccnd3-/-

**Figure 2.4 TCRβ recombination and TCRβ-mediated Ccnd3-dependent DN thymocyte proliferative expansion cooperate in αβ T cell development.** *A.* Representative flow cytometry analysis of CD4 and CD8 expression on total thymocytes isolated from littermate or age-matched Ccnd3$^{-/-}$ (n=4) and Rag1$^{C/C}$Ccnd3$^{-/-}$ (n=5) mice. The average number of total thymocytes for each genotype is indicated in parentheses, and the frequencies of cells in the DN, DP, CD4$^{+}$ SP, and CD8$^{+}$ SP quadrants are indicated on the plots. *B*. Graph showing the average numbers of DN and DP thymocytes from Ccnd3$^{-/-}$ and Rag1$^{C/C}$Ccnd3$^{-/-}$ mice. Error bars are standard error of the mean. The line with an asterisk above indicates a significant difference ($p \leq 0.05$). *A and B*. This experiment was independently performed three times, each time on at least one mouse of each genotype. *C.* Representative flow cytometry analysis of TCRβ and Vβ10 or Vβ14 expression on total thymocytes isolated from littermate or age-matched Ccnd3$^{-/-}$ and Rag1$^{C/C}$Ccnd3$^{-/-}$ mice. The frequencies of cells in the depicted TCRβ$^{intermediate}$ gate are indicated. *D.* Graph showing the average frequencies of TCRβ$^{intermediate}$ cells expressing Vβ10 or Vβ14 in thymocytes from Ccnd3$^{-/-}$ (n=4) and Rag1$^{C/C}$Ccnd3$^{-/-}$ (n=5) mice. Error bars are standard error of the mean. Lines with asterisks above indicate significant differences ($p \leq 0.05$). *C and D*. This experiment was independently performed three times, each time on at least one mouse of each genotype.

**Figure 2.5**

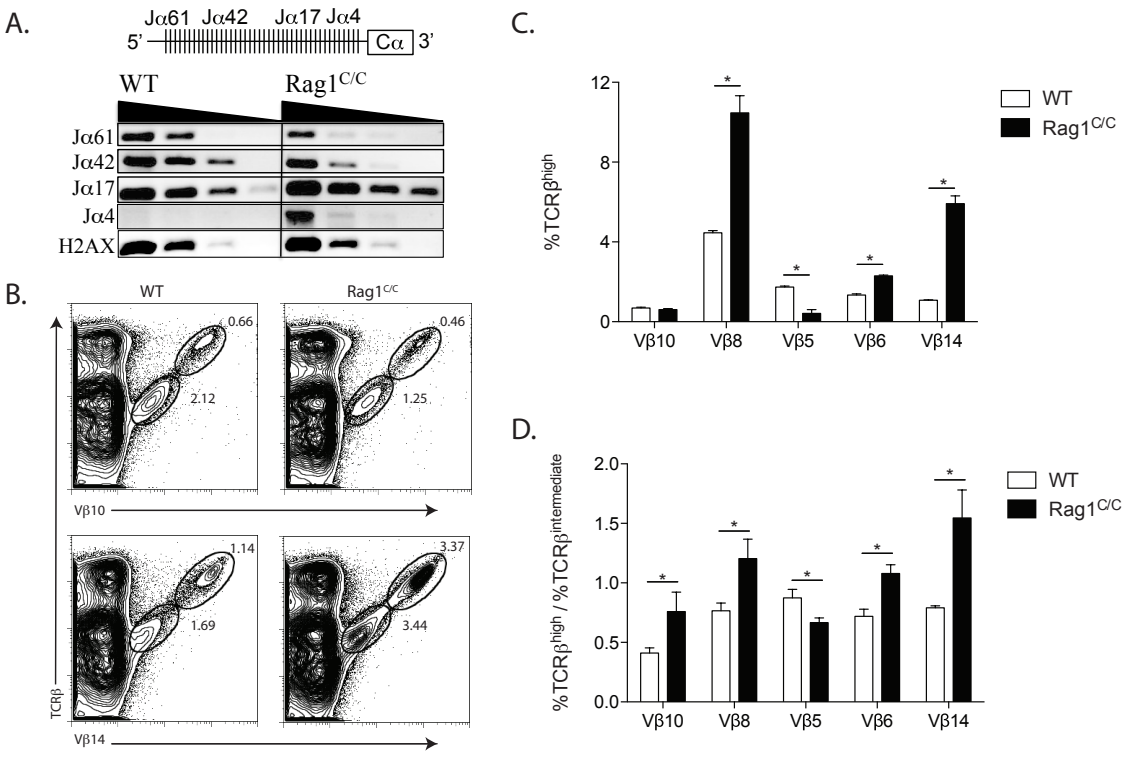
A.
Jα61 Jα42 Jα17 Jα4
5'
Cα
3'
WT
Rag1C/C
Jα61
Jα42
Jα17
Jα4
H2AX
B.
WT
Rag1C/C
0.66
2.12
0.46
1.25
Vβ10
1.14
1.69
3.37
3.44
TCRβ
Vβ14
C.
%TCRβhigh
12
8
4
0
WT
Rag1C/C
Vβ10
Vβ8
Vβ5
Vβ6
Vβ14
D.
%TCRβhigh / %TCRβintermediate
2.0
1.5
1.0
0.5
0.0
WT
Rag1C/C
Vβ10
Vβ8
Vβ5
Vβ6
Vβ14

**Figure 2.5. Rag1$^{C/C}$ mice exhibit altered Jα utilization in Vα-to-Jα rearrangements and abnormal changes in Vβ repertoire during αβ TCR selection.** *A.* Schematic of the Jα-Cα region of the TCRα locus *(Upper)*. Representative PCR analysis of Vα3 rearrangements to the indicated Jα gene segments or H2αx as a loading control on 5-fold dilutions of genomic DNA from sort-purified CD4$^{+}$CD8$^{+}$ WT (n=3) and Rag1$^{C/C}$ (n=3) thymocytes (*Lower*). *B.* Representative flow cytometry analysis of TCRβ and Vβ10 or Vβ14 expression on total thymocytes isolated from littermate or age-matched WT (n=3) and Rag1$^{C/C}$ (n=3) mice. The frequencies of cells in the depicted TCRβ$^{intermediate}$ and TCRβ$^{high}$ gates are indicated. *C.* Graph showing the average frequencies of TCRβ$^{high}$ cells expressing Vβ10, Vβ8, Vβ5, Vβ6, or Vβ14 in thymocytes from mice of the indicated genotypes. Error bars are standard error of the mean. Lines with asterisks above indicate significant differences ($p \leq 0.05$). *D.* Graph showing the average ratios of the frequencies of TCRβ$^{high}$ and TCRβ$^{intermediate}$ cells in thymocytes from WT and Rag1$^{C/C}$ mice. Error bars are standard error of the mean. Lines with asterisks above indicate significant differences ($p \leq 0.05$). *A* - *D*. These experiments were independently performed three times, each time on one mouse of each genotype.

**Figure 2.6**

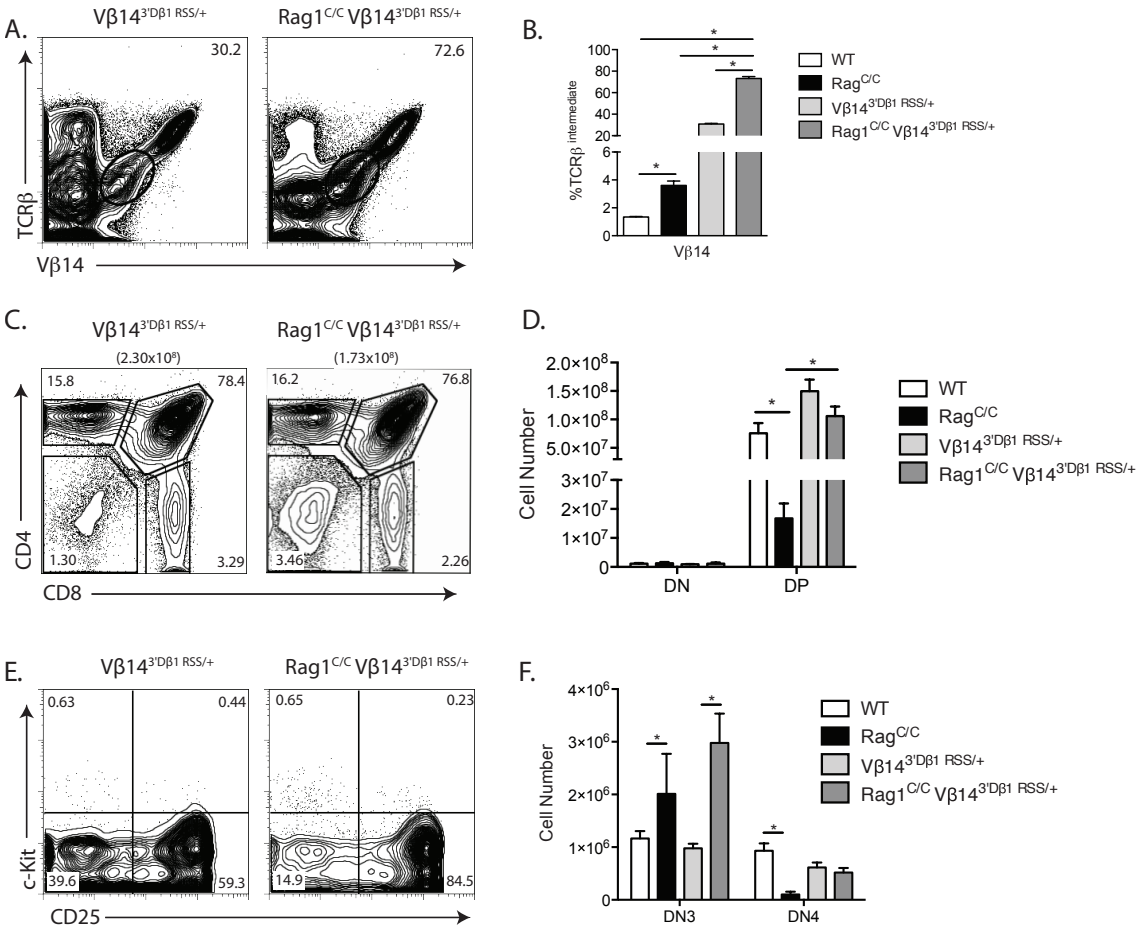
A.
Vβ14 3'Dβ1 RSS/+
Rag1 C/C Vβ14 3'Dβ1 RSS/+
30.2
72.6
TCRβ
Vβ14
B.
% TCRβ intermediate
Vβ14
WT
Rag C/C
Vβ14 3'Dβ1 RSS/+
Rag1 C/C Vβ14 3'Dβ1 RSS/+
C.
(2.30x10⁸)
(1.73x10⁸)
15.8
78.4
1.30
3.29
16.2
76.8
3.46
2.26
CD4
CD8
D.
Cell Number
DN
DP
E.
0.63
0.44
39.6
59.3
0.65
0.23
14.9
84.5
c-Kit
CD25
F.
Cell Number
DN3
DN4

**Figure 2.6. Replacement of the Vβ14 RSS with the more efficient 3'Dβ1 RSS increases Vβ14 recombination frequency and rescues αβ T cell development in Rag1$^{C/C}$ mice.** *A.* Representative flow cytometry analysis of TCRβ and Vβ14 expression on total thymocytes isolated from littermate or age-matched Vβ14$^{3'D\beta1RSS/+}$ (n=3) and Rag1$^{C/C}$Vβ14$^{3'D\beta1RSS/+}$ (n=3) mice. The frequencies of cells in the depicted TCRβ$^{intermediate}$ gates are indicated. *B*. Graph showing the average frequencies of TCRβ$^{intermediate}$ cells expressing Vβ14 in thymocytes from mice of the indicated genotypes. Significant differences of *p<0.05 indicated. *A and B*. This experiment was independently performed three times, each time on at least one mouse of each genotype. *C.* Representative flow cytometry analysis of CD4 and CD8 expression on total thymocytes isolated from littermate or age-matched Vβ14$^{3'D\beta1RSS/+}$ (n=3) and Rag1$^{C/C}$Vβ14$^{3'D\beta1RSS/+}$ (n=3) mice. The average number of total thymocytes for each genotype is indicated in parentheses, and the frequencies of DN, DP, CD4$^+$ SP, and CD8$^+$ SP cell populations are indicated on the plots. *D*. Graph showing the average number of DN and DP cells from mice of the indicated genotypes. Error bars are standard error of the mean. Significant differences of *p<0.05 indicated. *C and D*. This experiment was independently performed three times, each time on at least one mouse of each genotype. *E.* Representative flow cytometry analysis of c-Kit and CD25 expression on DN thymocytes isolated from littermate or age-matched Vβ14$^{3'D\beta1RSS/+}$ (n=3) and Rag1$^{C/C}$Vβ14$^{3'D\beta1RSS/+}$ (n=3) mice with the frequencies of DN1, DN2, DN3, and DN4 cell populations indicated. *F.* Graph showing the average numbers of DN3 and DN4 cells from mice of the indicated genotypes. Error bars are standard error of the mean. Significant differences of *p<0.05 indicated. This experiment was independently performed three times on a total of three mice of each genotype. *C and D*. This experiment was independently performed three times, each time on at least one mouse of each genotype.

## CHAPTER 3

## RAG1 enhances IgL Accessibility and Promotes B Cell Development by Transducing Pro-Survival Signals Upon IgL Recombination


### Abstract

The RAG1/RAG2 (RAG) endonuclease catalyzes the assembly of antigen receptor genes by cleaving accessible Ig and TCR gene segments. In addition to functioning with RAG2 as a nuclease, the RAG1 protein has been proposed to employ its amino-terminus to regulate V(D)J recombination by promoting Ig/TCR locus accessibility and signaling in response to RAG DNA cleavage. We show here that *Rag1*$^{C/C}$ mice expressing an amino-terminus truncated, cleavage-competent Rag1 protein exhibit a pronounced impairment in the development of Ig$\lambda^+$ B cells and a less severe defect in the generation of Ig$\kappa^+$ B cells. We demonstrate that *Rag1*$^{C/C}$ pre-B cells exhibit lower than normal *Ig*$\lambda$ recombination and accessibility and that full-length Rag1 protein enhances *Ig*$\kappa$ and *Ig*$\lambda$ accessibility independent of RAG endonuclease activity. We show that *Rag1*$^{C/C}$ pre-B cells cannot signal transcriptional activation of the pro-survival Pim2 kinase upon RAG cleavage of *Ig*$\kappa$ loci. Finally, we demonstrate that expression of the anti-apoptotic BCL2 protein rescues Ig$\lambda^+$ B cell development in *Rag1*$^{C/C}$ mice. Our data indicate that RAG1 has critical functions that enhance *Ig*$\kappa$ and *Ig*$\lambda$ accessibility and that transduce pro-survival signals during *Ig*$\kappa$ recombination to promote Ig$\kappa^+$ and Ig$\lambda^+$ B cell development and thereby establish a normal Ig$\kappa^+$ and Ig$\lambda^+$ B cell repertoire.

**Introduction**

A broad lymphocyte antigen receptor repertoire comprised of immunoglobulin (Ig) heavy (H) and Igκ or Igλ light (L) chain-positive B cells and T cell receptor (TCR) αβ or γδ chain-positive T cells is critical for effective adaptive immunity. The lymphocyte-specific RAG endonuclease generates Ig and TCR diversity by catalyzing assembly of Ig and TCR genes in developing B and T cells, respectively (Liang et al., 2002). RAG cleavage between two participating variable (V), diversity (D), or joining (J) gene segments and their flanking recombination signal sequences (RSSs) yields hairpin-sealed coding ends and blunt signal ends (Fugmann et al., 2000). The RAG proteins then function with classical non-homologous end-joining factors, the Ataxia Telangiectasia mutated (ATM) kinase, and ATM substrates to stabilize, process, and repair these DNA ends, creating V(D)J coding joins and signal joins (Fugmann et al., 2000; Schatz and Swanson, 2011). V(D)J coding joins form the second exons of Ig and TCR genes that, along with downstream constant region exons, encode Ig or TCR proteins. The number of possible joining events and the imprecision in coding join formation cooperate to create enormous antigen receptor diversity. The lymphocyte lineage- and development stage-directed modulation of Ig and TCR locus accessibility and topology controls initiation of V(D)J recombination to ensure the development of mature $Ig\kappa^+$ and $Ig\lambda^+$ B cells and $\alpha\beta^+$ and $\gamma\delta^+$ T cells expressing a broad antigen receptor repertoire (Alt et al., 2013; Boboila et al., 2012; Helmink and Sleckman, 2012; Lieber, 2010).

Mouse $Ig\kappa^+$ and $Ig\lambda^+$ B cells develop in the bone marrow (BM) through a differentiation program that links the assembly and selection of Ig genes with cellular survival and continued developmental progression (Degner-Leisso and Feeney, 2010; Guo et al., 2011; Jhunjhunwala et al., 2009; Seitan et al., 2011; Shih and Krangel, 2013;

Xiang et al., 2013; Xiang et al., 2011). BM common lymphoid progenitor cells differentiate into pro-B cells that activate *Rag1/Rag2* transcription, *IgH* accessibility, and *IgH* compaction by chromosome looping, which leads to $D_H$-to-$J_H$ recombination and subsequent $V_H$-to-$DJ_H$ rearrangements in G1 phase cells (Clark et al., 2014). The assembly and expression of in-frame *IgH* genes generates Igμ proteins that can pair with λ5 and VpreB surrogate light chains to form pre-B cell receptors (pre-BCRs) (Alt et al., 2013; Cobb et al., 2006). Pre-BCRs activate intracellular signals that rescue pro-B cells from death, halt *Rag1/Rag2* transcription, inhibit $V_H$ accessibility and looping, and induce differentiation of pro-B cells into large cycling pre-B cells (Alt et al., 2013; Cobb et al., 2006; Melchers, 2005). The IL-7 cytokine drives proliferation of large cycling pre-B cells (Alt et al., 2013; Cobb et al., 2006; Herzog et al., 2009; Melchers, 2005). After several cellular divisions, large pre-B cells attenuate IL-7 signaling, arrest in G1 phase, and differentiate into small pre-B cells. This transition coincides with re-initiation of *Rag1/Rag2* transcription and activation of *Igκ* locus accessibility and looping to promote *Vκ*-to-*Jκ* recombination (Corfe and Paige, 2012; Malin et al., 2010a; Milne and Paige, 2006). The expression of in-frame *Igκ* genes generates Igκ proteins that can pair with Igμ peptides to form $Ig\kappa^+$ BCRs. Receptors that do not bind self-antigens activate signals that cease *Rag1/Rag2* transcription and promote differentiation of immature transitional B cells that migrate to the spleen and develop into mature B cells (Clark et al., 2014; Malin et al., 2010b). In contrast, auto-reactive BCRs transduce signals that either induce apoptosis to eliminate self-reactive cells or re-initiate *Rag1/Rag2* transcription and *Igκ* recombination to provide cells chances to assemble innocuous BCRs through receptor editing (Pillai and Cariappa, 2009). Pre-B cells also can initiate *Vλ*-to-*Jλ* recombination of accessible *Igλ* loci, which can lead to expression of $Ig\lambda^+$ BCRs that signal

differentiation into mature Igλ$^+$ B cells (Nemazee, 2006; Rajewsky, 1996; Schlissel, 2007). Although most pre-B cells recombine *Igκ* loci before *Igλ* loci, the mechanisms by which pre-B cells initiate recombination of *Igκ* versus *Igλ* loci and differentiate into Igκ$^+$ versus Igλ$^+$ B cells remain enigmatic (Nemazee, 2006).

The RAG1 and RAG2 proteins are each comprised of ”core” regions, defined as the minimal sequences required for DNA cleavage *in vitro*, and noncore regions that exhibit additional biochemical activities (Matthews and Oettinger, 2009; Sadofsky, 2004b; Schatz and Swanson, 2011b). In humans, mutations that truncate or disrupt noncore regions of RAG1 or RAG2 can cause severe combined immunodeficiency (SCID) or Omenn Syndrome, a SCID-like condition with more substantial defects in the development of B cells than T cells, altered TCR repertoire, autoimmunity, and atopy (Luning Prak et al., 2011; Oberdoerffer et al., 2003). Mice expressing "core", but not full-length, Rag1 (*Rag1*$^{C/C}$ mice) or Rag2 (*Rag2*$^{C/C}$ mice) protein exhibit reduced levels and altered repertoires of D-to-J and V-to-DJ rearrangements at *IgH* and *Tcrβ* loci in pro-B/T cells, and develop lower numbers of pre- and mature B and T cells (Santagata et al., 2000; Sobacchi et al., 2006; Wong and Roth, 2007). Evidence indicates that the shared phenotypes of humans and mice compromised in noncore regions of RAG1 or RAG2 result from decreased recombinase activity (Akamatsu et al., 2003; Dudley et al., 2003; Liang et al., 2002). Yet, considering that the noncore regions of RAG1 and RAG2 each exhibit distinct biochemical activities, RAG1 and RAG2 likely regulate antigen receptor gene assembly through different mechanisms (Horowitz and Bassing, 2014; Lee et al., 2014; Liang et al., 2002). The carboxy-terminus noncore RAG2 region contains a PHD domain that binds tri-methylated histone H3 proteins along transcribing genes to increase V(D)J recombination (Matthews and Oettinger, 2009; Sadofsky, 2004; Schatz and Swanson, 2011) and a motif that restricts RAG2 expression and therefore RAG

cleavage to G1 phase cells (Liu et al., 2007; Matthews et al., 2007). The amino-terminus noncore regions of Rag1 include a Really Interesting New Gene (RING) domain with E3 ubiquitin ligase activity and sequences that interact with a distinct ubiquitin ligase complex, a kinase, histones, DNA damage response proteins, and at least one transcription factor (Li et al., 1996). The discoveries of these biochemical activities have led to hypotheses linking the noncore regions of RAG1 to modulating antigen receptor gene assembly through ubiquitylating proteins to promote Ig/TCR locus accessibility and transducing signals following incursion of RAG DNA breaks (Coster et al., 2012; Grazini et al., 2010; Jones et al., 2011; Kassmeier et al., 2012; Kim et al., 2013; Maitra and Sadofsky, 2009; Raval et al., 2008; Yurchenko et al., 2003). However, evidence for roles of the noncore RAG1 regions in regulating these or other aspects of antigen receptor gene assembly within the context of developing lymphocytes *in vivo* remain unreported.

The mouse Ig$\kappa^+$ and Ig$\lambda^+$ B cell developmental program provides a physiologic experimental system to elucidate potential functions of the noncore RAG1 regions in modulating V(D)J recombination *in vivo*. Changes in the control of *Ig$\kappa$* or *Ig$\lambda$* accessibility can affect recombination of *Ig$\kappa$* or *Ig$\lambda$* loci, and as a result, alter the frequencies of Ig$\kappa^+$ and Ig$\lambda^+$ B cells (Dudley et al., 2003; Grazini et al., 2010; Horowitz and Bassing, 2014; Jones et al., 2011; Sadofsky, 2004; Simkus et al., 2007). In addition, RAG cleavage of *Ig$\kappa$* loci during *V$\kappa$*-to-*J$\kappa$* recombination activates intracellular signals that promote pre-B cell survival by inducing transcription of *Pim2* (Beck et al., 2009; Gorman et al., 1996; Inlay et al., 2002; Takeda et al., 1993; Xu et al., 1996; Zou et al., 1993), which encodes a pro-survival kinase that facilitates the development of Ig$\lambda^+$ B cells (Bednarski et al., 2012; Bredemeyer et al., 2008). By analyzing Ig$\kappa^+$ and Ig$\lambda^+$ B cell development in *Rag1$^{C/C}$* mice, we demonstrate here that the Rag1 protein has non-cleavage functions that enhance IgL locus accessibility, transduce pro-survival signals during IgL

recombination to promote Igκ$^+$ and Igλ$^+$ B cell development, and establish a normal Igκ$^+$ and Igλ$^+$ B cell repertoire.

**Materials and Methods**

**Mice.** *Rag1$^{c/c}$* (Derudder et al., 2009), *EμBCL2* (Dudley et al., 2003), *IgH$^{Tg}$* (Strasser et al., 1991), *κ$^{MS}$* (Mandik-Nayak et al., 2006), *Rag1*$^{-/-}$ (Ait-Azzouzene et al., 2005), *Rag1$^{D708A}$* (Mombaerts et al., 1992), and *Rag2$^{del352/del352}$* (Ji et al., 2010b) mice were used and bred together generate all of the mice described in this study. All experimental mice were of a mixed 129SvEv and C57BL/6 background and were littermate or age-matched mice between 4-6 weeks of age unless otherwise noted. All studies were conducted in accordance with national guidelines and approved by the Institutional Animal Care and Use Committee of the Children's Hospital of Philadelphia.

**Flow cytometry and cell sorting.** Cells isolated from BM and spleens were depleted of red blood cells with $NH_4Cl$ lysis buffer and FC receptors were blocked using anti-CD16/CD32 (2.4G2; BD). Single cell suspensions were stained in PBS containing 2% BSA using the following antibodies: PE anti-mouse Igκ (187.1; BD), PE-Cy7 anti-mouse B220 (RA3-6B2; BD), PE-Cy7 anti-mouse CD19 (1D3: BD), FITC anti-mouse CD43 (S7; BD), PE anti-mouse CD21/CD35 (7G6; BD), biotin anti-mouse CD23 (B3B4; BD), APC anti-mouse IgM (II/41; BD), PE anti-mouse Igκ (187.1; BD), FITC anti-mouse Igλ (R26-46; BD), and FITC anti-Streptavadin (BD). Data was acquired on a FACSCalibur (BD Biosciences, San Jose, CA) using CellQuest software (BD Biosciences) and analyzed using FlowJo software (Tree Star). Cell sorting was conducted using a MoFlo Astrios (Beckman Coulter, Inc.) using PE-Cy7 anti-mouse CD19 and FITC anti-mouse CD43 to identify pre-B cells.

**BrdU labeling.** A BrdU Flow kit (BD Pharmingen) was used for labeling of DNA with BrdU (5-bromo-2-deoxyuridine) according to the manufacturer's instructions. Intraperitoneal injections of 0.2 mg/ml BrdU in 100uL were performed on mice every 12 hours over a 72-hour period. BM cells were analyzed by flow cytometry. Control mice were not injected with BrdU.

***Vλ1-Jλ1* recombination assays.** PCR reactions with the *Igλ* and HuR control primers were performed on DNA (100 ng and 1:5 serial dilutions) from sorted pre-B cells. PCR conditions were 94°C for 3 min; 40 cycles of 94°C for 45 s, 65°C for 90 s, 72°C for 2.5 min; and 72°C for 10 min. Primers used to detect *Vλ1-Jλ1* recombination and *HuR* loading control were: *Vλ1* forward, 5'- GCCATTTCCCAGGCTGTTGTGACTCAGG-3' and *Jλ1* reverse, 5'-AGGACAGTCAGTTTGGTTCC-3'; *HuR* forward, 5'-AGGCAGATGAGCACATGTGA-3', *HuR* reverse, 5'-AGGCTCTGGGATGAAACCTA-3'.

**RT-PCR.** Total RNA was isolated from sorted pre-B cells using the Trizol Reagent (Ambion). RNA was incubated with DNAse (Promega) to destroy contaminating DNA. cDNA was synthesized using ProtoScript First Strand cDNA synthesis Kit (New England BioLabs) as described (Liang et al., 2002). Primers used to detect *Jκ* and *Jλ* germline transcripts were: *Jκ1* forward, 5'- ACCAAGCTGGAAATCAAACG-3' and *Jκ1* reverse, 5'-CCAGCTTTGCTTACGGAGTT-3'; *Jλ1* forward 5'-AGCTGCATACATCACAGATGC-3' and *Jλ1* reverse, 5'-AGGTGGAAACAGGGTGACTG-3'. Levels of *Pim2, Jκ1, and Jλ1* were calculated using ΔΔCt analysis relative to levels of *Hprt1* in *WT* or *Rag1*$^{-/-}$cells as indicated.

**StyI restriction enzyme digests.** Nuclei were isolated and digested with Sty1 as described (Brady et al., 2010). Nuclease sensitivity was determined by performing qPCR using described primers and methods (Trotter and Archer, 2012).

**Primary pre-B cell cultures.** BM was isolated from 4-6 week old mice and cultured for 5-7 days at 5 x $10^6$ cells/ml in medium containing 1ng/mL IL-7 (Bevington and Boyes, 2013; Grange and Boyes, 2007). For IL-7 withdrawal experiments, cells were harvested, washed in PBS, and re-suspended at 5 x $10^6$ cells/ml in medium lacking IL-7 for the time indicated.

**Abl pre-B cell studies.** Two independent *EμBCL2:Artemis*$^{-/-}$ and two independent *EμBCL2:Artemis*$^{-/-}$ Abl lines were made from two *EμBCL2:Artemis*$^{-/-}$ and two *EμBCL2:Artemis*$^{-/-}$ mice, respectively. STI571 treatments were conducted using 5 μM STI571 as described (Bednarski et al., 2012; Steinel et al., 2013). Irradiation with 4 Gy was carried out as described (Bednarski et al., 2012; Bredemeyer et al., 2008).

**Southern blot analysis.** Southern blot analysis of RAG coding ends at the Igκ locus was performed on DNA digested with *Bam*HI as described (Bednarski et al., 2012; Bredemeyer et al., 2008; Muljo and Schlissel, 2003; Steinel et al., 2013).

## Results

### The noncore regions of Rag1 promote Igλ$^+$ B cell development and help establish a normal Igκ$^+$ and Igλ$^+$ B cell repertoire.

To identify potential unique functions of the noncore regions of Rag1 in modulating V(D)J recombination *in vivo*, we first quantified Igκ$^+$ and Igλ$^+$ B cells in *Rag1*$^{C/C}$, *Rag2*$^{C/C}$, and wild-type (*WT*) mice at 4-6 weeks of age when the mature B cell compartment is still expanding (Bednarski et al., 2012; Bredemeyer et al., 2008; Steinel et al., 2013). We observed equivalent frequencies of BM and splenic Igκ$^+$ B cells between *Rag1*$^{C/C}$ mice and *WT* mice and modestly lower frequencies of these populations in *Rag2*$^{C/C}$ mice (Figure 3.1, A and B). In contrast, we observed 2-3-fold lower frequencies of BM and splenic Igλ$^+$ B cells in *Rag1*$^{C/C}$ mice compared to *WT* mice, but 3-5-fold greater frequencies of these populations in *Rag2*$^{C/C}$ mice relative to *WT* mice and 8-fold greater frequencies of these populations in *Rag2*$^{C/C}$ mice relative to Rag1$^{C/C}$ mice (Figure 3.1 A and B). The numbers of Igκ$^+$ B cells were below normal but comparable between *Rag1*$^{C/C}$ and *Rag2*$^{C/C}$ mice, while Igλ$^+$ B cell numbers were lower than normal in *Rag1*$^{C/C}$ and Rag2$^{C/C}$ mice (Figure 3.1 C). Consistent with the greater loss of Igλ$^+$ versus Igκ$^+$ B cells in *Rag1*$^{C/C}$ mice, the level of *Vλ*-to-*Jλ* recombination (Figure 3.1 D), but not *Vκ*-to-*Jκ* recombination (Allman et al., 1993), is lower than normal in *Rag1*$^{C/C}$ pre-B cells. Finally, as compared to *WT* and *Rag1*$^{C/C}$ mice, we detected ~3-fold higher frequencies of dual-Igκ$^+$/Igλ$^+$ B cells in the BM and spleens of *Rag2*$^{C/C}$ mice (Figure 3.1 A and E). These distinct phenotypes suggest that the noncore regions of RAG1 and RAG2 have unique functions in regulating IgL recombination and Igκ$^+$ and Igλ$^+$ B cell development. Yet, this interpretation is confounded because this strain of *Rag2*$^{C/C}$ mice (Dudley et al., 2003; Liang et al., 2002) was recently shown to express a

more extensively truncated Rag2 protein (amino acids 1-352) than the core Rag2 protein (amino acids 1-383)(Liang et al., 2002). These renamed *Rag2*$^{del352/del352}$ mice exhibit a V(D)J joining defect not observed in *Rag1*$^{C/C}$ mice (Gigi et al., 2014; Liang et al., 2002) that, as explained in our discussion, could account for increased frequencies of Ig$\lambda^+$ and dual-Ig$\kappa^+$/Ig$\lambda^+$ B cells. Thus, our comparison of B cell development between *Rag1*$^{C/C}$ and *Rag2*$^{del352/del352}$ mice cannot distinguish whether the more pronounced impairment in generation of Ig$\lambda^+$ versus Ig$\kappa^+$ B cells in *Rag1*$^{C/C}$ mice is caused by decreased recombinase activity versus loss of unique functions of noncore regions of Rag1.

Since the only additional strain of *Rag2*$^{C/C}$ mice (Deriano et al., 2011) is not available, we conducted three independent and complementary experiments to assess whether lower recombinase activity in *Rag1*$^{C/C}$ mice contributes to the more impaired development of Ig$\lambda^+$ versus Ig$\kappa^+$ B cells. First, we assayed the rates at which Ig$\kappa^+$ and Ig$\lambda^+$ B cells arise from pre-B cells in 4-6 week old *Rag1*$^{C/C}$ and *WT* mice, reasoning that lower recombinase activity would delay the rate of appearance of Ig$\lambda^+$ B cells more than the rate of appearance of Ig$\kappa^+$ B cells since *Ig*$\kappa$ recombination and development of Ig$\kappa^+$ cells occurs before *Ig*$\lambda$ recombination and development of Ig$\lambda^+$ cells (Akamatsu et al., 2003). To do this, we conducted repeated intraperitoneal injection of BrdU into *WT* and *Rag1*$^{C/C}$ mice to label B lineage cells as they differentiate from the pro-B cell stage to the pre-B cell stage, and then over time quantified the numbers and frequencies of BrdU$^+$ BM Ig$\kappa^+$ and Ig$\lambda^+$ B cells. At all time points assayed, we detected fewer Ig$\kappa^+$ and Ig$\lambda^+$ B cells that had incorporated BrdU in *Rag1*$^{C/C}$ mice as compared to *WT* mice (Figure 3.2 A), consistent with the lower than normal numbers of pre-B cells in *Rag1*$^{C/C}$ mice (Nemazee, 2006; Rajewsky, 1996). In contrast, we detected no differences in the rates of BrdU incorporation into Ig$\kappa^+$ B cells between *Rag1*$^{C/C}$ and *WT* mice or into Ig$\lambda^+$ B cells

between *Rag1*$^{C/C}$ and *WT* mice (Figure 3.2 B), demonstrating that Ig$\kappa^+$ and Ig$\lambda^+$ B cells each develop at a normal rate in *Rag1*$^{C/C}$ mice. Second, we quantified Ig$\kappa^+$ and Ig$\lambda^+$ B cells in *Rag1*$^{C/C}$ and *WT* mice at 5 months of age when the mouse mature B cell compartment has completely expanded (Dudley et al., 2003), reasoning that the size of the *Rag1*$^{C/C}$ Ig$\lambda^+$ B cell pool would normalize over time if the impaired development of these cells is caused by lower recombination efficiency. We observed similar numbers of total, immature transitional (T)2, and mature marginal zone and follicular B cells between the spleens of 5-month-old *Rag1*$^{C/C}$ and *WT* mice (Figure 3.2 C), revealing that older *Rag1*$^{C/C}$ mice contain normal sized pools of mature B cells. Still, we detected the same patterns of lower frequencies and numbers of BM (Figure 3.2 D - F) and splenic (unpublished data) Ig$\lambda^+$ B cells in these *Rag1*$^{C/C}$ mice compared to *WT* control mice, indicating that the impaired generation of Ig$\lambda^+$ B cells persists in older mice with a replete mature B cell compartment. Consistent with this notion, these older *Rag1*$^{C/C}$ mice exhibit a similar lower output of immature T1 B cells from pre-B cells as younger *Rag1*$^{C/C}$ mice (Figure 3.2 C). Finally, we quantified Ig$\lambda^+$ B cells in *WT* and *Rag1*$^{C/C}$ mice that can only develop Ig$\lambda^+$ B cells, reasoning that forcing *Ig*$\lambda$ expression would normalize Ig$\lambda^+$ B cell development if reduced recombinase activity were the cause of impaired Ig$\lambda^+$ B cell development in *Rag1*$^{C/C}$ mice. Transgenic $\kappa$-macroself ($\kappa^{MS}$) mice expressing a membrane-tethered anti-Ig$\kappa$-reactive antibody develop only Ig$\lambda^+$ B cells since all developing $\kappa^{MS}$ Ig$\kappa^+$ B cells are auto-reactive and edit to Ig$\lambda$ expression (Allman et al., 1993). Thus, we made and analyzed $\kappa^{MS}$*Rag1*$^{C/C}$ mice, which only develop Ig$\lambda^+$ B cells (Figure 3.2 G). We found lower numbers of BM (Figure 3.2 H) and splenic (unpublished data) Ig$\lambda^+$ B cells in $\kappa^{MS}$*Rag1*$^{C/C}$ mice compared to $\kappa^{MS}$ mice, demonstrating that *Rag1*$^{C/C}$ mice have a defect in producing Ig$\lambda^+$ B cells even when forced to do so via editing of

auto-reactive Igκ$^+$ B cells. Collectively, these data suggest that the more impaired development of Igλ$^+$ versus Igκ$^+$ B cells in *Rag1*$^{C/C}$ mice is not simply due to lower recombinase activity, but likely is caused by loss of unique functions of the noncore Rag1 regions.

**The noncore regions of Rag1 promote Igκ$^+$ B cell development.**

Our data above show that *Rag1*$^{C/C}$ mice exhibit a pronounced defect in the generation of Igλ$^+$ B cells from pre-B cells. However, they are equivocal as to whether *Rag1*$^{C/C}$ mice have a similar defect in Igκ$^+$ B cell development, as decreased numbers of Igκ$^+$ B cells may result solely from fewer pre-B cells caused by impaired IgH recombination and resultant expansion of pro-B cells (Ait-Azzouzene et al., 2005). To evaluate whether the noncore regions of Rag1 promote Igκ$^+$ B cell development, we generated and analyzed *Rag1*$^{C/C}$ mice expressing an *IgH* transgene that drives pro-B to pre-B cell expansion independent of endogenous *IgH* gene assembly. For this experiment, we chose *IgH* transgenic (*IgH*$^{Tg}$) mice that generate auto-reactive BCRs at a higher frequency than normal (Mandik-Nayak et al., 2006) so that we also could evaluate whether the noncore Rag1 regions promote Igλ$^+$ B cell development in a setting where creation of these cells from receptor editing would be increased. Consistent with increased receptor editing, we detected a lower frequency of Igκ$^+$ B cells and a greater frequency of Igλ$^+$ B cells in *IgH*$^{Tg}$ mice compared to *WT* mice (Figure 3.3 A and B). Reflecting roles for noncore Rag1 regions in promoting Igλ$^+$ B cell development, we observed a higher frequency of Igκ$^+$ B cells and lower frequency and number of Igλ$^+$ B cells in *IgH*$^{Tg}$*Rag1*$^{C/C}$ mice relative to *IgH*$^{Tg}$ mice (Figure 3.3 A - C). Notably, despite similar numbers of pre-B cells in *IgH*$^{Tg}$ and *IgH*$^{Tg}$*Rag1*$^{C/C}$ mice (Figure 3.3 D), we

detected a 2-fold reduction in Igκ$^+$ B cell numbers in *IgH$^{Tg}$Rag1$^{C/C}$* mice relative to *IgH$^{Tg}$* mice (Figure 3.3 C), showing that *Rag1$^{C/C}$* mice are compromised in the ability to generate Igκ$^+$ B cells from pre-B cells. These data demonstrate that the noncore regions of Rag1 promote both Igκ$^+$ and Igλ$^+$ B cell development.

**The Rag1 protein promotes *Igκ* and *Igλ* locus accessibility independent of RAG endonuclease activity.**

The noncore regions of Rag1 have been suggested to promote accessibility of Ig/TCR loci for V(D)J recombination (Dudley et al., 2003). To test whether the impaired development of Igλ$^+$ and Igκ$^+$ B cells in *Rag1*$^{C/C}$ mice reflects critical function of the noncore Rag1 regions in enhancing IgL locus accessibility, we first quantified steady-state levels of Igλ and Igκ germline transcripts in pre-B cells sort-purified from *Rag1*$^{C/C}$ and *WT* mice (Figure 3.4 A). We measured germline *Jλ1* transcripts because Rag1 binds D and J but not V segments (Ji et al., 2010), and *Jλ1* is the most frequently rearranged *Jλ* segment (Grazini et al., 2010; Sadofsky, 2004). We detected a 2-fold lower level of germline *Jλ1* transcripts in *Rag1*$^{C/C}$ pre-B cells compared to *WT* pre-B cells (Figure 3.4 B), consistent with a role for the noncore regions of Rag1 in stimulating *Igλ* accessibility. In contrast to *Jλ1* transcripts, we detected no difference in the levels of germline *Jκ1* transcripts between *Rag1*$^{C/C}$ and *WT* pre-B cells (Figure 3.4 B). These data suggest that the noncore Rag1 regions stimulate *Igλ* but not *Igκ* accessibility. However, the ability of accessible *Jκ* and *Jλ* gene segments to undergo recombination in *Rag1*$^{C/C}$ and *WT* cells and the potential differences in activation of pro-survival signals by RAG DSBs in *WT* and *Rag1*$^{C/C}$ pre-B cells complicate this interpretation. In addition, the heterogeneous nature of the pre-B cell population consisting of IL-7-responding cells with inaccessible *Igκ* loci and IL-7-attenuated cells with accessible *Igκ* loci could mask differences in *Jκ* accessibility between *Rag1*$^{C/C}$ and *WT* pre-B cells.

To definitively determine whether Rag1 enhances IgL locus accessibility, we quantified germline *Jλ* and *Jκ* transcripts in small non-cycling pre-B cells lacking Rag1 protein (*Rag1*$^{-/-}$ cells) or expressing a mutant full-length Rag1 protein that contains an

aspartic acid to alanine mutation at position 708 in the catalytic core (*Rag1*$^{D708A}$ cells). This Rag1$^{D708A}$ protein binds germline D/J segments and the Rag2 protein, but resulting RAG complexes cannot cleave DNA to initiate V(D)J recombination (Haque et al., 2013; Nadel et al., 1990; Sanchez et al., 1991). We first used v-Abl transformed pro-B (Abl) cell lines created from *Rag1*$^{-/-}$ mice or *Rag1*$^{D708A}$ mice. Proliferating Abl cells do not express RAG proteins or catalyze V(D)J recombination; addition of the Abl kinase inhibitor STI571 induces their differentiation into pre-B cells concomitant with their arrest in G1 phase, expression of Rag1/Rag2, and accessibility and recombination of IgL loci (Ji et al., 2010a). We placed *Rag1*$^{-/-}$ and *Rag1*$^{D708A}$ Abl cells in STI571 to cause a G1 arrest, induce Rag1/Rag2 protein expression, and activate IgL accessibility. In these cells, we detected no change in germline *Jκ1* transcripts, but a ~2-fold higher level of germline *Jλ*1 transcripts, in *Rag1*$^{D708A}$ cells as compared to *Rag1*$^{-/-}$ cells (Figure 3.4 C). We next assayed primary pre-B cells from *IgH*$^{Tg}$*Rag1*$^{-/-}$ mice and *IgH*$^{Tg}$*Rag1*$^{-/-}$ mice expressing the *Rag1*$^{D708A}$ transgene (*IgH*$^{Tg}$*Rag1*$^{D708A}$ mice). The expression of a pre-assembled *IgH* transgene in *Rag1*$^{-/-}$ or R*ag1*$^{D708A}$ mice promotes differentiation of pre-B cells (Muljo and Schlissel, 2003). Since IL-7 drives pre-B cell proliferation and represses IgL accessibility and *Rag1/Rag2* expression (Ji et al., 2010a), we cultured primary BM cells from *IgH*$^{Tg}$*Rag1*$^{-/-}$ and *IgH*$^{Tg}$*Rag1*$^{D708A}$ mice in IL-7 to isolate and expand pre-B cells lacking RAG expression. We then withdrew IL-7 from the culture medium to cause a G1 arrest, induce Rag1 and Rag2 protein expression, and activate IgL accessibility (Corfe and Paige, 2012; Malin et al., 2010b; Milne and Paige, 2006). Using this system, we observed ~2-fold higher levels of germline *Jκ1* and *Jλ1* transcripts in these *IgH*$^{Tg}$*Rag1*$^{D708A}$ cells compared to control *IgH*$^{Tg}$*Rag1*$^{-/-}$ cells (Figure 3.4 D), revealing a role for Rag1 in enhancing *Igλ* and *Igκ* accessibility. Collectively, these data indicate that

the Rag1 protein stimulates IgL locus accessibility independent of RAG endonuclease activity.

To more rigorously assess whether RAG1 enhances IgL locus accessibility, we quantified the sensitivity of germline *Igκ* and Igλ segments to restriction enzyme digestion. We measured the ability of the StyI restriction enzyme to cleave at Jκ3 and Jλ1 in nuclei isolated from STI571-treated *Rag1*$^{-/-}$ and *Rag1*$^{D708A}$ Abl cells and IL-7-withdrawn *IgH*$^{Tg}$*Rag1*$^{-/-}$ and *IgH*$^{Tg}$ *Rag1*$^{D708A}$ primary pre-B cells. After incubating nuclei with or without Sty1, we conducted qPCR to amplify across Sty1 sites in *Jκ3* or *Jλ1* and then calculated the percent of cleaved DNA at each segment as a measure of accessibility (Figure 3.4 A). Using Abl cell lines, we detected ~3-5-fold greater accessibility of *Jκ3* and *Jλ1* in cells expressing Rag1$^{D708A}$ relative to cells lacking Rag1 protein (Figure 3.4 E). We next assayed primary pre-B cells from *IgH*$^{Tg}$*Rag1*$^{-/-}$ mice and *IgH*$^{Tg}$*Rag1*$^{D708A}$ mice. In these cells, we observed ~2-fold higher accessibility of *Jκ3* and *Jλ1* in cells expressing Rag1$^{D708A}$ relative to cells lacking Rag1 protein (Figure 3.4 F). Based on the increased levels of transcripts and Sty1 digestion of Jκ3 and Jλ1 segments in pre-B cells expressing Rag1$^{D708A}$ relative to pre-B cells lacking Rag1 protein, we conclude that Rag1 stimulates IgL locus accessibility independent of RAG endonuclease activity.

**The noncore regions of Rag1 activate pro-survival signals following RAG cleavage of *Igκ* loci.**

RAG cleavage of *Igκ* loci activates intracellular signals that promote pre-B cell survival by inducing transcription of *Pim2* (Bednarski et al., 2012; Steinel et al., 2013). *Pim2* encodes a protein kinase required for the development of a normal frequency of Igλ$^{+}$ B cells (Bednarski et al., 2012; Bredemeyer et al., 2008). Accordingly, the impaired

development of Igκ$^+$ and Igλ$^+$ B cells in *Rag1$^{C/C}$* mice could arise from decreased induction of *Pim2* expression upon RAG cleavage during *Vκ*-to-*Jκ* recombination. To evaluate whether noncore Rag1 regions are necessary to activate *Pim2* transcription following RAG cleavage of *Igκ* loci, we first quantified steady-state *Pim2* transcripts in pre-B cells from *Rag1$^{C/C}$* and *WT* mice. We detected ~2-fold lower levels of *Pim2* transcripts in *Rag1$^{C/C}$* pre-B cells as compared to WT pre-B cells (Figure 3.5 A). This observation is consistent with a role for noncore Rag1 regions in activating *Pim2* expression after RAG cleavage. However, it also could reflect a role for Rag1 in control of *Pim2* transcription independent of RAG cleavage. Thus, we next quantified *Pim2* transcripts following IL-7 withdrawal from *IgH$^{Tg}$Rag1$^{-/-}$* and *IgH$^{Tg}$Rag1$^{D708A}$* primary pre-B cells. We observed no induction of *Pim2* transcripts in *IgH$^{Tg}$Rag1$^{-/-}$* or *IgH$^{Tg}$Rag1$^{D708A}$* pre-B cells (Figure 3.5 B), indicating Rag1 does not control *Pim2* transcription in the absence of RAG endonuclease activity. Accordingly, our data suggest that the noncore Rag1 regions are required for RAG DNA cleavage in pre-B cells to transduce signals that activate *Pim2* transcription.

To unequivocally identify whether the noncore regions of Rag1 are necessary to activate *Pim2* expression in response to RAG DNA cleavage, we used Abl cell lines established from mice lacking the Artemis non-homologous end-joining factor and expressing the anti-apoptotic *EμBCL2* transgene. RAG DNA cleavage in *Artemis$^{-/-}$* cells generates chromosomal DNA double strand breaks (DSBs) that cannot be processed and repaired (Derudder et al., 2009). BCL2 expression prevents apoptosis from DSBs, enabling accumulation of un-repaired RAG DSBs at *Igκ* loci in *Artemis$^{-/-}$* cells and thus amplification of signals from RAG DSBs (Moshous et al., 2001; Rooney et al., 2003). Thus, to determine whether the noncore regions of Rag1 are necessary to activate *Pim2* transcription during *Igκ* recombination, we created and analyzed *Artemis$^{-/-}$* and

*Artemis*$^{-/-}$*Rag1*$^{C/C}$ Abl cells. Reflecting the normal level of *Vκ*-to-*Jκ* recombination in *Rag1*$^{C/C}$ pre-B cells (Bednarski et al., 2012; Bredemeyer et al., 2008; Savic et al., 2009; Steinel et al., 2013), we detected similar amounts of RAG DSBs at *Jκ* segments in *Artemis*$^{-/-}$ and *Artemis*$^{-/-}$*Rag1*$^{C/C}$ cells (Figure 3.5 C and D). Consistent with published data (Dudley et al., 2003), we detected a ~5-fold induction of *Pim2* transcript levels following STI571 addition to *Artemis*$^{-/-}$ Abl cells (Figure 3.5 D). In contrast, we observed no induction of *Pim2* transcripts following STI571 treatment of *Artemis*$^{-/-}$*Rag1*$^{C/C}$ Abl cells (Figure 3.5 E), suggesting that the noncore regions of Rag1 are necessary for RAG DSBs to signal activation of *Pim2* expression. Although we observed consistent results between two independent lines of each genotype, we considered that v-Abl immortalization of *Artemis*$^{-/-}$*Rag1*$^{C/C}$ cells might have disrupted the ability of DSBs to activate *Pim2* transcription. To test this possibility, we evaluated the ability of DSBs induced by ionizing radiation (IR) to activate *Pim2* expression in *Artemis*$^{-/-}$ and *Artemis*$^{-/-}$*Rag1*$^{C/C}$ Abl cells. We observed that IR triggers a ~2-fold increase of *Pim2* transcripts in our experimental *Artemis*$^{-/-}$ and *Artemis*$^{-/-}$*Rag1*$^{C/C}$ lines (Figure 3.5 F), showing that *Artemis*$^{-/-}$*Rag1*$^{C/C}$ Abl pre-B cells exhibit normal ability to induce *Pim2* expression in response to exogenous DSBs. Collectively, our data indicate that the non-core regions of Rag1 are necessary for RAG DSBs to signal transcriptional activation of *Pim2* expression during *Igκ* recombination.

Pim2 promotes survival of pre-B cells rearranging *Igκ* genes (Bredemeyer et al., 2008) and *Pim2*$^{-/-}$ mice exhibit an identical reduction in the frequency of Igλ$^{+}$ B cells as *Rag1*$^{C/C}$ mice (Bednarski et al., 2012; Derudder et al., 2009)(Figure 3.1). To evaluate whether the noncore regions of Rag1 promote Igλ$^{+}$ B cell development by enabling RAG DSBs to enhance pre-B cell survival and thereby provide more opportunities for *Vλ*-to-*Jλ*

recombination, we made and analyzed *Rag1*$^{C/C}$ mice expressing the anti-apoptotic *E*$\mu$*BCL2* transgene. Here, we observed no differences in the numbers or frequencies of Ig$\kappa^+$ B cells and Ig$\lambda^+$ B cells between *E*$\mu$*BCL2:Rag1*$^{C/C}$ mice and control *E*$\mu$*BCL2* mice (Figure 3.6 A - C), indicating that providing pre-B cells a constitutive pro-survival signal rescues the impaired development of Ig$\lambda^+$ B cells in *Rag1*$^{C/C}$ mice. To assess whether BCL2 also rescues Ig$\lambda$ accessibility, we quantified germline *J*$\lambda$*1* transcripts in *E*$\mu$*BCL2* and *E*$\mu$*BCL2:Rag1*$^{C/C}$ pre-B cells. We detected a ~2-fold reduced level of *J*$\lambda$*1* transcripts in *E*$\mu$*BCL2:Rag1*$^{C/C}$ cells as compared to *E*$\mu$*BCL2* cells (Figure 3.6 D), identical to the difference in *J*$\lambda$*1* transcripts between *Rag1*$^{C/C}$ and *WT* mice (Figure 3.4 C), confirming that neither BCL2 expression nor enhanced survival of pre-B cells increases *Ig*$\lambda$ accessibility. These data demonstrate that the noncore regions of Rag1 are required for RAG DSBs to transduce signals that activate *Pim2* to enhance pre-B cell survival, promote Ig$\lambda^+$ B cell development, and ensure generation of a normal Ig$\kappa^+$ and Ig$\lambda^+$ B cell repertoire.

**Discussion**

Here, we have analyzed *Rag1*$^{C/C}$ mice and *Rag1*$^{-/-}$ and Rag1$^{D708A}$ pre-B cells to identify potential unique non-cleavage functions of RAG1 in regulating V(D)J recombination *in vivo*. Our data show that *Rag1*$^{C/C}$ mice exhibit pronounced defects in *Vλ*-to-*Jλ* recombination and development of Igλ$^+$ B cells from pre-B cells and a less severe deficiency in generation of Igκ$^+$ B cells from pre-B cells. Our data also demonstrate that the noncore regions of Rag1 both enhance IgL locus accessibility independent of RAG endonuclease activity and signal up-regulation of *Pim2* expression in response to RAG cleavage of *Igκ* loci. Our finding that BCL2 expression rescues Igλ$^+$ B cell development in *Rag1*$^{C/C}$ mice indicates that the noncore regions of Rag1 promote Igλ$^+$ B cell development, at least in part, by activating *Pim2* expression following the incursion of RAG DSBs during *Igκ* recombination. This result provides causal evidence that the ability of the noncore Rag1 regions to activate a pro-survival genetic program during IgL recombination is critical for facilitating Igλ$^+$ B cell development and establishing a normal broad Igκ$^+$ and Igλ$^+$ B cell repertoire. The Pim2-dependent pro-survival signaling function of the noncore regions of Rag1 also may promote the generation of Igκ$^+$ B cells from pre-B cells; however, our experiments do not directly address this potential mechanism. In addition, our experiments cannot provide a conclusion as to whether Rag1-dependent enhancement of IgL locus accessibility promotes Igλ$^+$ and Igκ$^+$ B cell development by stimulating kinetics of IgL gene assembly. Determining contributions of accessibility and pro-survival signaling functions of the noncore Rag1 regions in promoting Igλ$^+$ and Igκ$^+$ B cell development requires elucidating precise mechanisms through which Rag1 mediates these two distinct functions and then generating and analyzing mice with only one of these Rag1 functions inactivated.

Our data that *Rag1*$^{C/C}$ pre-B cells expressing truncated cleavage-competent "core" Rag1 protein exhibit lower than normal levels of germline transcripts and restriction enzyme sensitivity of *Igλ* gene segments reveals that noncore Rag1 regions enhance IgL locus accessibility beyond levels achieved by transcriptional enhancers and promoters. The noncore RAG1 regions contain a RING domain with E3 ubiquitin ligase activity, as well as amino acids that bind the VprBP kinase, which in turn associates with the RING E3 ubiquitin ligase complex DDB1/Cul4A/Roc1 (Bednarski et al., 2012; Derudder et al., 2009). The RAG1 RING domain promotes histone H3 and H3.3 mono-ubiquitylation (Kassmeier et al., 2012; Yurchenko et al., 2003), which at other loci can drive accessibility and transcription by reducing core histone interactions with DNA (Jones et al., 2011; Yurchenko et al., 2003). In response to DNA damage by ultraviolet radiation, DDB1/Cul4A/Roc1 ubiquitylates histones H3 and H4, weakening nucleosome interactions with DNA to promote accessibility to repair factors (Zentner and Henikoff, 2013). *RAG1* mutations that impair RAG1 intrinsic ubiquitin ligase activity and likely alter RAG1 protein structure decrease RAG endonuclease activity within the context of $D_H$-to-$J_H$ recombination in a pro-B cell line (Wang et al., 2006). Accordingly, the noncore RAG1 regions might promote IgL accessibility through RAG1-mediated and/or RAG1-dependent ubiquitylation of histones over RAG1-bound $J_L$ gene segments to enhance removal of nucleosomes from $J_L$ RSSs. Building on an existing model (Grazini et al., 2010; Simkus et al., 2007), RAG1 auto-ubiquitylation, or DDB1/Cul4A/Roc1 ubiquitylation of RAG1, on lysine 233 of the noncore region of RAG1 might promote conformational changes in RAG1 that foster interactions with proteins that stimulate accessibility. However, the noncore RAG1 regions could increase accessibility independent of ubiquitylation by recruiting transcriptional co-activators, such as GMEB1 (Simkus et al., 2007) or chromatin-modifying enzymes. Studies testing the effects of

specific mutations of noncore Rag1 regions and/or Rag1-interacting proteins using *Rag1*$^{D708A}$ cells should help elucidate precise molecular mechanisms by which Rag1 stimulates IgL locus accessibility.

Our finding that full-length, cleavage-incompetent Rag1$^{D708A}$ protein enhances *Igκ* and *Igλ* locus accessibility, while *Rag1*$^{C/C}$ pre-B cells exhibit reduced accessibility and recombination of *Igλ* but not *Igκ* gene segments, has implications for mechanisms that regulate antigen receptor gene assembly. One is that the "core", rather than noncore, regions of RAG1 might enhance *Igκ* accessibility, possibly by recruiting transcription factors and/or chromatin-modifying enzymes. A second possibility is that the 2-fold reduction in *Jκ* accessibility in *Rag1*$^{C/C}$ pre-B cells causes a similar decrease in *Vκ*-to-*Jκ* recombination that is not discernable by PCR analysis of *Igκ* rearrangements. A third possibility is that $J_L$ gene segment accessibility is rate-limiting for *Igλ* but not *Igκ* recombination, so that a 2-fold reduction in *Jλ* accessibility impairs *Vλ*-to-*Jλ* rearrangements while a 2-fold reduction in *Jκ* accessibility has no effect on *Vκ*-to-*Jκ* rearrangements. The current model for V-to-(D)J rearrangements is that the RAG proteins bind accessible D/J segments and then capture and cleave accessible V segments placed in proximity of RAG-D/J recombination centers via chromosome looping (Maitra and Sadofsky, 2009). Evidence suggests that capture/cleavage of accessible V segments is rate limiting for Igκ and TCRβ loci (Ji et al., 2010b; Schatz and Ji, 2011). These loci have large V clusters that contain numerous V segments organized in chromosome loops and recombine across genomic distances of 0.5-2 Mb to D/J gene segments through long-range chromosome looping. While control of *Vλ* recombination has not been investigated in-depth, the *Igλ* locus contains two V-J domains, each containing one Vλ that rearranges to Jλs across distances of 30-80 kb (Bassing et al.,

2008; Casellas et al., 2002; Wu et al., 2003; Xiang et al., 2013). These features of *Vλ*-to-*Jλ* recombination more closely resemble D-to-J recombination of *TCRβ* and *IgH* loci than V-to-(D)J recombination of *Igκ*, *TCRβ*, and *IgH* loci. Considering that *Rag1*$^{C/C}$ mice have similar reductions in Dβ-to-Jβ and $D_H$-to-$J_H$ recombination as Vλ-to-Jλ recombination (Sanchez et al., 1991; Vettermann and Schlissel, 2010), the ability of noncore Rag1 regions to promote recombination by enhancing chromatin accessibility may be most critical for rearrangements that do not proceed via long-range chromosome looping. The creation and analysis of mice expressing specific mutant Rag1 or Rag1$^{D708A}$ proteins should help identify roles and functions of noncore Rag1 regions in promoting accessibility and recombination of each antigen receptor locus.

Our discovery that RAG DSBs induced at *Igκ* loci in *Artemis*$^{-/-}$*Rag1*$^{C/C}$ pre-B cells are unable to up-regulate *Pim2* expression indicates that the noncore regions of Rag1 are necessary for RAG DSBs to transduce signals that activate a pro-survival genetic program. DSBs induced by IR or RAG in pre-B cells activate the ATM kinase, which phosphorylates the NF-κB essential modifier (NEMO) protein to trigger NFκB-mediated *Pim2* transcription (Dudley et al., 2003). The expression of *Pim2* increases pre-B cell survival by antagonizing pro-apoptotic signals (Bednarski et al., 2012; Bredemeyer et al., 2008; Li et al., 2001). In response to IR DSBs, ATM-mediated phosphorylation of nuclear NEMO enables cIAP-mediated mono-ubiquitylation of NEMO, which is required to activate NF-κB following DSBs (Bednarski et al., 2012; Bredemeyer et al., 2008; Muljo and Schlissel, 2003; Steinel et al., 2013). Thus, in response to RAG DSBs, noncore Rag1 regions may activate *Pim2* transcription through RAG1-mediated and/or RAG1-dependent ubiquitylation of ATM-phosphorylated NEMO proteins. This notion is supported by observations that both mice with conditional deletion of *NEMO* in the B cell lineage (*mb1-cre NEMO*$^{f}$ mice) and *Pim2*$^{-/-}$ mice exhibit similar decreases in frequencies

of Igλ$^+$ B cells as *Rag1*$^{C/C}$ mice, and BCL2 expression rescues the frequency of Igλ$^+$ B cells in *mb1-cre NEMO*$^f$ mice (Hinz et al., 2010; Wu et al., 2006). It has been shown that noncore Rag1 regions bind the DSB repair/response protein MDC1, which is phosphorylated by ATM and amplifies a subset of ATM signals (Derudder et al., 2009). We find that *Mdc1*$^{-/-}$ mice exhibit normal Igκ$^+$/Igλ$^+$ B cell ratios (unpublished data), indicating that the noncore regions of Rag1 do not signal ATM-mediated activation of the NEMO-NF-κB-Pim2 pathway by recruiting MDC1 to RAG-cleaved IgL loci. Considering that RAG DSBs also signal gene expression changes via ATM-dependent/NF-κB-independent and ATM/NF-κB-independent pathways (Lou et al., 2006), the noncore regions of Rag1 may transduce ATM-dependent and/or ATM-independent signals that function in parallel with the ATM-NEMO-NF-κB signals to activate *Pim2* transcription. The analysis of intracellular signaling pathways and gene expression changes following the induction of RAG DSBs in *Artemis*$^{-/-}$*Rag1*$^{C/C}$ pre-B cells and *Artemis*$^{-/-}$ pre-B cells with specific mutations of Rag1 and/or Rag1-interacting proteins should help elucidate mechanisms by which Rag1 transduces signals in response to RAG cleavage of IgL loci.

Our finding that *Rag1*$^{C/C}$ and *Rag2*$^{del352/del352}$ mice exhibit opposite deviations from normal Igκ$^+$/Igλ$^+$ B cell ratio provides new insights into how pre-B cells integrate RAG DSB signaling and repair to promote Igκ$^+$ and Igλ$^+$ B cell development. *Rag1*$^{C/C}$ mice have no discernable defect in V(D)J joining (Bredemeyer et al., 2008), indicating that their pre-B cells are defective in pro-survival signaling from RAG DSBs but not repair of RAG DSBs. Our data shows that loss of these pro-survival signals leads to loss of pre-B cells that would normally develop into Igλ$^+$ B cells. *Rag2*$^{del352/del352}$ mice exhibit destabilization of RAG-cleaved DNA ends and therefore impaired V(D)J joining (Deriano et al., 2011), suggesting that their pre-B cells are defective in RAG DSB repair but not

pro-survival signaling from RAG cleavage of IgL loci. It remains to be determined how the destabilization of RAG-cleaved DNA ends increases the development of Igλ$^+$ B cells relative to Igκ$^+$ B cells. One possibility is that RAG-cleaved Igλ loci are inherently more stable than RAG-cleaved Igκ loci due to the simpler organization and smaller size of Igλ loci. Consistent with this notion, *Rag2*$^{del352/del352}$ mice exhibit normal levels of *IgH* and *TCRβ* D-to-J rearrangements across short genomic distances but severely reduced levels of *IgH* and *TCRβ* V-to-DJ rearrangements across large genomic distances (Deriano et al., 2011). The observation that *Atm*$^{-/-}$ mice have normal Igκ$^+$/Igλ$^+$ B cell ratios was used to argue that activation of *Pim2* by RAG DSBs does not promote Igλ$^+$ B cell development (Liang et al., 2002). In addition to their DSB pro-survival signaling defect, *Atm*$^{-/-}$ mice exhibit destabilization of RAG-cleaved DNA ends and impaired V(D)J joining (Derudder et al., 2009). This suggests that increased Igλ$^+$ B cell development from defective V(D)J joining counters decreased generation of Igλ$^+$ B cells from loss of pro-survival signaling. Impaired V(D)J joining and normal DSB signaling may enable pre-B cells with un-repaired RAG-cleaved Igκ loci to initiate Igλ recombination, leading to the assembly of in-frame *VJκ* and *VJλ* coding joins in a greater than normal fraction of pre-B cells, which may explain the increased frequency of dual-Igκ$^+$/Igλ$^+$ B cells in *Rag2*$^{del352/del352}$ mice. The expression of *Rag2*$^{del352}$ at a ~10-fold higher level than full-length Rag2 (Bredemeyer et al., 2006) also might enable cells to be temporarily refractory to RAG DSB-induced, ATM-mediated suppression of Rag1 and Rag2 protein expression (Liang et al., 2002). Similarly, the absence of a conserved consensus ATM phosphorylation motif (amino acids serine 365 and glutamic acid 366) might allow *Rag2*$^{del352}$ to escape ATM-dependent phosphorylation and resultant suppression of RAG nuclease activity before loss of RAG expression. Future generation and analysis of

*Atm*$^{-/-}$*Rag1*$^{C/C}$ mice, *EμBCL2:Atm*$^{-/-}$ mice, and *Rag2*$^{S365A/S365A}$ mice could be used to elucidate precise mechanisms through which pre-B cells integrate RAG DSB signaling and repair to promote Igκ$^{+}$ and Igλ$^{+}$ B cell development.

Our demonstration of non-cleavage functions of RAG1 in modulating accessibility and signaling has broad implications beyond mechanisms that regulate V(D)J recombination. In addition to the ATM-NF-κB pathway, RAG DSBs signal through undefined ATM-dependent and ATM-independent pathways to activate a transcriptional program including genes that encode proteins that regulate the selection of lymphocytes based on antigen-receptor specificity (Bednarski et al., 2012; Bredemeyer et al., 2008; Steinel et al., 2013). Thus, the noncore regions of Rag1 may additionally be critical for activating these and possibly additional unidentified signaling pathways to modulate positive and negative lymphocyte selection, ensuring creation of a robust self-tolerant adaptive immune system. Notably, humans with mutations in noncore RAG1 regions that do not affect RAG recombinase activity develop Omenn syndrome (Bednarski et al., 2012; Bredemeyer et al., 2008; Muljo and Schlissel, 2003; Steinel et al., 2013). Our data suggest that impaired signaling in response to RAG DSBs may contribute to the immune deficiency and autoimmunity of these Omenn Syndrome patients. Further, a recent study has revealed that RAG endonuclease activity in a subset of common lymphoid progenitors leads to elevated expression of DSB repair/response genes in mature NK cells, imparting these innate immune cells with enhanced ability to survive virus-driven proliferation (Lee et al., 2014). This function of RAG outside of V(D)J recombination also is important for endowing mature T cells and other innate lymphoid cell types with a cellular fitness that protects them from apoptosis upon immune response-driven proliferation (Karo et al., 2014). These data lead us to speculate that the accessibility and signaling functions of the noncore Rag1 regions that we have demonstrated here

may be important for the RAG endonuclease to instil cellular fitness in multiple cell types. Therefore, in addition to serving as an essential subunit of the V(D)J recombinase, the RAG1 protein has physiologic functions outside of catalysis of Ig and TCR gene assembly that are critical for the development of an effective immune system.

## Figures

## Figure 3.1

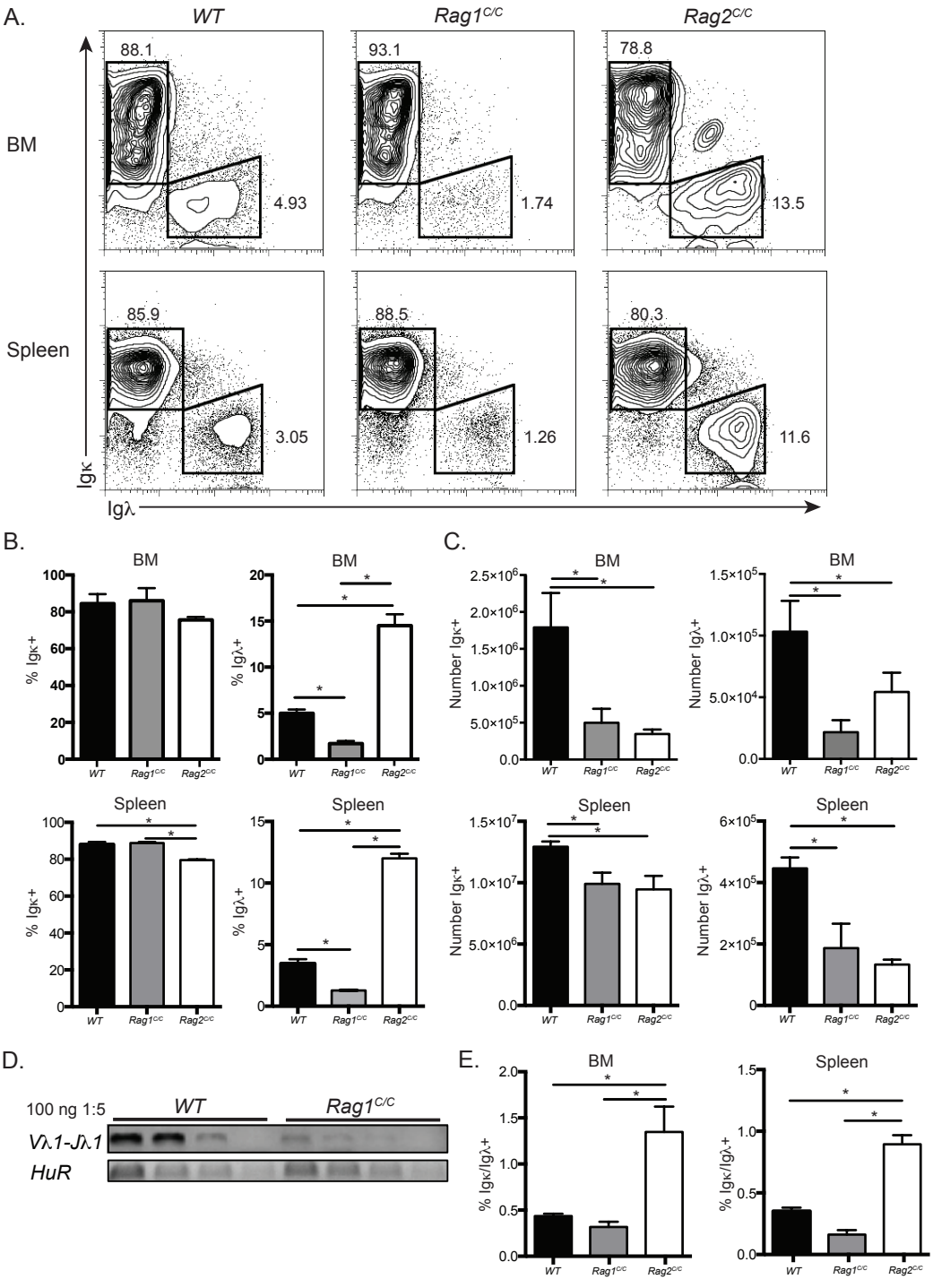

**Figure 3.1. Noncore Rag1 promotes Ig$\lambda^+$ B cell development.** (A) Representative FACS analysis of Ig$\kappa$ and Ig$\lambda$ expression on BM and splenic B cells isolated from the indicated mice. (B and C) Graphs showing average frequencies (B) and numbers (C) of BM and splenic Ig$\kappa^+$ and Ig$\lambda^+$ B cells isolated from the indicated mice. (D) Representative PCR analysis of *V$\lambda$1*-to-*J$\lambda$1* rearrangements or *HuR* as a loading control on serial 5-fold dilutions of genomic DNA from *WT* or *Rag1$^{C/C}$* pre-B cells. (E) Graphs showing the average frequencies of dual-Ig$\kappa$/Ig$\lambda$ expression on BM and splenic B cells of the indicated mice. (B, C, and E) Data are from five independent experiments conducted on five *WT*, nine *Rag1$^{C/C}$*, and three *Rag2$^{C/C}$* mice of the same age. Error bars are SEM. *; $p<0.05$.

**Figure 3.2**

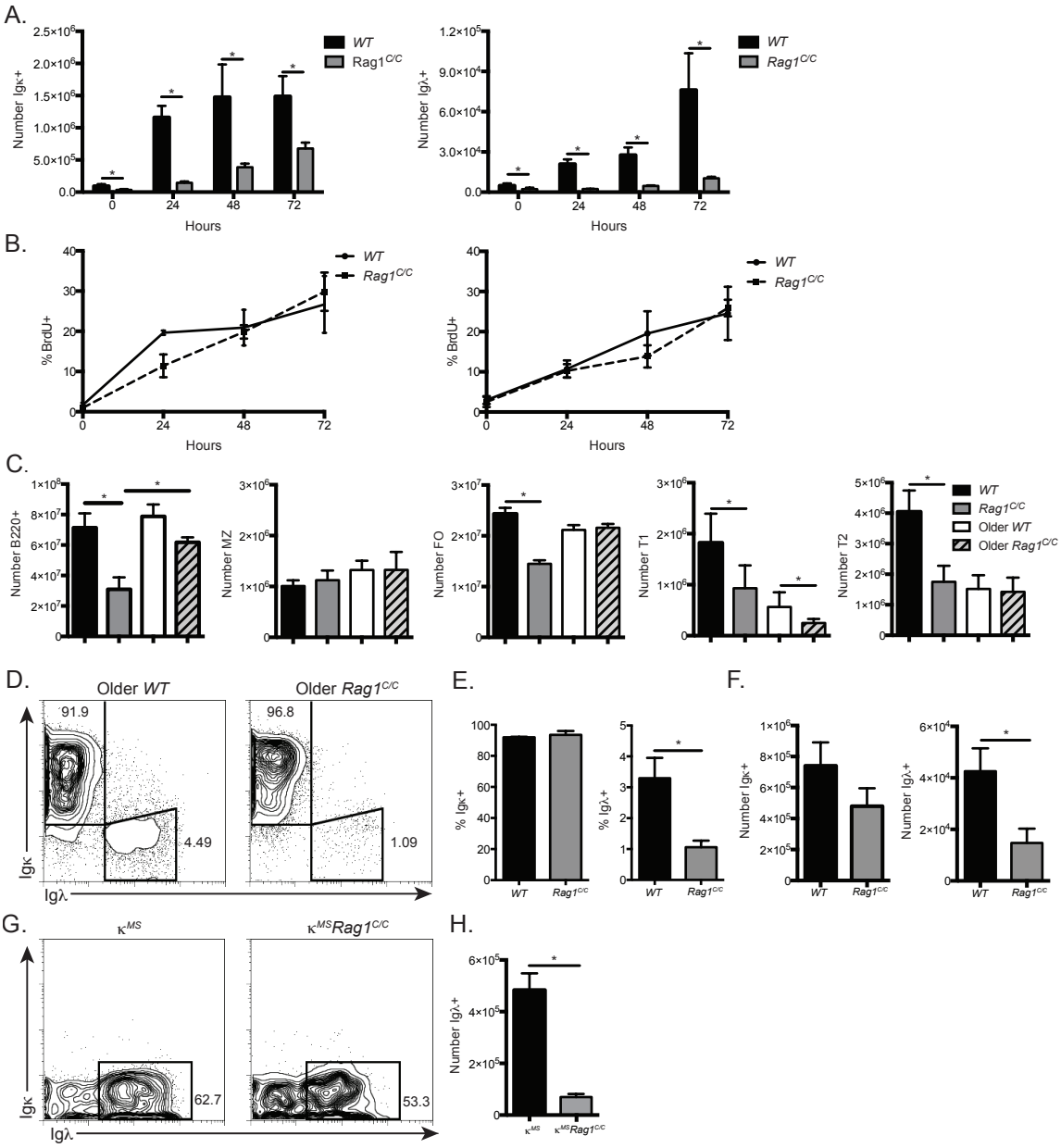
A.
Number Igκ+
Number Igλ+
WT
Rag1C/C
Hours
B.
% BrdU+
C.
Number B220+
Number MZ
Number FO
Number T1
Number T2
Older WT
Older Rag1C/C
D.
Older WT
Older Rag1C/C
91.9
4.49
96.8
1.09
Igκ
Igλ
E.
% Igκ+
% Igλ+
F.
Number Igκ+
Number Igλ+
G.
κMS
κMSRag1C/C
62.7
53.3
H.
Number Igλ+

**Figure 3.2 Impaired Igλ$^+$ B cell development in *Rag1$^{C/C}$* mice is not due to decreased recombinase activity.** (A and B) Graphs showing the average numbers (A) and frequencies (B) of BrdU$^+$ BM B cells isolated from the indicated mice at the indicated time points following intraperitoneal injection of BrdU. Data were collected from three *WT* and three *Rag1$^{C/C}$* mice at 4-6 weeks of age per time point. Error bars are SEM. *; $p<0.05$. (C) Graphs showing the average numbers of total splenic B220$^+$, marginal zone (MZ), follicular (FO), T1, and T2 B cells from the indicated mice. Data are from six independent experiments conducted on eight *WT* and eleven *Rag1$^{C/C}$* mice at 4-6 weeks of age, and three independent experiments on six *WT* and six *Rag1$^{C/C}$* mice at 5-months of age. Error bars are SEM. *; $p<0.05$. (D) Representative FACS analysis of Igκ and Igλ expression on BM B cells from the indicated mice. (E and F) Graphs indicating the average frequencies (E) and numbers (F) of BM B cells from the indicated mice. Data are from three independent experiments conducted on six *WT* and six *Rag1$^{C/C}$* mice at 5-months of age. Error bars are SEM. *; $p<0.05$. (G) Representative FACS analysis of Igκ and Igλ expression on BM B cells from the indicated mice. (H) Graphs showing the average numbers of BM B cells from the indicated mice. Data are from three independent experiments conducted on three $\kappa^{MS}$ and three $\kappa^{MS}$*Rag1$^{C/C}$* mice at 4-6 weeks of age.

**Figure 3.3**

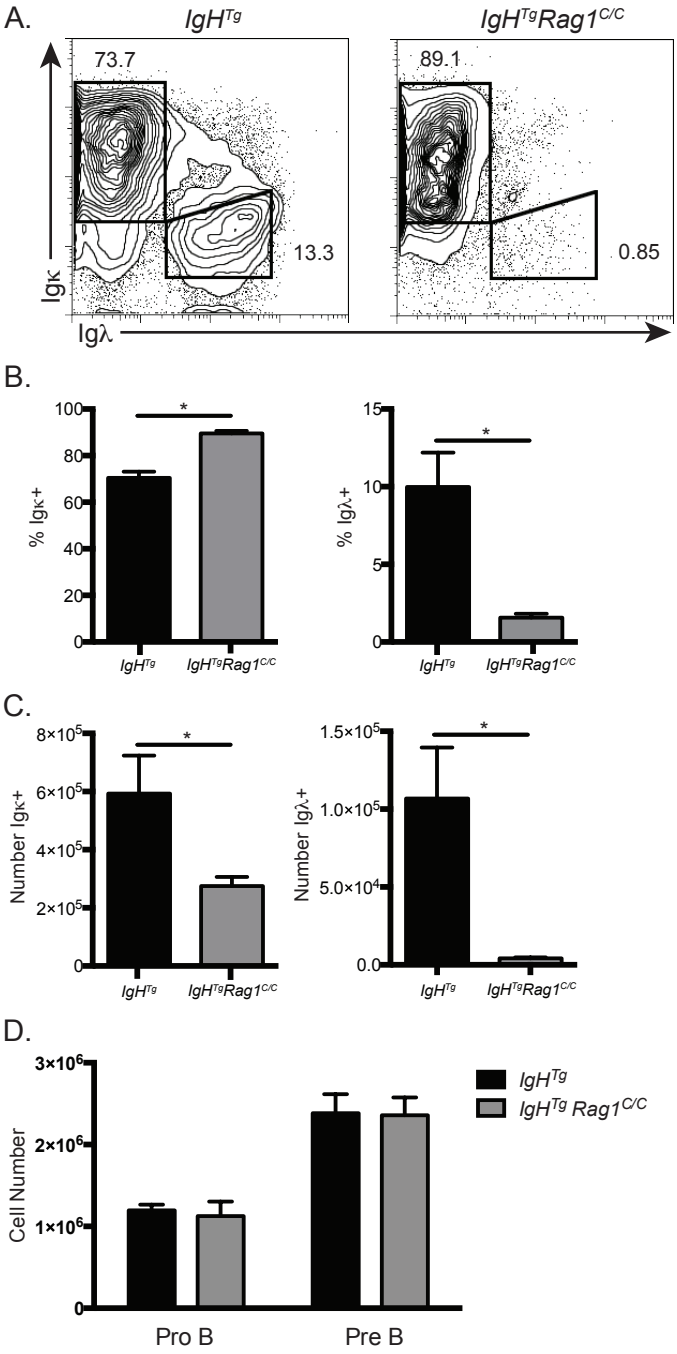
A.
IgH^Tg
IgH^TgRag1^C/C
73.7
13.3
89.1
0.85
Igκ
Igλ
B.
% Igκ+
% Igλ+
*
IgH^Tg
IgH^TgRag1^C/C
C.
Number Igκ+
Number Igλ+
D.
Cell Number
IgH^Tg
IgH^Tg Rag1^C/C
Pro B
Pre B

**Figure 3.3 Rag1 protein promotes Igκ- and Igλ- B cell development.** (A) Representative FACS analysis of Igκ and Igλ expression on BM B cells from the indicated mice. (B - C) Graphs indicating the average frequencies (B) and numbers (C) of BM $Ig\kappa^+$ and $Ig\lambda^+$ B cells from the indicated mice. (D) Graphs indicating the average numbers of pro-B and pre-B cells from the indicated mice. (B - D) Data are from three independent experiments conducted on six $IgH^{Tg}$ and twelve $IgH^{Tg}Rag1^{C/C}$ mice at 4-6 weeks of age. Error bars are SEM. *; $p<0.05$.

**Figure 3.4**

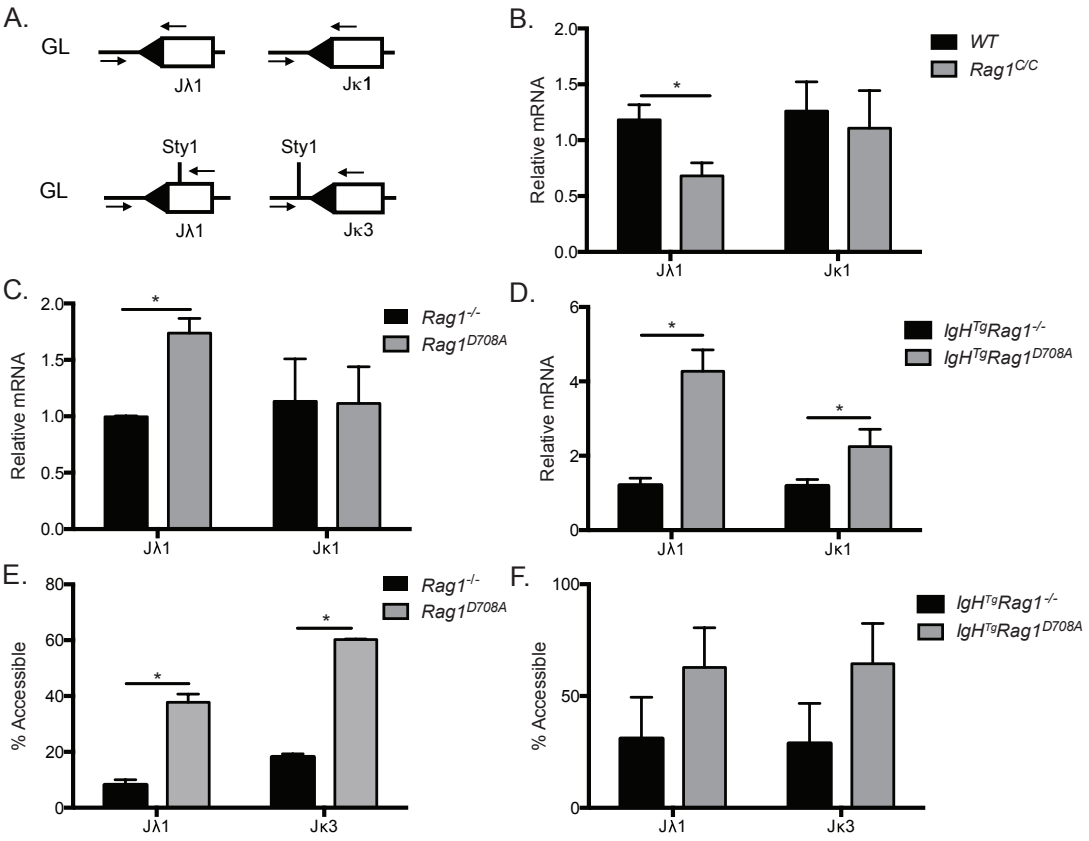
A.
GL
Jλ1
Jκ1
Sty1
Sty1
GL
Jλ1
Jκ3
B.
WT
Rag1C/C
Relative mRNA
2.0
1.5
1.0
0.5
0.0
*
Jλ1
Jκ1
C.
Rag1-/-
Rag1D708A
Relative mRNA
2.0
1.5
1.0
0.5
0.0
*
Jλ1
Jκ1
D.
IgHTgRag1-/-
IgHTgRag1D708A
Relative mRNA
6
4
2
0
*
*
Jλ1
Jκ1
E.
Rag1-/-
Rag1D708A
% Accessible
80
60
40
20
0
*
*
Jλ1
Jκ3
F.
IgHTgRag1-/-
IgHTgRag1D708A
% Accessible
100
50
0
Jλ1
Jκ3

**Figure 3.4 Rag1 protein promotes Igλ locus accessibility.** (A) Schematic of *Jλ1* and *Jκ1* segments with arrows indicating positions of PCR primers used to amplify germline transcripts from RNA or gene segments from Sty1-digested DNA. (B - D) Graphs showing average relative levels of germline *Jκ1* and *Jλ1* transcripts in primary pre-B cells purified from the indicated mice (B), STI571-treated Abl pre-B cells of the indicated genotypes (C), or IL-7 withdrawn primary pre-B cells cultured from the indicated mice (D). Data are from three independent experiments conducted on six *WT* and six $Rag1^{C/C}$ mice at 4-6 weeks of age (B), four independent experiments on Abl cell lines of each genotype (C), or five independent experiments on cells pooled from five mice of each genotype (D). Error bars are SEM. *; $p<0.05$. (E - F) Graphs depicting relative accessibility at *Jκ1* and *Jλ1* in STI571-treated Abl pre-B cells of the indicated genotypes (E) or in IL-7 withdrawn pre-B cells from mice of the indicated genotype. Data are from three independent experiments on Abl cell lines of each genotype (E) or five independent experiments on cells pooled from five mice of each genotype (F). Error bars are SEM. *; $p<0.05$.

**Figure 3.5**

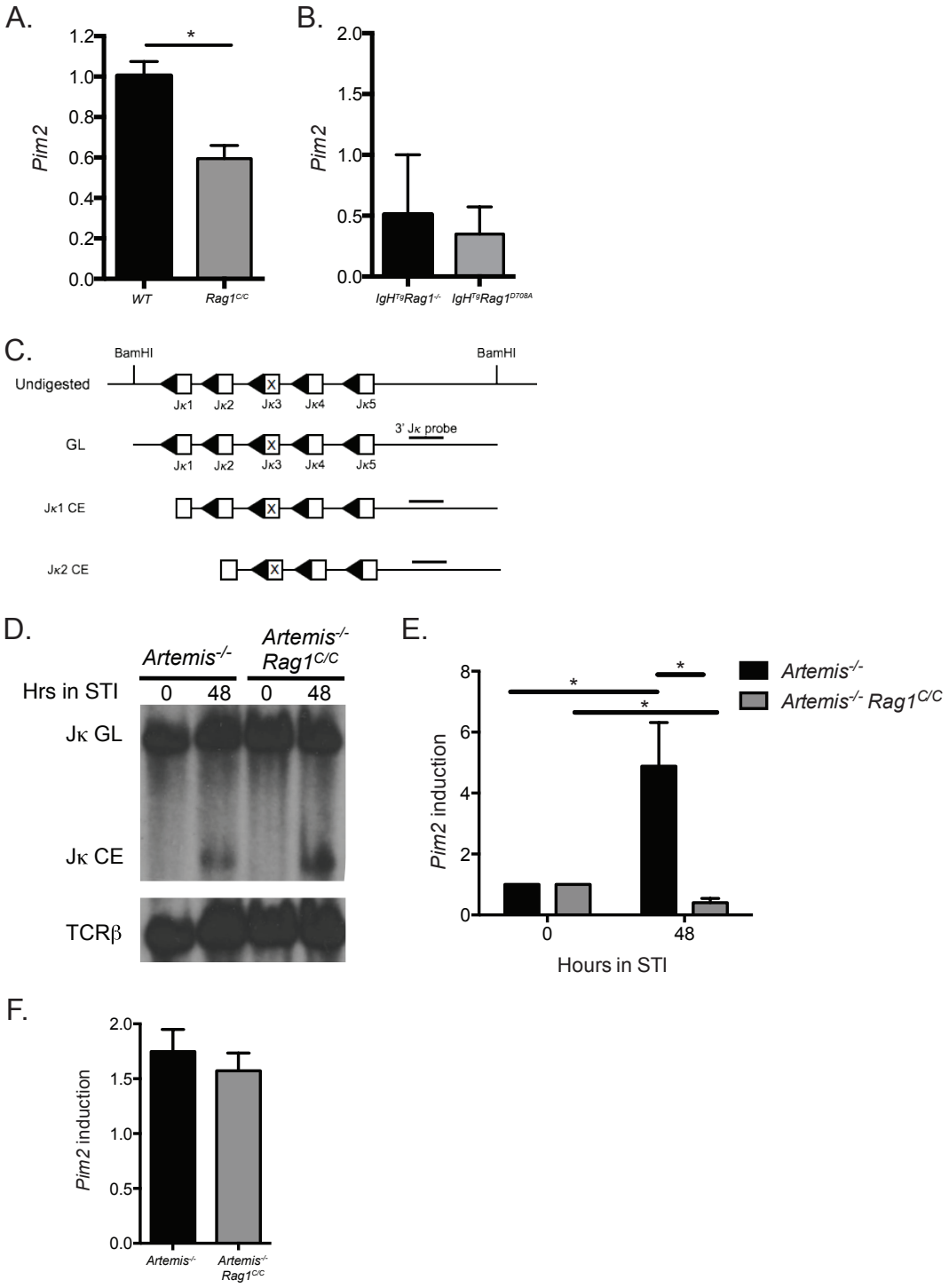
A.
Pim2
1.2
1.0
0.8
0.6
0.4
0.2
0.0
*
WT
Rag1C/C
B.
Pim2
2.0
1.5
1.0
0.5
0.0
IgHTgRag1-/-
IgHTgRag1D708A
C.
BamHI
BamHI
Undigested
Jκ1 Jκ2 Jκ3 Jκ4 Jκ5
GL
3' Jκ probe
Jκ1 CE
Jκ2 CE
D.
Artemis-/-
Artemis-/- Rag1C/C
Hrs in STI
0 48 0 48
Jκ GL
Jκ CE
TCRβ
E.
Artemis-/-
Artemis-/- Rag1C/C
Pim2 induction
8
6
4
2
0
0
48
Hours in STI
F.
Pim2 induction
2.0
1.5
1.0
0.5
0.0
Artemis-/-
Artemis-/- Rag1C/C

**Figure 3.5 Rag1 transduces pro-survival signals in pre-B cells undergoing IgL recombination.** (A - B) Average levels of *Pim2* transcripts in primary pre-B cells sorted from the indicated mice (A) or IL-7 withdrawn primary pre-B cells cultured from the indicated mice (B). Data are from three independent experiments conducted on six 4-6 week old mice of each genotype (A) or on IL-7 withdrawn cells pooled from five 4-6 week old mice of each genotype (B). Error bars are SEM. *; $p<0.05$. (C) Schematic of the *Jκ* locus in germline (GL) configuration or with coding ends (CEs) at the Jκ1/Jκ2 segments. The relative locations of the *BamH*1 sites and *3'Jκ* probe are indicated. (D) Representative Southern blot analysis of RAG-cleaved *Jκ* loci in STI571-treated Abl pre-B cells of the indicated genotypes. TCRβ probe is shown as a DNA loading control. (E) Graph depicting average levels of *Pim2* transcripts in STI571-treated Abl pre-B cells of the indicated genotypes. Data were collected from four independent experiments. Error bars are SEM. *; $p<0.05$. (F) Graph showing average levels of *Pim2* transcripts in Abl pre-B cells of the indicated genotypes after their exposure to 4 Gy IR. Data are from four independent experiments. Error bars are SEM. *, $p<0.05$.

**Figure 3.6**

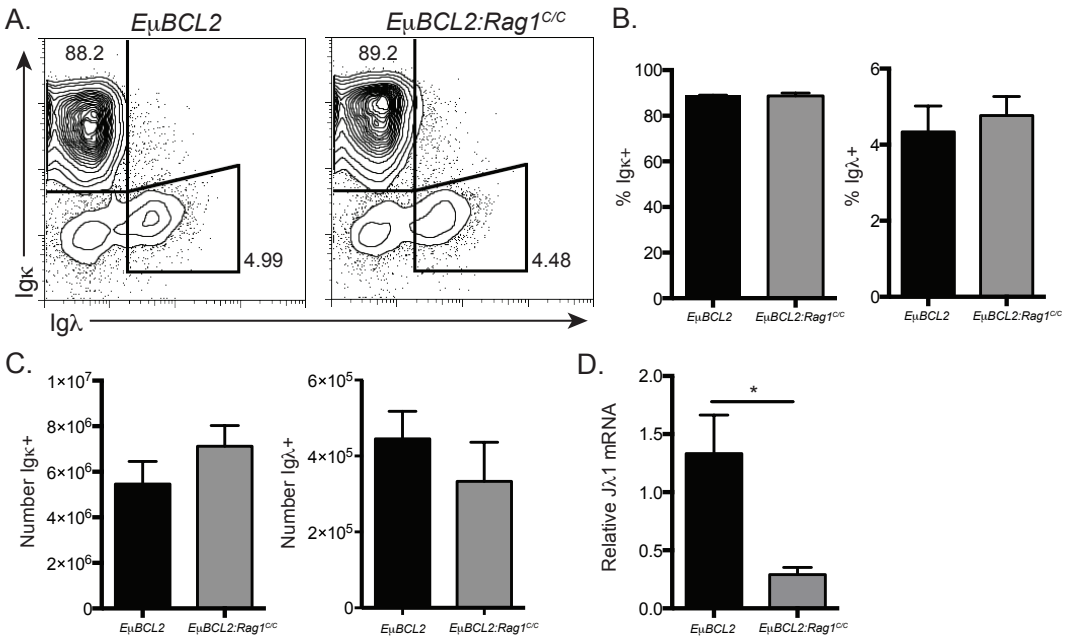


**Figure 3.6 Ectopic BCL2 expression rescues Igλ$^+$ B cells in *Rag1$^{C/C}$* mice**. (A) Representative FACS analysis of Igκ and Igλ expression on BM B cells of the indicated mice. (B - C) Graphs indicating the average frequencies (B) and numbers (C) of Igκ$^+$ and Igλ$^+$ B cells from the indicated mice. Data are from three independent experiments conducted on four *EμBCL2* and four *EμBCL2:Rag1$^{C/C}$* mice at 4-6 weeks of age. Error bars are SEM. *; p<0.05. (D) Graph showing average relative levels of germline Jκ and Jλ1 transcripts in primary pre-B cells sorted from the indicated mice. Data are from three independent experiments conducted on three *EμBCL2* and three *EμBCL2:Rag1$^{C/C}$* mice at 4-6 weeks of age. Error bars are SEM. *; p<0.05.

## CHAPTER 4

## Potential Roles for RAG DSB Signaling in NK Cell Development[2]


### Abstract

In developing B/T lymphocytes, the RAG1/2 endonuclease complex catalyzes the assembly of antigen receptors (AgRs) via a series of programmed DNA double strand breaks (DSBs) at AgR loci. Natural killer (NK) cells are an innate lymphocyte lineage that express germline-encoded receptors and do not require the RAG proteins for development. Yet, approximately 40% of mature NK cells derive from common lymphoid progenitors (CLPs) that have expressed RAG during ontogeny. Recent evidence suggests that NK cells that develop in the absence of RAG DSBs are phenotypically more terminally differentiated and functionally less "fit" than those with a history of RAG expression. The RAG proteins are comprised of "core" regions that together possess DNA endonuclease activity and "non-core" regions that are dispensable for RAG cleavage. The RAG1 protein has been proposed to employ its non-core regions to regulate V(D)J recombination by promoting survival and differentiation signals in response to RAG DSBs. We show here that *Rag1*$^{C/C}$ mice, which express the core-Rag1 protein, exhibit a pronounced impairment in the development of CD27$^{-}$ CD11b$^{+}$ mature NK cells relative to mice expressing wildtype Rag1 protein, full-length cleavage-dead Rag1 protein, and Rag1-deficient mice. These preliminary data suggest that through its non-core regions, RAG1 may function outside of the canonical lymphocyte lineage to promote normal NK cell development.


[2] Experiments described in this chapter were conducted with EnJun Yang and Taku Kambayashi

## Introduction

Natural killer (NK) cells are an innate subset of lymphocytes that control intracellular pathogens and tumors through cytotoxic effector functions and the secretion of activating cytokines. Like B/T lymphocytes, NK cells undergo “licensing” to establish tolerance to self-proteins, undergo proliferative expansion during infection, and generate antigen-specific recall responses on secondary antigenic stimulation. However, the mechanisms regulating NK cell development, NK cell lineage commitment, and NK cell effector function are not well understood (Karo et al., 2014).

The RAG1/2 endonuclease complex catalyzes the assembly of antigen receptors (AgRs) via a series of programmed DSBs in developing B/T lymphocytes. Although RAG expression is not required for NK cell development, approximately 40% of mature NK cells derive from common lymphoid progenitors (CLPs) that have previously expressed RAG during ontogeny (Sun and Lanier, 2011). Recent evidence suggests that NK cells developing in the absence of RAG DSBs are functionally distinct and less fit during an immune response (Borghesi et al., 2004; Pilbeam et al., 2008). Further, NK cells that either lack RAG1 protein expression ($Rag1^{-/-}$) or NK cells that express full-length, but cleavage-dead Rag1 protein ($Rag1^{D708A}$) mice develop with delayed kinetics (Karo et al., 2014), and exhibit a more terminally differentiated phenotype, hyper-responsiveness during infection, decreased expression of DNA damage response factors, and diminished survival capacity in response to virus-driven proliferation (Andrews and Smyth, 2010). These findings suggest a requirement for RAG DSBs and or RAG-DSB-induced signalling in normal NK cell ontogeny.

RAG DSBs in pre-B cells induce a program of genes involved in cell survival and lymphocyte differentiation pathways (Karo et al., 2014). The RAG1 and RAG2 proteins are each comprised of “core” regions, which together possess DNA endonuclease

activity, and “non-core” regions, which are dispensable for RAG cleavage. Non-core Rag1 possesses intrinsic E3 ubiquitin ligase activity and can interact with a separate ubiquitin ligase complex, a kinase, histones, DNA damage response proteins, and at least one transcription factor (Bednarski and Sleckman, 2012; Bredemeyer et al., 2008; Helmink and Sleckman, 2012). These activities of non-core RAG1 have been proposed to generate survival and differentiation signals in response to RAG DSBs ((Coster et al., 2012; Grazini et al., 2010; Jones et al., 2011; Kassmeier et al., 2012; Kim et al., 2013; Maitra and Sadofsky, 2009; Raval et al., 2008; Yurchenko et al., 2003); Chapter 3). Mice expressing truncated Rag1 core protein ($Rag1^{C/C}$ mice) exhibit impaired lymphocyte development associated with defects in generating survival signals following RAG DSBs (Dudley Horowitz; Chapter 3). Thus, to begin to determine whether non-core RAG1 has a role in generating survival and/or differentiation signals in NK cell ontogeny, we assayed NK cell development in $Rag1^{C/C}$ mice. We show here that *$Rag1^{C/C}$* mice exhibit a pronounced impairment in the $CD27^{-}$ $CD11b^{+}$ mature NK cell populations relative to wildtype, $Rag1^{D708A}$ and $Rag1^{-/-}$ mice. These preliminary data support findings that RAG DSBs promote normal NK cell development and may further suggest that RAG1 functions outside of the canonical lymphocyte lineage to generate signals required for NK cell fitness.

## Materials and Methods

**Mice.** Wildtype (129SvEv), *Rag1*$^{C/C}$ (Horowitz and Bassing, 2014), and *Rag1*$^{D708A}$ (Dudley et al., 2003) mice were bred with *Rag1*$^{-/-}$ (Ji et al., 2010b) to generate mice on a mixed 129SvEv and C57BL/6 background. All mice described in this study were 4-weeks old and either littermate or age-matched. All studies were conducted in accordance with national guidelines and approved by the Institutional Animal Care and Use Committee of the Children's Hospital of Philadelphia.

### Flow Cytometry

Single cell suspensions were isolated from spleens and stained as in (Mombaerts et al., 1992). Data was acquired on a FACSCanto (BD Biosciences, San Jose, CA) using Diva software (BD Biosciences) and analyzed using FlowJo software (Tree Star).

## Results

### Potential Roles for RAG DSB-Signaling in NK Cell Development

To identify potential functions of the non-core regions of Rag1 in modulating NK cell development, we first quantified mature $CD27^-$ $CD11b^+$ splenic NK cells from mice expressing either wildtype, full-length cleavage-dead Rag1 ($Rag1^{D708A}$), and core-Rag1 ($Rag1^{C/C}$) proteins that were bred to C57BL/6 $Rag1^{-/-}$ mice to reduce variation between background strains. Thus, we generated and analysed $Rag1^{+/-}$, $Rag^{D708A/-}$, $Rag1^{C/-}$, and $Rag1^{-/-}$ mice at 4 weeks of age when the mature NK cell compartment is still expanding (May et al., 2013). We observed decreased frequencies of mature splenic $CD27^-$ $CD11b^+$ NK cells between $Rag1^{+/-}$ mice and $Rag1^{-/-}$ mice (Figure 4), suggesting that RAG1 protein promotes mature NK cell development. We also observed an increase in the frequency of $CD27^-$ $CD11b^+$ NK cells in $Rag1^{D708A/-}$ mice relative to either $Rag1^{+/-}$ or $Rag1^{/-}$ mice (Figure 4), indicating that the absence of RAG DSBs in CLPs yields NK cells that are more terminally differentiated (Andrews and Smyth, 2010). In contrast, we observed ~2-3-fold lower frequencies of splenic $CD27^-$ $CD11b^+$ NK cells in $Rag1^{C/C}$ mice compared to $Rag1^{+/-}$, $Rag1^{/-}$, or $Rag1^{D708A/-}$ mice, indicating that $Rag1^{C/C}$ mice exhibit an impaired mature splenic NK cell compartment. These data suggest that both RAG DSBs and non-core regions of RAG1 promote normal splenic NK cell development.

## Discussion

Natural killer (NK) cells control viral infections and tumors through activation of germline-encoded receptors. NK cells do not require RAG proteins for their development. Yet, RAG endonuclease activity in a subset of CLPs leads to elevated expression of DSB repair/response genes in mature NK cells, imparting these innate immune cells with enhanced ability to survive virus-driven proliferation (Karo et al., 2014). RAG DSBs also appear important for endowing mature T cells and other innate lymphoid cell types with a cellular "fitness" that protects them from apoptosis during bouts of immune response-driven proliferation (Karo et al., 2014). Data shown here indicates that mice developing in the absence of RAG1 protein and/or RAG DSBs exhibit impaired mature NK cell populations. This finding supports a requirement for RAG DSBs in normal NK cell development (Karo et al., 2014). Additional data shown here also indicates that non-core RAG1 regions may be required for RAG-DSB-induced NK cell fitness. The experiment shown here cannot account for potential quantitative differences in the frequency of RAG DSBs generated among CLPs in $Rag1^{C/C}$ mice versus wildtype CLPs. Yet, the data are suggestive of a qualitative difference in RAG DSB-induced signals in $Rag1^{C/C}$ CLPs that impair NK cell development in these mice. Thus, future analyses should determine whether $Rag1^{C/C}$ CLPs have undergone equivalent frequencies of RAG DSBs prior to committing to the NK cell lineage. Subsequent studies on NK cells having experienced equivalent levels of RAB DSBs at the CLP stage can be used for gene expression analyses to determine which, if any, RAG DSB-induced genes are regulated by non-core Rag1 in NK cells. Further, these preliminary data allow for speculation that non-core Rag1 regions transduce a subset of signals in CLPs that may be important for multiple downstream lymphocyte lineages. Thus, in addition to serving

as an essential subunit of the V(D)J recombinase, the RAG1 protein may function outside of the canonical lymphocyte lineage to establish an effective immune system.

**Figure 4.**

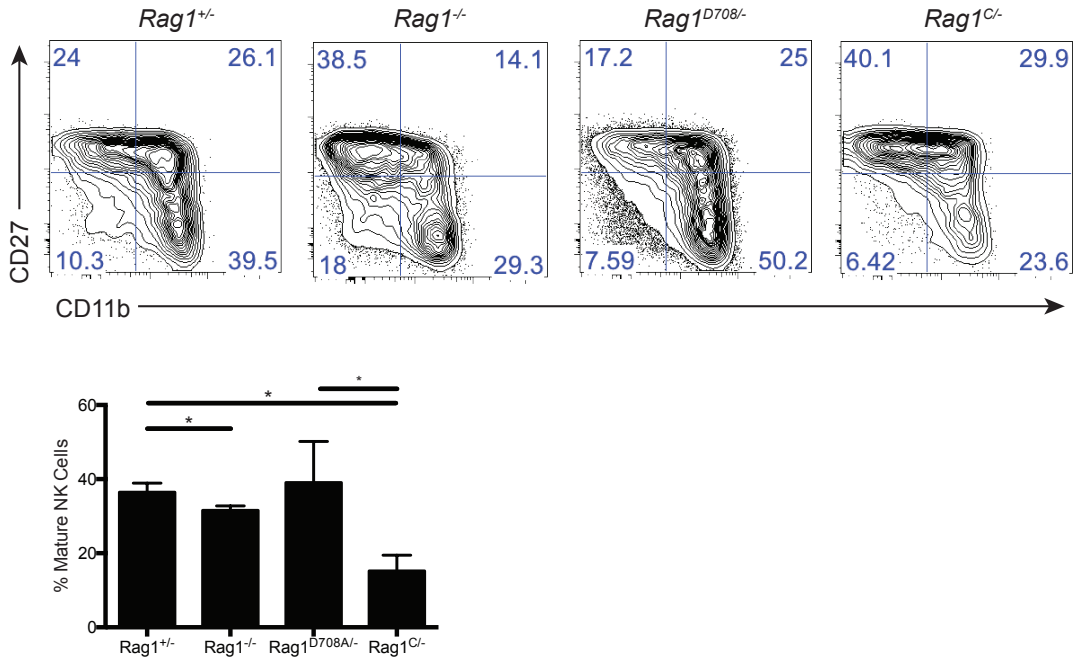


**Figure 4.** Rag1$^{C/C}$ mice have altered NK cell development. Representative flow cytometry plots and quantitation of CD27$^{-}$ CD11b$^{+}$ splenic NK cells from two independent experiments on 3 mice each of the indicated genotype.

# CHAPTER 5

# Discussion

## I. Overview

Nearly 25 years ago, the RAG1 and RAG2 proteins were identified as the V(D)J recombinase based on their ability to catalyze rearrangement of recombination substrates in non-lymphoid cells (Karo et al., 2014). Subsequent studies identified the essential "core" domains of RAG1 and RAG2 required for DNA endonuclease activity, providing critical tools for defining the fundamental mechanisms of V(D)J recombination (Oettinger et al., 1990; Schatz and Baltimore, 1988; Schatz et al., 1989). Mutating the remaining "non-core" domains of RAG1 or RAG2 preserves V(D)J recombination activity on plasmid and extra-chromosomal substrates (Sadofsky, 2004; Sadofsky et al., 1993), but reduces recombination frequencies at TCRβ and *IgH* loci leading to altered TCRβ and IgH repertoires and defects in early B/T cell development in mice (Lee et al., 2014; Santagata et al., 2000; Wong and Roth, 2007) and causes fatal immunodeficiencies in people (Akamatsu et al., 2003; Dudley et al., 2003; Horowitz and Bassing, 2014; Liang et al., 2002). Thus, one outstanding question in the field of V(D)J recombination is how mutations in RAG1 or RAG2 that preserve V(D)J recombination result in altered AgR repertoire and impaired lymphocyte development *in vivo*. Recent studies have identified several functional biochemical domains in both the RAG1 and RAG2 proteins that serve critical functions in normal AgR assembly and lymphocyte development overall (Lee et al., 2014). For instance, non-core Rag2 binds histones at sites of active transcription, ties V(D)J recombination to the cell cycle, and prevents genomic instability (Matthews and Oettinger, 2009; Schatz and Ji, 2011). Non-core Rag1 possesses intrinsic E3 ubiquitin ligase activity and can interact with a separate ubiquitin ligase complex, a kinase, histones, DNA damage response proteins, and at least one transcription factor

(Li et al., 1996; Liu et al., 2007; Matthews et al., 2007). These interactions have led to suggested roles for RAG1 in modulating AgR gene assembly *in vivo* via ubiquitylating histones and/or other proteins, promoting AgR locus accessibility, regulating RAG endonuclease activity, repairing RAG DSBs, and/or transducing gene expression changes following RAG DSBs (Coster et al., 2012; Grazini et al., 2010; Jones et al., 2011; Kassmeier et al., 2012; Kim et al., 2013; Maitra and Sadofsky, 2009; Raval et al., 2008; Yurchenko et al., 2003). However, data supporting either these RAG1 protein-protein interactions or RAG1 biochemical activities and their relevance *in vivo* is lacking. The data presented in Chapter 2 of this thesis demonstrates roles for non-core Rag1 in $\alpha\beta$ T cell development by promoting diverse Vβ recombination and normal $\alpha\beta$ TCR selection. Additional data presented in Chapter 3 of this thesis indicates roles for Rag1 in promoting late B cell development by enhancing accessibility of AgR loci prior to recombination and by generating survival signals in response to RAG breaks. Future site-directed analyses of non-core Rag1 regions *in vivo* may reveal the precise mechanisms by which non-core Rag1 modulates chromatin accessibility prior to RAG DSBs and promote gene expression changes following RAG DSBs. The final sections of this thesis seek to provide mechanistic insight underlying the phenotypes observed in $Rag1^{C/C}$ mice and to explain how RAG may function outside of classic V(D)J recombination in a cell-type and locus-specific manner.

**II. Non-Canonical Roles for RAG1 Protein: Pre-RAG DSBs**

Transcription-dependent opening of chromatin is associated with efficient V(D)J recombination (Coster et al., 2012; Grazini et al., 2010; Horowitz and Bassing, 2014; Jones et al., 2011; Kassmeier et al., 2012; Kim et al., 2013; Maitra and Sadofsky, 2009; Raval et al., 2008; Sadofsky, 2004; Yurchenko et al., 2003), and experiments described

in Chapter 3 of this thesis suggest roles for RAG1 protein in promoting chromatin accessibility of AgR loci prior to recombination. Analysis of unrearranged germline transcripts in both primary and Abelson-transformed pre-B cells indicate that the Igλ locus is less accessible in pre-B cells lacking non-core Rag1 regions relative to pre-B cells expressing full-length, wildtype Rag1. Further, analyses of both germline transcripts and restriction endonuclease sensitivity in primary pre-B cells expressing full-length, cleavage-dead Rag1 protein indicate that both the Igκ and Igλ locus is more accessible in pre-B cells expressing full-length Rag1 relative to pre-B cells that lack Rag1 protein altogether. Together, these data indicate that the RAG1 protein has roles in promoting both Igκ and Igλ locus accessibility that function independently of RAG endonuclease activity. How might this occur? Substrates for the Rag1 E3 ligase include histones H3 and variant histone H3.3, which is present at actively transcribing genes and promotes both transcriptional activation and accessibility by reducing core histone-DNA interactions (Hamel et al., 2014; Hesslein and Schatz, 2001; Krangel, 2007). Thus, one physiologic role for the RAG1 E3 ligase may be to ubiquitylate H3 and/or H3.3 prior to RAG cleavage to promote opening of chromatin and germline transcription to enhance AgR gene segment accessibility. Further, Rag1 RING domain auto-ubiquitylation at non-core Rag1 residue K233 is speculated to yield conformational changes in Rag1 that foster interactions with additional proteins (Grazini et al., 2010; Jones et al., 2011; Wang et al., 2006; Zentner and Henikoff, 2013), some of which may promote AgR gene segment accessibility. Along these lines, N-terminal non-core Rag1 interacts with the VprBP component of the VprBP/ROC1/DDB1 E3 ligase complex, which ubiquitylates histones H3 and H4 and promotes chromatin accessibility (Jones and Gellert, 2003). Thus, RAG1-bound VprBP could serve to scaffold the ROC1/Cul4/DDB1 E3 ligase (Kassmeier et al., 2012; Wang et al., 2006) to promote Igκ/Igλ gene segment

accessibility through ROC1/Cul4/DDB1-mediated histone ubiquitylation. Additionally, non-core RAG1 binds the transcription factor Gmeb1 (Kassmeier et al., 2012), and RAG-binding of the transcription factors Runx1 and c-Fos at TCRδ and TCRβ loci, respectively, increases Rag recruitment subsequent Rag cleavage at these loci (Maitra and Sadofsky, 2009). Thus, Gmeb1 or another yet-unidentified transcriptional co-activator recruited to AgR loci by Rag1 could increase Igκ/Igλ accessibility independent of Rag1 E3 ligase activity. Future analyses of mice expressing specific Rag1 RING mutants, VprBP/ROC1/DDB1-binding mutants, or Gmeb1-binding mutants in the context of a full-length, cleavage-dead Rag1 protein may identify how non-core Rag1 region promote AgR gene segment accessibility.

Based on findings shown in Chapter 3 that full-length, cleavage-dead Rag1 enhances *Igκ* and *Igλ* locus accessibility, while *Rag1*$^{C/C}$ pre-B cells exhibit reduced accessibility at both *Igλ* and *Igκ* gene segments but only exhibit reduced *Igλ* recombination, could suggest locus-specific mechanisms by which RAG1 might regulates AgR assembly. The *Igλ* locus contains two V/J gene arrays, each containing one or two Vλ gene segments that rearrange to a Jλ gene segment ~30-80 kb away (Cieslak et al., 2014; Wang et al., 2008) (Figure 1.1). Thus, *Vλ*-to-*Jλ* rearrangements closely resemble the small-scale D-to-J rearrangements of *TCRβ* and *IgH* loci rather than large-scale V-to-(D)J recombination of *Igκ*, *TCRβ*, and *IgH* loci, which are separated by ~0.5-3 Mb (Sanchez et al., 1991; Vettermann and Schlissel, 2010). Since *Rag1*$^{C/C}$ mice have similar reductions in Dβ-to-Jβ and $D_H$-to-$J_H$ recombination (Schatz and Ji, 2011) as Vλ-to-Jλ recombination (Figure 3.1), the ability of non-core Rag1 regions to promote recombination by enhancing AgR gene accessibility may be most critical for rearrangements that do not proceed via long-range chromosome looping

(Dudley et al., 2003). This possibility is supported by data in Chapter 3 showing that a 2-fold reduction in *Jλ* accessibility impairs *Vλ*-to-*Jλ* rearrangements while a 2-fold reduction in *Jκ* accessibility has no effect on *Vκ*-to-*Jκ* rearrangements (Guo et al., 2011; Majumder et al., 2015; Shih and Krangel, 2013). It is also possible that the 2-fold reduction in *Jκ* accessibility in *Rag1*$^{C/C}$ pre-B cells results in similar decreases in *Vκ*-to-*Jκ* recombination, but that these differences are not detectable by PCR (Dudley et al., 2003). However, the data presented here supports a view in which local $J_L$ gene segment accessibility appears limiting for small-scale rearrangements, which occur in *Igλ* but not *Igκ* recombination.

The current model for V-to-(D)J rearrangements is that RAG proteins bind accessible D/J segments and then capture and cleave accessible V segments placed in proximity of RAG-D/J recombination centers via chromosome looping (Dudley et al., 2003). Evidence suggests that capture/cleavage of accessible V segments is limiting for Igκ and TCRβ loci (Ji et al., 2010b; Schatz and Ji, 2011). These loci have large V clusters that contain dozens of V segments organized in chromosome loops and recombine across genomic distances of 0.5-2 Mb to D/J gene segments through long-range chromosomal interactions (Figure 1.1). Rag1$^{C/C}$ mice have defects in early T cell development associated with reduced D-J and V-DJ recombination at the TCRβ locus (Bassing et al., 2008; Casellas et al., 2002; Wu et al., 2003; Xiang et al., 2013). The experiments in Chapter 2 of this thesis show that non-core Rag1 regions drive Vβ-to-DβJβ recombination and promote diverse Vβ usage in both primary and secondary Vβ-DβJβ rearrangements. Further, exchanging a single inefficient Vβ RSS for a consensus RSS is sufficient to partially rescue the overall αβ T cell developmental defects observed Rag1$^{C/C}$ mice (Figure 2.6). The relative usage of a given Vβ gene segment during recombination is likely a function of Vβ RSS accessibility, changes in locus topology that

place Vβ segments near DβJβ joins, and the on-off rates of RAG proteins at Vβ RSSs within the pre-cleavage synaptic complex (Dudley et al., 2003). Thus, non-core RAG1 regions may promote or preserve changes in TCRβ topology that help assemble or stabilize synaptic complexes for a subset of Vβ segments. This may explain how replacement of a single RSS out of a possible ~30 possible Vβ RSSs with one containing a consensus sequence is enough to partially rescue αβ T cell development. Overcoming Vβ RSS inefficiency in this manner might occur via Rag1-medated ubiquitylation of histone H3, which can remove nucleosomes and promote accessibility (Bassing et al., 2008; Schatz and Ji, 2011; Wu et al., 2003). Future analyses of Vβ usage in mice expressing Rag1 RING mutations or Rag1-VprBP/ROC1/DDB1-binding mutants may elucidate how non-core Rag1 overcomes Vβ RSS inefficiencies.

Differences in accessibility and transcription among germline Vβ and Jα gene segments are observed in DN and DP thymocytes, whereas changes in TCRα locus topology control Jα usage in Vα-Jα rearrangements (Wang et al., 2006; Zentner and Henikoff, 2013). Data shown in Chapter 2 of this thesis shows that Vα3 rearrangements are biased toward 3'Jα segments in DP cells of $Rag1^{C/C}$ mice. These data suggest that non-core RAG1 regions may modulate Jα gene segment utilization via promoting Jα gene accessibility. Based on the prediction that large-scale rearrangements are not limited by small decreases in local J gene segment accessibility, any potential decreases in Vα/Jα gene segment accessibility may have only slight impact on Jα recombination in DP cells (Chen et al., 2001; Krangel, 2007; Krangel, 2009). Further, the experiments shown here cannot differentiate whether this apparent skewing of the Jα repertoire results from decreased Jα accessibility/recombination at the TCRα locus itself in DP cells versus altered αβ TCR chain pairing observed in DP cells as a result of skewed Vβ usage at the DN3 stage (Figure 2.3). Future analyses of Jα germline transcripts in mice

expressing a pre-assembled TCRβ transgene on a Rag1$^{D708A}$ background are necessary to unequivocally assess roles for Rag1 Jα gene segment accessibility.

Point mutations in the RAG1 RING domain that partially or completely abrogate RAG1 ubiquitylation activity cause Omenn syndrome in humans (Dudley et al., 2003; Horowitz and Bassing, 2014). Recently the Rag1$^{C325Y/C325Y}$ mouse was generated, which lacks Rag1 E3 ligase activity and exhibits more severe D-J and V-DJ at IgH and TCRβ loci than deletion of the entire Rag1 non-core region (Lee et al., 2014; Simkus et al., 2007). These data support the requirement for RAG1 histone H3 ubiquitylation in normal V(D)J recombination and lymphocyte development in vivo. However, because these mouse studies were conducted on a Rag1 cleavage-sufficient background, the relative contribution of Rag1-H3 ubiquitylation to accessibility at AgR loci versus roles for Rag1-H3 ubiquitylation in stabilizing the RAG synaptic complex, and/or the response to RAG DSBs is unclear. Ongoing studies using full-length, cleavage-dead Rag1 with the RAG1-C325Y mutation may determine whether the RAG1 E3 ligase promotes V(D)J recombination via AgR gene segment accessibility prior to RAG DSBs.

**III. Non-Canonical Roles for RAG1 Protein: Post-RAG DSB**

RAG DSBs in pre-B cells change expression of a catalog of genes involved in cell survival and lymphocyte differentiation pathways, among others (Deng et al., 2015; Dudley et al., 2003). One gene induced downstream of ATM/NF-κB signals encodes the pro-survival kinase Pim2, which is required for the survival of pre-B cells undergoing RAG DSBs (Bednarski and Sleckman, 2012; Bredemeyer et al., 2008; Helmink and Sleckman, 2012) and necessary for the development of Igλ$^{+}$ B cells (Bednarski et al., 2012). Experiments shown in Chapter 3 of this thesis demonstrate that RAG DSBs induced at *Igκ* loci in *Artemis*$^{-/-}$*Rag1*$^{C/C}$ pre-B cells are unable to up-regulate *Pim2*

expression. This finding indicates that, in addition to catalyzing RAG breaks, the RAG1 protein transduces pro-survival signals through its non-core regions and in response to RAG breaks. DNA DSBs induced by IR or by RAG in pre-B cells activate the ATM kinase, which phosphorylates the NF-κB essential modifier (NEMO) to trigger NF-κB-mediated *Pim2* transcription (Derudder et al., 2009). The expression of *Pim2* increases pre-B cell survival by antagonizing pro-apoptotic signals (Bednarski et al., 2012; Bredemeyer et al., 2008; Li et al., 2001). Nuclear NF-κB signaling in response to exogenous DNA DSBs relies on phosphorylation of the NEMO by ATM and subsequent ubiquitylation of NEMO by an E3 ubiquitin ligase complex (Bednarski et al., 2012; Bredemeyer et al., 2008; Muljo and Schlissel, 2003; Steinel et al., 2013). However, the E3 ligase responsible for NF-κB activation in response to RAG DSBs is currently unknown. Thus, in response to RAG DSBS, either the RAG1 E3 ligase, RAG1-bound to the VprBP/Roc1/Cul4/DDB E3 ligase complex, or a RAG1 bound to a separate E3 ligase complex may activate *Pim2* transcription through RAG1-mediated NEMO ubiquitylation. This notion is supported by observations that both mice with B cell lineage deletion of *NEMO (mb1-cre NEMO$^{f}$* mice*)* and *Pim2$^{-/-}$* mice exhibit similar decreases in the frequencies of Igλ$^{+}$ B cells as *Rag1$^{C/C}$* mice, and BCL2 expression rescues the frequency of Igλ$^{+}$ B cells in *mb1-cre NEMO$^{f}$* mice (Wu et al., 2010) and in Rag1$^{c/c}$ mice (Figure 3.6). Further, experiments described in this thesis have uncovered additional ATM- and NF-κB dependent genes induced by non-core Rag1 regions (data not shown), indicating this response is not specific for *Pim2* alone. Considering that RAG DSBs also signal gene expression changes via ATM-dependent/NF-κB-independent and ATM/NF-κB-independent pathways (Derudder et al., 2009), non-core Rag1 regions may transduce additional signals that fall in these other pathways, as well. Thus, future gene expression

profiling arrays in *Artemis*$^{-/-}$*Rag1*$^{C/C}$ pre-B cells and *Artemis*$^{-/-}$ pre-B cells are necessary to elucidate these signals.

The data presented in Chapter 2 demonstrating that *Rag1*$^{C/C}$ and *Rag2*$^{del352/del352}$ mice exhibit oppositely skewed Ig$\kappa^+$/Ig$\lambda^+$ B cell ratios may offer insight into how pre-B cells integrate RAG DSB signalling and repair to promote Ig$\kappa^+$ and Ig$\lambda^+$ B cell development. *Rag1*$^{C/C}$ mice have no discernable defect in V(D)J joining (Bredemeyer et al., 2008), indicating that their pre-B cells are defective in pro-survival signalling from RAG DSBs but not in the repair of RAG DSBs. Further, data in Chapter 3 shows that failure to induce pro-survival signals following RAG DSBs leads to loss of pre-B cells that would normally develop into Ig$\lambda^+$ B cells (Figure 3.1 versus Figure 3.6). *Rag2*$^{del352/del352}$ mice exhibit destabilization of RAG-cleaved DNA ends and therefore impaired V(D)J joining (Deriano et al., 2011), suggesting that their pre-B cells are defective in RAG DSB repair but not RAG DSB-induced pro-survival signalling. The observation that Atm$^{-/-}$ mice have normal Ig$\kappa^+$/Ig$\lambda^+$ B cell ratios, has been used to argue that activation of *Pim2* by RAG DSBs does not promote Ig$\lambda^+$ B cell development (Deriano et al., 2011). However, in addition to lacking RAG DSB pro-survival signals, *Atm*$^{-/-}$ mice exhibit destabilization of RAG-cleaved DNA ends and impaired V(D)J joining (Derudder et al., 2009). This suggests that increased Ig$\lambda^+$ B cell development from defective V(D)J joining (as in both *Atm*$^{-/-}$ and *Rag2*$^{del352/del352}$ mice) may counteract the decreased generation of Ig$\lambda^+$ B cells from loss of pro-survival signalling (as in Atm$^{-/-}$ mice only). Impaired V(D)J joining and normal DSB signalling may enable pre-B cells with un-repaired RAG-cleaved Ig$\kappa$ loci to initiate Ig$\lambda$ recombination, leading to the assembly of in-frame *VJ*$\kappa$ and *VJ*$\lambda$ coding joins in a greater than normal fraction of pre-B cells, which may explain the both the increased frequency of Ig$\lambda^+$ B cells as well as the increased frequency dual-Ig$\kappa^+$/Ig$\lambda^+$ B cells in

*Rag2*$^{del352/del352}$ mice (Figure 3.1). In line with this hypothesis, we find that germline deletion of ATM in Rag1$^{C/C}$ mice or in *Eμ*BCL2 *mice* yields normal Igκ/Igλ ratios (data not shown), indicating that the role of ATM in the formation of stable coding ends supersedes ATM-mediated Pim2 induction downstream of RAG DSBs at Igκ.

**IV. Implications for RAG1 Outside of RAG Cleavage**

Humans with mutations in non-core RAG1 regions that do not affect RAG recombinase activity develop Omenn syndrome (Bredemeyer et al., 2006). Data here demonstrating non-cleavage functions of RAG1 in modulating accessibility and signalling has broad implications beyond mechanisms that regulate V(D)J recombination. In addition to the ATM-NF-κB pathway, RAG DSBs signal through undefined ATM-dependent and ATM-independent pathways to activate a transcriptional program of genes that encode proteins that regulate the selection of lymphocytes based on antigen-receptor specificity (Lee et al., 2014). Thus, the non-core regions of Rag1 may additionally be critical for activating these and possibly additional unidentified signalling pathways to modulate positive and negative lymphocyte selection, ensuring creation of a robust self-tolerant adaptive immune system. Further, the normal human B cell repertoire is 40% Igλ$^+$. The impaired ability of RAG1 to promote the development of Igλ$^+$ cells results in loss of 5% of all mouse B cells, but could potentially result in loss of ~20% of all human mature B cells. Yet, Igκ/Igλ ratios have not been examined in OS or other SCID-like condition with non-core RAG1 mutations. Together, the data presented here suggest that impaired signalling in response to RAG DSBs may contribute to the immune deficiency and autoimmunity of Omenn Syndrome patients. Thus, further elucidation of the roles for non-core RAG1 are necessary and may generate new therapeutics for Omenn Syndrome patients.

**IV. Implications for RAG1 in Other Cell Types**

In contrast to B/T cells, innate lymphocytes, including natural killer (NK) and innate lymphoid cells (ILCs), do not require RAG for development (Bednarski et al., 2012; Bredemeyer et al., 2008; Muljo and Schlissel, 2003; Steinel et al., 2013). However, ~40% of mature NK cells derive from RAG-expressing progenitor cells. Two recent studies have revealed that RAG endonuclease activity in a subset of common lymphoid progenitors (CLPs) leads to elevated expression of DSB repair/response genes in mature NK cells, imparting these innate immune cells with enhanced ability to survive virus-driven proliferation (Andrews and Smyth, 2010; Karo et al., 2014). RAG-deficient NK cells demonstrate increased basal levels of apoptosis and DNA damage and have altered expression of genes involved in the response to and repair of RAG DSBs, suggesting that RAG DSBs in CLPs signal gene expression changes that promote the survival and differentiation of mature NK cell subsets. This function of RAG outside of V(D)J recombination also is important for endowing mature T cells and ILCs with a cellular fitness that protects them from apoptosis during immune response-driven proliferation (Andrews and Smyth, 2010; Karo et al., 2014). Data shown in Chapter 4 of this thesis demonstrate that NK cells in $Rag1^{C/C}$ mice have maturation defects relative to NK cells isolated from $Rag1^{-/-}$, $Rag1^{D708A}$, and wildtype mice (Figure 4). While these preliminary data cannot account for potential quantitative differences in RAG DSBs among CLPs in $Rag1^{C/C}$ mice, these data are suggestive of a qualitative difference in RAG DSBs in $Rag1^{C/C}$ CLPs that impair NK cell development in these mice. These data lead us to speculate that the signalling functions of non-core Rag1 regions may be important for the RAG endonuclease to instil cellular fitness in multiple cell lineages. Therefore, in addition to serving as an essential subunit of the V(D)J recombinase, the

RAG1 protein likely serves additional physiologic functions outside of catalysis of Ig and TCR gene assembly that are critical for the development of a robust immune system.

## V. Conclusions

The appearance of the RAG locus in the genomes of jawed vertebrates, coincident with the appearance of major histocompatibility loci, and seven AgR loci, marks a watershed moment for adaptive immunity (Karo et al., 2014). The diversity afforded by RAG-mediated AgR assembly likely provided a protective advantage through the increased ability to recognize, respond, and establish memory to a large number of potential antigens (Flajnik and Kasahara, 2010). The “core” domains of both RAG proteins are highly evolutionarily conserved (Cooper and Alder, 2006; Pancer and Cooper, 2006), as are portions of RAG “non-core” regions, including the RAG1 RING domain (Jones and Gellert, 2003). The identification of E3 ligase activity within the RAG1 RING domain, as well as multiple RAG1 protein-protein interactions, suggests additional roles for RAG1 beyond DNA cleavage. Data presented in this thesis demonstrates that RAG1 not only catalyzes V(D)J recombination but also promotes accessibility of AgR genes prior to recombination and promotes pro-survival signals in response to V(D)J recombination. Dispensing with non-core regions, which comprise 40% of the Rag1 protein, does not prevent V(D)J recombination activity *in vitro* (Sadofsky, 2004), but leads to lymphocyte development defects, restricted AgR repertoires, and both autoimmunity and immune deficiencies, *in vivo* (Sadofsky, 2004; Sadofsky et al., 1993). These data suggest that biochemical activities of the non-core regions of RAG1 may have evolved under selective pressure to fine-tune V(D)J recombination in ways that both maximize diversity in AgR gene usage and minimize

risks associated with RAG-mediated DNA DSBs. Thus, the physiological roles for the V(D)J recombinase extend far beyond the generation of RAG DSBs.

## BIBLIOGRAPHY


Abarrategui, I., and M.S. Krangel. 2009. Germline transcription: a key regulator of accessibility and recombination. *Advances in experimental medicine and biology* 650:93-102.

Ait-Azzouzene, D., L. Verkoczy, J. Peters, A. Gavin, P. Skog, J.L. Vela, and D. Nemazee. 2005. An immunoglobulin C kappa-reactive single chain antibody fusion protein induces tolerance through receptor editing in a normal polyclonal immune system. *The Journal of experimental medicine* 201:817-828.

Akamatsu, Y., R. Monroe, D.D. Dudley, S.K. Elkin, F. Gartner, S.R. Talukder, Y. Takahama, F.W. Alt, C.H. Bassing, and M.A. Oettinger. 2003. Deletion of the RAG2 C terminus leads to impaired lymphoid development in mice. *Proceedings of the National Academy of Sciences of the United States of America* 100:1209-1214.

Aleman, K., J.G. Noordzij, R. de Groot, J.J. van Dongen, and N.G. Hartwig. 2001. Reviewing Omenn syndrome. *European journal of pediatrics* 160:718-725.

Allman, D.M., S.E. Ferguson, V.M. Lentz, and M.P. Cancro. 1993. Peripheral B cell maturation. II. Heat-stable antigen(hi) splenic B cells are an immature developmental intermediate in the production of long-lived marrow-derived B cells. *Journal of immunology* 151:4431-4444.

Alt, F.W., Y. Zhang, F.L. Meng, C. Guo, and B. Schwer. 2013. Mechanisms of programmed DNA lesions and genomic instability in the immune system. *Cell* 152:417-429.

Amin, R.H., and M.S. Schlissel. 2008. Foxo1 directly regulates the transcription of recombination-activating genes during B cell development. *Nature immunology* 9:613-622.

Andrews, D.M., and M.J. Smyth. 2010. A potential role for RAG-1 in NK cell development revealed by analysis of NK cells during ontogeny. *Immunology and cell biology* 88:107-116.

Bain, G., E.C. Maandag, D.J. Izon, D. Amsen, A.M. Kruisbeek, B.C. Weintraub, I. Krop, M.S. Schlissel, A.J. Feeney, M. van Roon, and et al. 1994. E2A proteins are required for proper B cell development and initiation of immunoglobulin gene rearrangements. *Cell* 79:885-892.

Bassing, C.H., F.W. Alt, M.M. Hughes, M. D'Auteuil, T.D. Wehrly, B.B. Woodman, F. Gartner, J.M. White, L. Davidson, and B.P. Sleckman. 2000. Recombination signal sequences restrict chromosomal V(D)J recombination beyond the 12/23 rule. *Nature* 405:583-586.

Bassing, C.H., S. Whitlow, R. Mostoslavsky, K. Yang-Iott, S. Ranganath, and F.W. Alt. 2008. Vbeta cluster sequences reduce the frequency of primary Vbeta2 and Vbeta14 rearrangements. *European journal of immunology* 38:2564-2572.

Beck, K., M.M. Peak, T. Ota, D. Nemazee, and C. Murre. 2009. Distinct roles for E12 and E47 in B cell specification and the sequential rearrangement of immunoglobulin light chain loci. *The Journal of experimental medicine* 206:2271-2284.

Bednarski, J.J., A. Nickless, D. Bhattacharya, R.H. Amin, M.S. Schlissel, and B.P. Sleckman. 2012. RAG-induced DNA double-strand breaks signal through Pim2 to promote pre-B cell survival and limit proliferation. *The Journal of experimental medicine* 209:11-17.

Bednarski, J.J., and B.P. Sleckman. 2012. Lymphocyte development: integration of DNA damage response signaling. *Advances in immunology* 116:175-204.

Bevington, S., and J. Boyes. 2013. Transcription-coupled eviction of histones H2A/H2B governs V(D)J recombination. *The EMBO journal* 32:1381-1392.

Blackman, M.A., P. Marrack, and J. Kappler. 1989. Influence of the major histocompatibility complex on positive thymic selection of V beta 17a+ T cells. *Science* 244:214-217.

Boboila, C., F.W. Alt, and B. Schwer. 2012. Classical and alternative end-joining pathways for repair of lymphocyte-specific and general DNA double-strand breaks. *Advances in immunology* 116:1-49.

Borghesi, L., L.Y. Hsu, J.P. Miller, M. Anderson, L. Herzenberg, L. Herzenberg, M.S. Schlissel, D. Allman, and R.M. Gerstein. 2004. B lineage-specific regulation of V(D)J recombinase activity is established in common lymphoid progenitors. *The Journal of experimental medicine* 199:491-502.

Brady, B.L., and C.H. Bassing. 2011. Differential regulation of proximal and distal Vbeta segments upstream of a functional VDJbeta1 rearrangement upon beta-selection. *Journal of immunology* 187:3277-3285.

Brady, B.L., M.A. Oropallo, K.S. Yang-Iott, T. Serwold, K. Hochedlinger, R. Jaenisch, I.L. Weissman, and C.H. Bassing. 2010. Position-dependent silencing of germline Vss segments on TCRss alleles containing preassembled VssDJssCss1 genes. *Journal of immunology* 185:3564-3573.

Brady, B.L., L.J. Rupp, and C.H. Bassing. 2013. Requirement for dicer in survival of proliferating thymocytes experiencing DNA double-strand breaks. *Journal of immunology* 190:3256-3266.

Bredemeyer, A.L., B.A. Helmink, C.L. Innes, B. Calderon, L.M. McGinnis, G.K. Mahowald, E.J. Gapud, L.M. Walker, J.B. Collins, B.K. Weaver, L. Mandik-Nayak, R.D. Schreiber, P.M. Allen, M.J. May, R.S. Paules, C.H. Bassing, and B.P. Sleckman. 2008. DNA double-strand breaks activate a multi-functional genetic program in developing lymphocytes. *Nature* 456:819-823.

Bredemeyer, A.L., G.G. Sharma, C.Y. Huang, B.A. Helmink, L.M. Walker, K.C. Khor, B. Nuskey, K.E. Sullivan, T.K. Pandita, C.H. Bassing, and B.P. Sleckman. 2006. ATM stabilizes DNA double-strand-break complexes during V(D)J recombination. *Nature* 442:466-470.

Caglayan Sozmen, S., S. Isik, Z. Arikan Ayyildiz, K. Yildiz, Y. Cakir, E. Ozer, S. Asilsoy, N. Uzuner, O. Karaman, and O. Anal. 2015. Cyclosporin Treatment Improves Skin Findings in Omenn Syndrome. *Pediatric dermatology*

Carpenter, A.C., K.S. Yang-Iott, L.H. Chao, B. Nuskey, S. Whitlow, F.W. Alt, and C.H. Bassing. 2009. Assembled DJ beta complexes influence TCR beta chain selection and peripheral V beta repertoire. *Journal of immunology* 182:5586-5595.

Casellas, R., M. Jankovic, G. Meyer, A. Gazumyan, Y. Luo, R. Roeder, and M. Nussenzweig. 2002. OcaB is required for normal transcription and V(D)J recombination of a subset of immunoglobulin kappa genes. *Cell* 110:575-585.

Chaumeil, J., M. Micsinai, P. Ntziachristos, L. Deriano, J.M. Wang, Y. Ji, E.P. Nora, M.J. Rodesch, J.A. Jeddeloh, I. Aifantis, Y. Kluger, D.G. Schatz, and J.A. Skok. 2013. Higher-order looping and nuclear organization of Tcra facilitate targeted rag cleavage and regulated rearrangement in recombination centers. *Cell reports* 3:359-370.

Chaumeil, J., and J.A. Skok. 2012. The role of CTCF in regulating V(D)J recombination. *Current opinion in immunology* 24:153-159.

Chen, F., L. Rowen, L. Hood, and E.V. Rothenberg. 2001. Differential transcriptional regulation of individual TCR V beta segments before gene rearrangement. *Journal of immunology* 166:1771-1780.

Cieslak, A., S. Le Noir, A. Trinquand, L. Lhermitte, D.M. Franchini, P. Villarese, S. Gon, J. Bond, M. Simonin, L. Vanhille, C. Reimann, E. Verhoeyen, J. Larghero, E. Six, S. Spicuglia, I. Andre-Schmutz, A. Langerak, B. Nadel, E. Macintyre, D. Payet-Bornet, and V. Asnafi. 2014. RUNX1-dependent RAG1 deposition instigates human TCR-delta locus rearrangement. *The Journal of experimental medicine* 211:1821-1832.

Clark, M.R., M. Mandal, K. Ochiai, and H. Singh. 2014. Orchestrating B cell lymphopoiesis through interplay of IL-7 receptor and pre-B cell receptor signalling. *Nature reviews. Immunology* 14:69-80.

Cobb, R.M., K.J. Oestreich, O.A. Osipovich, and E.M. Oltz. 2006. Accessibility control of V(D)J recombination. *Advances in immunology* 91:45-109.

Cooper, M.D., and M.N. Alder. 2006. The evolution of adaptive immune systems. *Cell* 124:815-822.

Corfe, S.A., and C.J. Paige. 2012. The many roles of IL-7 in B cell development; mediator of survival, proliferation and differentiation. *Seminars in immunology* 24:198-208.

Coster, G., A. Gold, D. Chen, D.G. Schatz, and M. Goldberg. 2012. A dual interaction between the DNA damage response protein MDC1 and the RAG1 subunit of the V(D)J recombinase. *The Journal of biological chemistry* 287:36488-36498.

Degner, S.C., T.P. Wong, G. Jankevicius, and A.J. Feeney. 2009. Cutting edge: developmental stage-specific recruitment of cohesin to CTCF sites throughout immunoglobulin loci during B lymphocyte development. *Journal of immunology* 182:44-48.

Degner-Leisso, S.C., and A.J. Feeney. 2010. Epigenetic and 3-dimensional regulation of V(D)J rearrangement of immunoglobulin genes. *Seminars in immunology* 22:346-352.

Deng, Z., H. Liu, and X. Liu. 2015. RAG1-mediated ubiquitylation of histone H3 is required for chromosomal V(D)J recombination. *Cell research* 25:181-192.

Deriano, L., J. Chaumeil, M. Coussens, A. Multani, Y. Chou, A.V. Alekseyenko, S. Chang, J.A. Skok, and D.B. Roth. 2011. The RAG2 C terminus suppresses genomic instability and lymphomagenesis. *Nature* 471:119-123.

Derudder, E., E.J. Cadera, J.C. Vahl, J. Wang, C.J. Fox, S. Zha, G. van Loo, M. Pasparakis, M.S. Schlissel, M. Schmidt-Supprian, and K. Rajewsky. 2009. Development of immunoglobulin lambda-chain-positive B cells, but not editing of immunoglobulin kappa-chain, depends on NF-kappaB signals. *Nature immunology* 10:647-654.

Dudley, D.D., J. Sekiguchi, C. Zhu, M.J. Sadofsky, S. Whitlow, J. DeVido, R.J. Monroe, C.H. Bassing, and F.W. Alt. 2003. Impaired V(D)J recombination and lymphocyte development in core RAG1-expressing mice. *The Journal of experimental medicine* 198:1439-1450.

Ebert, A., S. McManus, H. Tagoh, J. Medvedovic, G. Salvagiotto, M. Novatchkova, I. Tamir, A. Sommer, M. Jaritz, and M. Busslinger. 2011. The distal V(H) gene cluster of the Igh locus contains distinct regulatory elements with Pax5 transcription factor-dependent activity in pro-B cells. *Immunity* 34:175-187.

Flajnik, M.F., and M. Kasahara. 2010. Origin and evolution of the adaptive immune system: genetic events and selective pressures. *Nature reviews. Genetics* 11:47-59.

Fugmann, S.D., A.I. Lee, P.E. Shockett, I.J. Villey, and D.G. Schatz. 2000. The RAG proteins and V(D)J recombination: complexes, ends, and transposition. *Annual review of immunology* 18:495-527.

Gigi, V., S. Lewis, O. Shestova, M. Mijuskovic, L. Deriano, W. Meng, E.T. Luning Prak, and D.B. Roth. 2014. RAG2 mutants alter DSB repair pathway choice in vivo and illuminate the nature of 'alternative NHEJ'. *Nucleic acids research* 42:6352-6364.

Gorman, J.R., N. van der Stoep, R. Monroe, M. Cogne, L. Davidson, and F.W. Alt. 1996. The Ig(kappa) enhancer influences the ratio of Ig(kappa) versus Ig(lambda) B lymphocytes. *Immunity* 5:241-252.

Grange, S., and J. Boyes. 2007. Chromatin opening is tightly linked to enhancer activation at the kappa light chain locus. *Biochemical and biophysical research communications* 363:223-228.

Grazini, U., F. Zanardi, E. Citterio, S. Casola, C.R. Goding, and F. McBlane. 2010. The RING domain of RAG1 ubiquitylates histone H3: a novel activity in chromatin-mediated regulation of V(D)J joining. *Molecular cell* 37:282-293.

Guo, C., H.S. Yoon, A. Franklin, S. Jain, A. Ebert, H.L. Cheng, E. Hansen, O. Despo, C. Bossen, C. Vettermann, J.G. Bates, N. Richards, D. Myers, H. Patel, M. Gallagher, M.S. Schlissel, C. Murre, M. Busslinger, C.C. Giallourakis, and F.W. Alt. 2011. CTCF-binding elements mediate control of V(D)J recombination. *Nature* 477:424-430.

Guo, J., A. Hawwari, H. Li, Z. Sun, S.K. Mahanta, D.R. Littman, M.S. Krangel, and Y.W. He. 2002. Regulation of the TCRalpha repertoire by the survival window of CD4(+)CD8(+) thymocytes. *Nature immunology* 3:469-476.

Hamel, K.M., M. Mandal, S. Karki, and M.R. Clark. 2014. Balancing Proliferation with Igkappa Recombination during B-lymphopoiesis. *Frontiers in immunology* 5:139.

Haque, S.F., S.L. Bevington, and J. Boyes. 2013. The Elambda Enhancer is Essential for V(D)J Recombination of the Murine Immunoglobulin Lambda Light Chain Locus. *Biochemical and biophysical research communications*

Helmink, B.A., and B.P. Sleckman. 2012. The response to and repair of RAG-mediated DNA double-strand breaks. *Annual review of immunology* 30:175-202.

Herzog, S., M. Reth, and H. Jumaa. 2009. Regulation of B-cell proliferation and differentiation by pre-B-cell receptor signalling. *Nature reviews. Immunology* 9:195-205.

Hesslein, D.G., and D.G. Schatz. 2001. Factors and forces controlling V(D)J recombination. *Advances in immunology* 78:169-232.

Hinz, M., M. Stilmann, S.C. Arslan, K.K. Khanna, G. Dittmar, and C. Scheidereit. 2010. A cytoplasmic ATM-TRAF6-cIAP1 module links nuclear DNA damage signaling to ubiquitin-mediated NF-kappaB activation. *Molecular cell* 40:63-74.

Horowitz, J.E., and C.H. Bassing. 2014. Noncore RAG1 regions promote Vbeta rearrangements and alphabeta T cell development by overcoming inherent inefficiency of Vbeta recombination signal sequences. *Journal of immunology* 192:1609-1619.

Hsu, L.Y., J. Lauring, H.E. Liang, S. Greenbaum, D. Cado, Y. Zhuang, and M.S. Schlissel. 2003. A conserved transcriptional enhancer regulates RAG gene expression in developing B cells. *Immunity* 19:105-117.

Inlay, M., F.W. Alt, D. Baltimore, and Y. Xu. 2002. Essential roles of the kappa light chain intronic enhancer and 3' enhancer in kappa rearrangement and demethylation. *Nature immunology* 3:463-468.

Janeway, C. 2005. Immunobiology : the immune system in health and disease. Garland Science, New York. xxiii, 823 p. pp.

Jhunjhunwala, S., M.C. van Zelm, M.M. Peak, and C. Murre. 2009. Chromatin architecture and the generation of antigen receptor diversity. *Cell* 138:435-448.

Ji, Y., A.J. Little, J.K. Banerjee, B. Hao, E.M. Oltz, M.S. Krangel, and D.G. Schatz. 2010a. Promoters, enhancers, and transcription target RAG1 binding during V(D)J recombination. *The Journal of experimental medicine* 207:2809-2816.

Ji, Y., W. Resch, E. Corbett, A. Yamane, R. Casellas, and D.G. Schatz. 2010b. The in vivo pattern of binding of RAG1 and RAG2 to antigen receptor loci. *Cell* 141:419-431.

Jones, J.M., A. Bhattacharyya, C. Simkus, B. Vallieres, T.D. Veenstra, and M. Zhou. 2011. The RAG1 V(D)J recombinase/ubiquitin ligase promotes ubiquitylation of acetylated, phosphorylated histone 3.3. *Immunology letters* 136:156-162.

Jones, J.M., and M. Gellert. 2003. Autoubiquitylation of the V(D)J recombinase protein RAG1. *Proceedings of the National Academy of Sciences of the United States of America* 100:15446-15451.

Jspeert, I., G.J. Driessen, M.J. Moorhouse, N.G. Hartwig, B. Wolska-Kusnierz, K. Kalwak, A. Pituch-Noworolska, I. Kondratenko, J.M. van Montfrans, E. Mejstrikova, A.C. Lankester, A.W. Langerak, D.C. van Gent, A.P. Stubbs, J.J. van Dongen, and M. van der Burg. 2014. Similar recombination-activating gene (RAG) mutations result in similar immunobiological effects but in different clinical phenotypes. *The Journal of allergy and clinical immunology* 133:1124-1133.

Jung, D., C. Giallourakis, R. Mostoslavsky, and F.W. Alt. 2006. Mechanism and control of V(D)J recombination at the immunoglobulin heavy chain locus. *Annual review of immunology* 24:541-570.

Kappler, J.W., N. Roehm, and P. Marrack. 1987. T cell tolerance by clonal elimination in the thymus. *Cell* 49:273-280.

Kappler, J.W., U. Staerz, J. White, and P.C. Marrack. 1988. Self-tolerance eliminates T cells specific for Mls-modified products of the major histocompatibility complex. *Nature* 332:35-40.

Karo, J.M., D.G. Schatz, and J.C. Sun. 2014. The RAG recombinase dictates functional heterogeneity and cellular fitness in natural killer cells. *Cell* 159:94-107.

Kassmeier, M.D., K. Mondal, V.L. Palmer, P. Raval, S. Kumar, G.A. Perry, D.K. Anderson, P. Ciborowski, S. Jackson, Y. Xiong, and P.C. Swanson. 2012. VprBP binds full-length RAG1 and is required for B-cell development and V(D)J recombination fidelity. *The EMBO journal* 31:945-958.

Kim, K., J.M. Kim, J.S. Kim, J. Choi, Y.S. Lee, N. Neamati, J.S. Song, K. Heo, and W. An. 2013. VprBP has intrinsic kinase activity targeting histone H2A and represses gene transcription. *Molecular cell* 52:459-467.

Kim, M.S., M. Lapkouski, W. Yang, and M. Gellert. 2015. Crystal structure of the V(D)J recombinase RAG1-RAG2. *Nature* 518:507-511.

Kondilis-Mangum, H.D., H.Y. Shih, G. Mahowald, B.P. Sleckman, and M.S. Krangel. 2011. Regulation of TCRbeta allelic exclusion by gene segment proximity and accessibility. *Journal of immunology* 187:6374-6381.

Krangel, M.S. 2007. T cell development: better living through chromatin. *Nature immunology* 8:687-694.

Krangel, M.S. 2009. Mechanics of T cell receptor gene rearrangement. *Current opinion in immunology* 21:133-139.

Kuo, T.C., and M.S. Schlissel. 2009. Mechanisms controlling expression of the RAG locus during lymphocyte development. *Current opinion in immunology* 21:173-178.

Lauring, J., and M.S. Schlissel. 1999. Distinct factors regulate the murine RAG-2 promoter in B- and T-cell lines. *Molecular and cellular biology* 19:2601-2612.

Lee, Y.N., F. Frugoni, K. Dobbs, J.E. Walter, S. Giliani, A.R. Gennery, W. Al-Herz, E. Haddad, F. LeDeist, J.H. Bleesing, L.A. Henderson, S.Y. Pai, R.P. Nelson, D.H. El-Ghoneimy, R.A. El-Feky, S.M. Reda, E. Hossny, P. Soler-Palacin, R.L. Fuleihan, N.C. Patel, M.J. Massaad, R.S. Geha, J.M. Puck, P. Palma, C. Cancrini, K. Chen, M. Vihinen, F.W. Alt, and L.D. Notarangelo. 2014. A systematic analysis of recombination activity and genotype-phenotype correlation in human recombination-activating gene 1 deficiency. *The Journal of allergy and clinical immunology* 133:1099-1108.

Li, J., G.W. Peet, D. Balzarano, X. Li, P. Massa, R.W. Barton, and K.B. Marcu. 2001. Novel NEMO/IkappaB kinase and NF-kappa B target genes at the pre-B to immature B cell transition. *The Journal of biological chemistry* 276:18579-18590.

Li, Z., D.I. Dordai, J. Lee, and S. Desiderio. 1996. A conserved degradation signal regulates RAG-2 accumulation during cell division and links V(D)J recombination to the cell cycle. *Immunity* 5:575-589.

Liang, H.E., L.Y. Hsu, D. Cado, L.G. Cowell, G. Kelsoe, and M.S. Schlissel. 2002. The "dispensable" portion of RAG2 is necessary for efficient V-to-DJ rearrangement during B and T cell development. *Immunity* 17:639-651.

Lieber, M.R. 2010. The mechanism of double-strand DNA break repair by the nonhomologous DNA end-joining pathway. *Annual review of biochemistry* 79:181-211.

Lin, W.C., and S. Desiderio. 1993. Regulation of V(D)J recombination activator protein RAG-2 by phosphorylation. *Science* 260:953-959.

Lin, W.C., and S. Desiderio. 1994. Cell cycle regulation of V(D)J recombination-activating protein RAG-2. *Proceedings of the National Academy of Sciences of the United States of America* 91:2733-2737.

Liu, Y., R. Subrahmanyam, T. Chakraborty, R. Sen, and S. Desiderio. 2007. A plant homeodomain in RAG-2 that binds Hypermethylated lysine 4 of histone H3 is necessary for efficient antigen-receptor-gene rearrangement. *Immunity* 27:561-571.

Lou, Z., K. Minter-Dykhouse, S. Franco, M. Gostissa, M.A. Rivera, A. Celeste, J.P. Manis, J. van Deursen, A. Nussenzweig, T.T. Paull, F.W. Alt, and J. Chen. 2006. MDC1 maintains genomic stability by participating in the amplification of ATM-dependent DNA damage signals. *Molecular cell* 21:187-200.

Luning Prak, E.T., M. Monestier, and R.A. Eisenberg. 2011. B cell receptor editing in tolerance and autoimmunity. *Annals of the New York Academy of Sciences* 1217:96-121.

MacDonald, H.R., R.K. Lees, R. Schneider, R.M. Zinkernagel, and H. Hengartner. 1988. Positive selection of CD4+ thymocytes controlled by MHC class II gene products. *Nature* 336:471-473.

Maitra, R., and M.J. Sadofsky. 2009. A WW-like module in the RAG1 N-terminal domain contributes to previously unidentified protein-protein interactions. *Nucleic acids research* 37:3301-3309.

Majumder, K., O.I. Koues, E.A. Chan, K.E. Kyle, J.E. Horowitz, K. Yang-Iott, C.H. Bassing, I. Taniuchi, M.S. Krangel, and E.M. Oltz. 2015. Lineage-specific compaction of Tcrb requires a chromatin barrier to protect the function of a long-range tethering element. *The Journal of experimental medicine* 212:107-120.

Malin, S., S. McManus, and M. Busslinger. 2010a. STAT5 in B cell development and leukemia. *Current opinion in immunology* 22:168-176.

Malin, S., S. McManus, C. Cobaleda, M. Novatchkova, A. Delogu, P. Bouillet, A. Strasser, and M. Busslinger. 2010b. Role of STAT5 in controlling cell survival and immunoglobulin gene recombination during pro-B cell development. *Nature immunology* 11:171-179.

Mandik-Nayak, L., J. Racz, B.P. Sleckman, and P.M. Allen. 2006. Autoreactive marginal zone B cells are spontaneously activated but lymph node B cells require T cell help. *The Journal of experimental medicine* 203:1985-1998.

Matthews, A.G., A.J. Kuo, S. Ramon-Maiques, S. Han, K.S. Champagne, D. Ivanov, M. Gallardo, D. Carney, P. Cheung, D.N. Ciccone, K.L. Walter, P.J. Utz, Y. Shi, T.G. Kutateladze, W. Yang, O. Gozani, and M.A. Oettinger. 2007. RAG2 PHD finger couples histone H3 lysine 4 trimethylation with V(D)J recombination. *Nature* 450:1106-1110.

Matthews, A.G., and M.A. Oettinger. 2009. RAG: a recombinase diversified. *Nature immunology* 10:817-821.

May, R.M., M. Okumura, C.J. Hsu, H. Bassiri, E. Yang, G. Rak, E.M. Mace, N.H. Philip, W. Zhang, T. Baumgart, J.S. Orange, K.E. Nichols, and T. Kambayashi. 2013. Murine natural killer immunoreceptors use distinct proximal signaling complexes to direct cell function. *Blood* 121:3135-3146.

Melchers, F. 2005. The pre-B-cell receptor: selector of fitting immunoglobulin heavy chains for the B-cell repertoire. *Nature reviews. Immunology* 5:578-584.

Milne, C.D., and C.J. Paige. 2006. IL-7: a key regulator of B lymphopoiesis. *Seminars in immunology* 18:20-30.

Mombaerts, P., J. Iacomini, R.S. Johnson, K. Herrup, S. Tonegawa, and V.E. Papaioannou. 1992. RAG-1-deficient mice have no mature B and T lymphocytes. *Cell* 68:869-877.

Moshous, D., I. Callebaut, R. de Chasseval, B. Corneo, M. Cavazzana-Calvo, F. Le Deist, I. Tezcan, O. Sanal, Y. Bertrand, N. Philippe, A. Fischer, and J.P. de Villartay. 2001. Artemis, a novel DNA double-strand break repair/V(D)J recombination protein, is mutated in human severe combined immune deficiency. *Cell* 105:177-186.

Muljo, S.A., and M.S. Schlissel. 2003. A small molecule Abl kinase inhibitor induces differentiation of Abelson virus-transformed pre-B cell lines. *Nature immunology* 4:31-37.

Nadel, B., P.A. Cazenave, and P. Sanchez. 1990. Murine lambda gene rearrangements: the stochastic model prevails over the ordered model. *The EMBO journal* 9:435-440.

Nadel, B., A. Tang, G. Lugo, V. Love, G. Escuro, and A.J. Feeney. 1998. Decreased frequency of rearrangement due to the synergistic effect of nucleotide changes in the heptamer and nonamer of the recombination signal sequence of the V kappa gene A2b, which is associated with increased susceptibility of Navajos to Haemophilus influenzae type b disease. *Journal of immunology* 161:6068-6073.

Nemazee, D. 2006. Receptor editing in lymphocyte development and central tolerance. *Nature reviews. Immunology* 6:728-740.

Notarangelo, L.D. 2010. Primary immunodeficiencies. *The Journal of allergy and clinical immunology* 125:S182-194.

Oberdoerffer, P., T.I. Novobrantseva, and K. Rajewsky. 2003. Expression of a targeted lambda 1 light chain gene is developmentally regulated and independent of Ig kappa rearrangements. *The Journal of experimental medicine* 197:1165-1172.

Oettinger, M.A., D.G. Schatz, C. Gorka, and D. Baltimore. 1990. RAG-1 and RAG-2, adjacent genes that synergistically activate V(D)J recombination. *Science* 248:1517-1523.

Oltz, E.M., and O. Osipovich. 2007. Targeting V(D)J recombinase: putting a PHD to work. *Immunity* 27:539-541.

Osipovich, O., R.M. Cobb, K.J. Oestreich, S. Pierce, P. Ferrier, and E.M. Oltz. 2007. Essential function for SWI-SNF chromatin-remodeling complexes in the promoter-directed assembly of Tcrb genes. *Nature immunology* 8:809-816.

Pancer, Z., and M.D. Cooper. 2006. The evolution of adaptive immunity. *Annual review of immunology* 24:497-518.

Perlot, T., and F.W. Alt. 2008. Cis-regulatory elements and epigenetic changes control genomic rearrangements of the IgH locus. *Advances in immunology* 99:1-32.

Pilbeam, K., P. Basse, L. Brossay, N. Vujanovic, R. Gerstein, A.N. Vallejo, and L. Borghesi. 2008. The ontogeny and fate of NK cells marked by permanent DNA rearrangements. *Journal of immunology* 180:1432-1441.

Pillai, S., and A. Cariappa. 2009. The follicular versus marginal zone B lymphocyte cell fate decision. *Nature reviews. Immunology* 9:767-777.

Rajewsky, K. 1996. Clonal selection and learning in the antibody system. *Nature* 381:751-758.

Raval, P., A.N. Kriatchko, S. Kumar, and P.C. Swanson. 2008. Evidence for Ku70/Ku80 association with full-length RAG1. *Nucleic acids research* 36:2060-2072.

Reynaud, D., I.A. Demarco, K.L. Reddy, H. Schjerven, E. Bertolino, Z. Chen, S.T. Smale, S. Winandy, and H. Singh. 2008. Regulation of B cell fate commitment and immunoglobulin heavy-chain gene rearrangements by Ikaros. *Nature immunology* 9:927-936.

Riegert, P., and S. Gilfillan. 1999. A conserved sequence block in the murine and human TCR J alpha region: assessment of regulatory function in vivo. *Journal of immunology* 162:3471-3480.

Rooney, S., F.W. Alt, D. Lombard, S. Whitlow, M. Eckersdorff, J. Fleming, S. Fugmann, D.O. Ferguson, D.G. Schatz, and J. Sekiguchi. 2003. Defective DNA repair and increased genomic instability in Artemis-deficient murine cells. *The Journal of experimental medicine* 197:553-565.

Rothenberg, E.V. 2014. Transcriptional control of early T and B cell developmental choices. *Annual review of immunology* 32:283-321.

Sadofsky, M.J. 2004. Recombination-activating gene proteins: more regulation, please. *Immunological reviews* 200:83-89.

Sadofsky, M.J., J.E. Hesse, J.F. McBlane, and M. Gellert. 1993. Expression and V(D)J recombination activity of mutated RAG-1 proteins. *Nucleic acids research* 21:5644-5650.

Sanchez, P., B. Nadel, and P.A. Cazenave. 1991. V lambda-J lambda rearrangements are restricted within a V-J-C recombination unit in the mouse. *European journal of immunology* 21:907-911.

Santagata, S., A. Villa, C. Sobacchi, P. Cortes, and P. Vezzoni. 2000. The genetic and biochemical basis of Omenn syndrome. *Immunological reviews* 178:64-74.

Savic, V., B. Yin, N.L. Maas, A.L. Bredemeyer, A.C. Carpenter, B.A. Helmink, K.S. Yang-Iott, B.P. Sleckman, and C.H. Bassing. 2009. Formation of dynamic gamma-H2AX domains along broken DNA strands is distinctly regulated by ATM and MDC1 and dependent upon H2AX densities in chromatin. *Molecular cell* 34:298-310.

Schatz, D.G., and D. Baltimore. 1988. Stable expression of immunoglobulin gene V(D)J recombinase activity by gene transfer into 3T3 fibroblasts. *Cell* 53:107-115.
Schatz, D.G., and Y. Ji. 2011. Recombination centres and the orchestration of V(D)J recombination. *Nature reviews. Immunology* 11:251-263.
Schatz, D.G., M.A. Oettinger, and D. Baltimore. 1989. The V(D)J recombination activating gene, RAG-1. *Cell* 59:1035-1048.
Schatz, D.G., and P.C. Swanson. 2011. V(D)J recombination: mechanisms of initiation. *Annual review of genetics* 45:167-202.
Schlissel, M.S. 2007. The regulation of receptor editing. *Advances in experimental medicine and biology* 596:173-179.
Seitan, V.C., B. Hao, K. Tachibana-Konwalski, T. Lavagnolli, H. Mira-Bontenbal, K.E. Brown, G. Teng, T. Carroll, A. Terry, K. Horan, H. Marks, D.J. Adams, D.G. Schatz, L. Aragon, A.G. Fisher, M.S. Krangel, K. Nasmyth, and M. Merkenschlager. 2011. A role for cohesin in T-cell-receptor rearrangement and thymocyte differentiation. *Nature* 476:467-471.
Shanbhag, N.M., I.U. Rafalska-Metcalf, C. Balane-Bolivar, S.M. Janicki, and R.A. Greenberg. 2010. ATM-dependent chromatin changes silence transcription in cis to DNA double-strand breaks. *Cell* 141:970-981.
Shih, H.Y., and M.S. Krangel. 2013. Chromatin architecture, CCCTC-binding factor, and V(D)J recombination: managing long-distance relationships at antigen receptor loci. *Journal of immunology* 190:4915-4921.
Sicinska, E., I. Aifantis, L. Le Cam, W. Swat, C. Borowski, Q. Yu, A.A. Ferrando, S.D. Levin, Y. Geng, H. von Boehmer, and P. Sicinski. 2003. Requirement for cyclin D3 in lymphocyte development and T cell leukemias. *Cancer cell* 4:451-461.
Simkus, C., P. Anand, A. Bhattacharyya, and J.M. Jones. 2007. Biochemical and folding defects in a RAG1 variant associated with Omenn syndrome. *Journal of immunology* 179:8332-8340.
Sobacchi, C., V. Marrella, F. Rucci, P. Vezzoni, and A. Villa. 2006. RAG-dependent primary immunodeficiencies. *Human mutation* 27:1174-1184.
Speiser, D.E., R.K. Lees, H. Hengartner, R.M. Zinkernagel, and H.R. MacDonald. 1989. Positive and negative selection of T cell receptor V beta domains controlled by distinct cell populations in the thymus. *The Journal of experimental medicine* 170:2165-2170.
Steinel, N.C., B.L. Brady, A.C. Carpenter, K.S. Yang-Iott, and C.H. Bassing. 2010. Posttranscriptional silencing of VbetaDJbetaCbeta genes contributes to TCRbeta allelic exclusion in mammalian lymphocytes. *Journal of immunology* 185:1055-1062.
Steinel, N.C., B.S. Lee, A.T. Tubbs, J.J. Bednarski, E. Schulte, K.S. Yang-Iott, D.G. Schatz, B.P. Sleckman, and C.H. Bassing. 2013. The ataxia telangiectasia mutated kinase controls Igkappa allelic exclusion by inhibiting secondary Vkappa-to-Jkappa rearrangements. *The Journal of experimental medicine* 210:233-239.
Strasser, A., S. Whittingham, D.L. Vaux, M.L. Bath, J.M. Adams, S. Cory, and A.W. Harris. 1991. Enforced BCL2 expression in B-lymphoid cells prolongs antibody responses and elicits autoimmune disease. *Proceedings of the National Academy of Sciences of the United States of America* 88:8661-8665.
Sun, J.C., and L.L. Lanier. 2011. NK cell development, homeostasis and function: parallels with CD8(+) T cells. *Nature reviews. Immunology* 11:645-657.
Takeda, S., Y.R. Zou, H. Bluethmann, D. Kitamura, U. Muller, and K. Rajewsky. 1993. Deletion of the immunoglobulin kappa chain intron enhancer abolishes kappa

chain gene rearrangement in cis but not lambda chain gene rearrangement in trans. *The EMBO journal* 12:2329-2336.

Trotter, K.W., and T.K. Archer. 2012. Assaying chromatin structure and remodeling by restriction enzyme accessibility. *Methods in molecular biology* 833:89-102.

Verkoczy, L., D. Ait-Azzouzene, P. Skog, A. Martensson, J. Lang, B. Duong, and D. Nemazee. 2005. A role for nuclear factor kappa B/rel transcription factors in the regulation of the recombinase activator genes. *Immunity* 22:519-531.

Vettermann, C., and M.S. Schlissel. 2010. Allelic exclusion of immunoglobulin genes: models and mechanisms. *Immunological reviews* 237:22-42.

Villa, A., L.D. Notarangelo, and C.M. Roifman. 2008. Omenn syndrome: inflammation in leaky severe combined immunodeficiency. *The Journal of allergy and clinical immunology* 122:1082-1086.

Villa, A., C. Sobacchi, L.D. Notarangelo, F. Bozzi, M. Abinun, T.G. Abrahamsen, P.D. Arkwright, M. Baniyash, E.G. Brooks, M.E. Conley, P. Cortes, M. Duse, A. Fasth, A.M. Filipovich, A.J. Infante, A. Jones, E. Mazzolari, S.M. Muller, S. Pasic, G. Rechavi, M.G. Sacco, S. Santagata, M.L. Schroeder, R. Seger, D. Strina, A. Ugazio, J. Valiaho, M. Vihinen, L.B. Vogler, H. Ochs, P. Vezzoni, W. Friedrich, and K. Schwarz. 2001. V(D)J recombination defects in lymphocytes due to RAG mutations: severe immunodeficiency with a spectrum of clinical presentations. *Blood* 97:81-88.

von Boehmer, H., and F. Melchers. 2010. Checkpoints in lymphocyte development and autoimmune disease. *Nature immunology* 11:14-20.

Wade, T., J. Bill, P.C. Marrack, E. Palmer, and J.W. Kappler. 1988. Molecular basis for the nonexpression of V beta 17 in some strains of mice. *Journal of immunology* 141:2165-2167.

Wang, H., L. Zhai, J. Xu, H.Y. Joo, S. Jackson, H. Erdjument-Bromage, P. Tempst, Y. Xiong, and Y. Zhang. 2006. Histone H3 and H4 ubiquitylation by the CUL4-DDB-ROC1 ubiquitin ligase facilitates cellular response to DNA damage. *Molecular cell* 22:383-394.

Wang, X., G. Xiao, Y. Zhang, X. Wen, X. Gao, S. Okada, and X. Liu. 2008. Regulation of Tcrb recombination ordering by c-Fos-dependent RAG deposition. *Nature immunology* 9:794-801.

Wayne, J., H. Suh, Z. Misulovin, K.A. Sokol, K. Inaba, and M.C. Nussenzweig. 1994. A regulatory role for recombinase activating genes, RAG-1 and RAG-2, in T cell development. *Immunity* 1:95-107.

Wilson, A., C. Marechal, and H.R. MacDonald. 2001. Biased V beta usage in immature thymocytes is independent of DJ beta proximity and pT alpha pairing. *Journal of immunology* 166:51-57.

Wong, S.Y., and D.B. Roth. 2007. Murine models of Omenn syndrome. *The Journal of clinical investigation* 117:1213-1216.

Wu, C., C.H. Bassing, D. Jung, B.B. Woodman, D. Foy, and F.W. Alt. 2003. Dramatically increased rearrangement and peripheral representation of Vbeta14 driven by the 3'Dbeta1 recombination signal sequence. *Immunity* 18:75-85.

Wu, Z.H., Y. Shi, R.S. Tibbetts, and S. Miyamoto. 2006. Molecular linkage between the kinase ATM and NF-kappaB signaling in response to genotoxic stimuli. *Science* 311:1141-1146.

Wu, Z.H., E.T. Wong, Y. Shi, J. Niu, Z. Chen, S. Miyamoto, and V. Tergaonkar. 2010. ATM- and NEMO-dependent ELKS ubiquitination coordinates TAK1-mediated IKK activation in response to genotoxic stress. *Molecular cell* 40:75-86.

Xiang, Y., S.K. Park, and W.T. Garrard. 2013. Vkappa gene repertoire and locus contraction are specified by critical DNase I hypersensitive sites within the Vkappa-Jkappa intervening region. *Journal of immunology* 190:1819-1826.

Xiang, Y., X. Zhou, S.L. Hewitt, J.A. Skok, and W.T. Garrard. 2011. A multifunctional element in the mouse Igkappa locus that specifies repertoire and Ig loci subnuclear location. *Journal of immunology* 186:5356-5366.

Xu, Y., L. Davidson, F.W. Alt, and D. Baltimore. 1996. Deletion of the Ig kappa light chain intronic enhancer/matrix attachment region impairs but does not abolish V kappa J kappa rearrangement. *Immunity* 4:377-385.

Yancopoulos, G.D., and F.W. Alt. 1985. Developmentally controlled and tissue-specific expression of unrearranged VH gene segments. *Cell* 40:271-281.

Yannoutsos, N., V. Barreto, Z. Misulovin, A. Gazumyan, W. Yu, N. Rajewsky, B.R. Peixoto, T. Eisenreich, and M.C. Nussenzweig. 2004. A cis element in the recombination activating gene locus regulates gene expression by counteracting a distant silencer. *Nature immunology* 5:443-450.

Yin, F.F., S. Bailey, C.A. Innis, M. Ciubotaru, S. Kamtekar, T.A. Steitz, and D.G. Schatz. 2009. Structure of the RAG1 nonamer binding domain with DNA reveals a dimer that mediates DNA synapsis. *Nature structural & molecular biology* 16:499-508.

Yurchenko, V., Z. Xue, and M. Sadofsky. 2003. The RAG1 N-terminal domain is an E3 ubiquitin ligase. *Genes & development* 17:581-585.

Zentner, G.E., and S. Henikoff. 2013. Regulation of nucleosome dynamics by histone modifications. *Nature structural & molecular biology* 20:259-266.

Zhang, F., L.R. Thomas, E.M. Oltz, and T.M. Aune. 2006a. Control of thymocyte development and recombination-activating gene expression by the zinc finger protein Zfp608. *Nature immunology* 7:1309-1316.

Zhang, L., T.L. Reynolds, X. Shan, and S. Desiderio. 2011. Coupling of V(D)J recombination to the cell cycle suppresses genomic instability and lymphoid tumorigenesis. *Immunity* 34:163-174.

Zhang, Z., C.R. Espinoza, Z. Yu, R. Stephan, T. He, G.S. Williams, P.D. Burrows, J. Hagman, A.J. Feeney, and M.D. Cooper. 2006b. Transcription factor Pax5 (BSAP) transactivates the RAG-mediated V(H)-to-DJ(H) rearrangement of immunoglobulin genes. *Nature immunology* 7:616-624.

Zou, Y.R., S. Takeda, and K. Rajewsky. 1993. Gene targeting in the Ig kappa locus: efficient generation of lambda chain-expressing B cells, independent of gene rearrangements in Ig kappa. *The EMBO journal* 12:811-820.